UNIVERSITY OF EDINBURGH

A STUDY OF THE HELICAL AERIAL

by

T. S. M. Maclean B.Sc.

A Thesis Submitted for the Degree of

Doctor of Philosophy

September 1959.

TABLE OF CONTENTS

Table of Contents (Contd)

CHAPTER I

Introduction

Historical Sketch

The first successful attempts of which there is record, to make use of a helical structure as an aerial, appear to have been made soon after 1930 when patents were taken out by Chireux[1] in the United States and Franklin[2] in this country. In both cases at least part of the radiation was in the Broadside direction, and as will be seen later, because the pattern bandwidth was therefore necessarily small these aerials found little application.

A new type of helical aerial radiating in the End-Fire direction was first proposed and investigated by Kraus[3] at Ohio State University (Claims to prior discovery are also made by Marston whose reports, however, were not available until three years after the first publication by Kraus). In this case the conception arose from the use of the travelling-wave tube, and Kraus's main contribution was in realising and putting into practice the idea that the circumferential dimension of the helix used there might profitably be increased until it was of the order of one wavelength, in order to make the helix a linear end-fire array. His first attempts were immediately successful and over the years 1947-1950 he was responsible for the detailed investigation of its properties that followed/

followed[4,5,6,7,8,9]. As a result a clear general picture of the aerial's operation was built up in terms of travelling waves along the helical conductor. This enabled the radiation pattern to be predicted for a given length of aerial, and explained the essentially non-reactive nature of the terminal impedance.

Nevertheless even at the end of these investigations it is clear that while sufficient information was available to design a helical aerial, one was left with no idea of what was responsible for its limitations of bandwidth for certain degrees of pitch angle or what would be the effect on bandwidth, axial ratio or impedance of minor alterations in the aerial structure. Similarly there were no means other than experimental of determining what effect, if any, would be produced by the presence of a centrally conducting mast or by encapsulation of the aerial in dielectric. What had been achieved was the building of a valuable superstructure of theory on the basis of many experimental results, but the theory was not, per se, capable of extrapolating beyond the evidence on which it was formed. It may perhaps be argued that the theory available did predict for simple helices the continuance of increased directivity patterns with moderate increases in aerial length. Nevertheless, it will be shown later that this is accompanied by a previously unknown decrease of aerial/

aerial bandwidth, so that even in this case it could give rise to misleading information.

These criticisms of the state of knowledge regarding the helical aerial from 1951 onwards are in no way intended as criticism of the work carried out by Kraus and his associates. Indeed their contributions are of permanent scientific as well as engineering value and it is not surprising that even the contributions of some significance[10,11,12] which have been made since that time have added relatively little to the knowledge for which Kraus has been responsible.

A third type of helical aerial has been proposed by Wheeler. This produced Broadside radiation by using a current which is uniform and in-phase throughout the whole length of the aerial. Consequently if it is to be used without the insertion of phase-shifting devices and end loading, its dimensions must be small compared with a wavelength, and its radiation resistance will accordingly be low.

Outline of New Approach

The approach which has been adopted by the author in the following pages is applicable to the first two types of helical aerial mentioned above The theory of the third kind is straightforward by comparison and has been adequately treated by Wheeler[13] and Kraus[19].

Main interest centres on the End-Fire type which has found by far the greater application and/

and which has presented the greater number of problems. It consists in treating the aerial as an infinitely long waveguide which allows the propagation of surface waves, the phase velocity of which can be determined from the characteristic equation. The initial justification for this approach is that the helical aerial is essentially a travelling wave aerial. The initial problem then was to find how the calculated values of phase velocity agreed with these which were previously available from experiment. This had previously been attempted for a pitch angle of 10° by Sensiper[14] but he unfortunately made the mistake of comparing the theoretical results for the infinite helix with the experimental results for one particular helix approximately 1.5 wavelengths long, of pitch angle 13°. Apart from the difference in pitch angles the unnoticed error consisted in assuming that the experimental values of phase velocity were independent of axial length. In fact one of the outstanding characteristics of the helical aerial, as judged from its radiation patterns, is that the phase velocity increases with axial length so as always to satisfy the increased directivity condition of Hansen and Woodyard[15]. This discovery was first made by T. E. Tice at Ohio State University before 1950. When therefore this correction is made to the comparison/

comparison of phase velocities, the agreement becomes outstandingly good instead of being merely approximate.

On the basis of this agreement it is immediately clear that the same method of approach i.e. treating the helix as an infinite wave-guide can then in principle be applied to other related and important practical problems such as a helix with a coaxial cylinder inside, two coaxial helices, a helix wound on a dielectric tube or encapsulated in a dielectric. In all these cases the validity of any solution obtained can be expected to hold as it does in the case of the simple helix, provided no further approximations are involved, and the original approximations are not violated by the presence of the additional material. Later chapters consider these problems in mathematical detail.

There is, however, one particular case when an approximation involved in the original solution is violated to some extent. This arises in the case of the cross-wound helix consisting of two helical wires wound in opposite directions, and of the same diameter. A solution to this problem which arose in the design of travelling-wave tubes, but which has an obvious application to aerials, which will be considered later, was obtained by Chodorow and Chu[16]. In this case the agreement with experiment is less good though/

though still useful.

It will be noted that the parameter of phase velocity arises naturally in the waveguide approach, and it cannot be emphasized sufficiently that even in a practical finite aerial this is not only the most important parameter, but indeed the only one which need be considered. Until this fact is realised even the simple helical aerial appears to present an insuperable number of variables e.g. helix diameter, pitch angle, axial length and conductor diameter, each of which has to be varied for every possible variation of the other three. The situation becomes even more complicated in some practical cases. Since the phase velocity, however, is a function of all of these variables, and is directly related to the radiation pattern of the aerial, it greatly simplifies an understanding of the problem if this single parameter alone is considered. The same simplification can also be used profitably in the case of the Yagi aerial[17] and is implicitly used in the treatment of dielectric aerials[18].

CHAPTER II

The Simple Helix

Wave Propagation Along an Infinite Helical Conductor.

This problem has been studied in the past primarily for its application to helices in travelling-wave tubes[20,14], by means of two different physical models. One model known as the Sheath Helix consists of a sheet of metal of width equal to the required helical pitch wound as a helix which is assumed to be conducting only in the helical direction. It will be seen from the boundary conditions given later that this model neglects the important periodicity of the helix. The other and better model, known as the Tape Helix consists of a uniform helix wound with a tape of finite width and zero thickness, assumed to be perfectly conducting in all directions. The two models are illustrated in Figure2.1. which is taken from Reference 21.

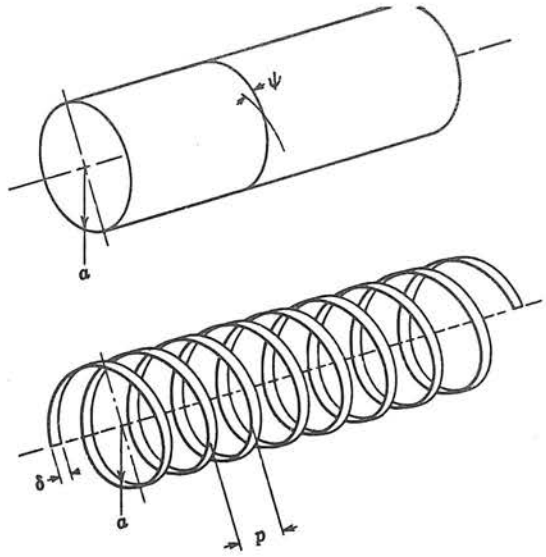

Figure 2.1. The sheath model and tape model helices. The sheath model is considered to conduct only in a direction making an angle ψ with a plane perpendicular to the axis.

2.1. The Sheath Helix

In this section a brief summary of the treatment developed by Sensiper[14] which is also given by Watkins[21], will be considered. This is more general than the original approach of Pierce[20] which although adequate for travelling wave tubes is not suitable for helical aerials, because of the angular variation of the fields there.

The scalar wave equations to be satisfied are

$$\nabla^2 E_z + k^2 E_z = 0 \qquad -- 2.1.1$$

and

$$\nabla^2 H_z + k^2 H_z = 0 \qquad -- 2.1.2$$

where E_z, H_z denote the axial components of electric and magnetic fields, and k is the free space phase constant. When written in cylindrical coordinates these give

$$\frac{1}{r}\frac{\partial}{\partial r}\left(r\frac{\partial E_z}{\partial r}\right) + \frac{1}{r^2}\frac{\partial^2 E_z}{\partial \theta^2} + \frac{\partial^2 E_z}{\partial z^2} + k^2 E_z = 0 \qquad -- 2.1.3$$

$$\text{and } \frac{1}{r}\frac{\partial}{\partial r}\left(r\frac{\partial H_z}{\partial r}\right) + \frac{1}{r^2}\frac{\partial^2 H_z}{\partial \theta^2} + \frac{\partial^2 H_z}{\partial z^2} + k^2 H_z = 0 \qquad -- 2.1.4$$

Assuming a solution of form $\begin{matrix} E_z \\ H_z \end{matrix} = f(r).e^{-jm\theta}.e^{-j\beta z} \qquad -- 2.1.5$

where β is the axial phase constant and m must be integral since the fields are to be single valued, there results

$$r^2\frac{\partial^2 f}{\partial r^2} + r\frac{\partial f}{\partial r} - \left[(\beta^2 - k^2)r^2 + m^2\right]f = 0 \qquad -- 2.1.6$$

For aerial operation a slow wave solution is desired to satisfy the condition of increased directivity, so that an appropriate choice is[22]

$$E_z = \left[A_m I_m(\gamma r) + C_m K_m(\gamma r)\right] e^{j m\theta} e^{-j\beta z} \quad -- 2.1.7$$

$$H_z = \left[B_m I_m(\gamma r) + D_m K_m(\gamma r)\right] e^{j m\theta} e^{-j\beta z} \quad -- 2.1.8$$

where A_m, B_m, C_m, D_m are constants and $\gamma^2 = \beta^2 - k^2$

Outside the helix the I_m functions are not suitable since their values become infinite as r tends to infinity. Likewise inside the helix the K_m functions must be discarded as these become infinite as r tends to zero.

Hence the desired solutions become

$$E_z^i = A_m^i I_m(\gamma r) e^{j m\theta} e^{-j\beta z} \qquad 0 < r < a \quad -- 2.1.10$$

$$E_z^e = A_m^e K_m(\gamma r) e^{j m\theta} e^{-j\beta z} \qquad a < r < \infty \quad -- 2.1.11$$

$$H_z^i = B_m^i I_m(\gamma r) e^{j m\theta} e^{-j\beta z} \qquad 0 < r < a \quad -- 2.1.12$$

$$H_z^e = B_m^e K_m(\gamma r) e^{j m\theta} e^{-j\beta z} \qquad a < r < \infty \quad -- 2.1.13$$

where a denotes the radius of the helix, and the superscripts i and e refer to regions internal and external to the helical surface respectively.

From these the remaining field quantities follow:-

$$E_r^i = \left[\frac{j\beta}{\gamma} A_m^i I_m'(\gamma r) - \frac{\omega\mu m}{\gamma^2 r} B_m^i I_m(\gamma r)\right] e^{j m\theta} e^{-j\beta z} \quad -- 2.1.14$$

$$E_\theta^i = \left[-\frac{m\beta}{\gamma^2 r} A_m^i I_m(\gamma r) - \frac{j\omega\mu}{\gamma} B_m^i I_m'(\gamma r)\right] e^{j m\theta} e^{-j\beta z} \quad -- 2.1.15$$

$$H_r^i = \left[\frac{m\omega\varepsilon}{\gamma^2 r} A_m^i I_m(\gamma r) + \frac{j\beta}{\gamma} B_m^i I_m'(\gamma r)\right] e^{j m\theta} e^{-j\beta z} \quad -- 2.1.16$$

$$H_\theta^i = \left[\frac{j\omega\varepsilon}{\gamma} A_m^i I_m'(\gamma r) - \frac{m\beta}{\gamma^2 r} B_m^i I_m(\gamma r)\right] e^{j m\theta} e^{-j\beta z} \quad -- 2.1.17$$

$$E_r^e = \left[\frac{j\beta}{\gamma} A_m^e K_m'(\gamma r) - \frac{\omega\mu m}{\gamma^2 r} B_m^e K_m(\gamma r)\right] e^{j m\theta} e^{-j\beta z} \quad -- 2.1.18$$

$$E_\theta^e = \left[-\frac{m\beta}{\gamma^2 r} A_m^e K_m(\gamma r) - \frac{j\omega\mu}{\gamma} B_m^e K_m'(\gamma r)\right] e^{j m\theta} e^{-j\beta z} \quad -- 2.1.19$$

$$H_r^e = \left[\frac{m\omega\varepsilon}{\gamma^2 r} A_m^e K_m(\gamma r) + \frac{j\beta}{\gamma} B_m^e K_m'(\gamma r)\right] e^{j m\theta} e^{-j\beta z} \quad -- 2.1.20$$

$$H_\theta^e = \left[\frac{j\omega\varepsilon}{\gamma} A_m^e K_m'(\gamma r) - \frac{m\beta}{\gamma^2 r} B_m^e K_m(\gamma r)\right] e^{j m\theta} e^{-j\beta z} \quad -- 2.1.21$$

The boundary conditions at the surface $r = a$ require that the tangential electric fields outside and inside the helix are continuous in the θ and z directions, and must be equated to zero along the direction of the helical winding, together with the requirement that the tangential magnetic field along the helical conductor is continuous. Formally the conditions are:

$$E_z^i = E_z^e \qquad -- 2.1.22$$

$$E_\theta^i = E_\theta^e \qquad -- 2.1.23$$

$$E_z^i = -E_\theta^i \cot\psi \qquad -- 2.1.24$$

$$H_z^i + H_\theta^i \cot\psi = H_z^e + H_\theta^e \cot\psi \qquad -- 2.1.25$$

where ψ is the pitch angle of the helix. Substituting the appropriate expressions for the fields in these equations and using the fact that a non-trivial solution will exist only if the determinant is zero gives

$$\begin{vmatrix} I_m(\gamma a) & 0 & -K_m(\gamma a) & 0 \\ -\frac{m\beta}{\gamma^2 a} I_m(\gamma a) & -j\frac{\omega\mu}{\gamma} I_m'(\gamma a) & \frac{m\beta}{\gamma^2 a} K_m(\gamma a) & j\frac{\omega\mu}{\gamma} K_m'(\gamma a) \\ \left[1 - \frac{m\beta\cot\psi}{\gamma^2 a}\right] I_m(\gamma a) & -j\frac{\omega\mu}{\gamma}\cot\psi I_m'(\gamma a) & 0 & 0 \\ j\frac{\omega\varepsilon}{\gamma}\cot\psi I_m'(\gamma a) & \left[1 - \frac{m\beta\cot\psi}{\gamma^2 a}\right] I_m(\gamma a) & -j\frac{\omega\varepsilon}{\gamma}\cot\psi K_m'(\gamma a) & \left[1 - \frac{m\beta\cot\psi}{\gamma^2 a}\right] -K_m(\gamma a) \end{vmatrix} = 0 \qquad -- 2.1.26$$

This leads quite simply to the characteristic equation

$$\frac{I_m'(\gamma a) K_m'(\gamma a)}{I_m(\gamma a) K_m(\gamma a)} = -\frac{(\gamma^2 a^2 - m\beta a \cot\psi)^2}{\gamma^2 a^2 \beta^2 a^2 \cot^2\psi} \qquad -- 2.1.27$$

2.2. The Tape Helix

This more exact representation of a physical helix was first dealt with by Sensiper[14] who was concerned primarily with its application to travelling-wave tubes. The tape width is δ and the pitch of the helix is denoted by h. Making use of Floquet's Theorem[21] the axial dependence of the fields, which must satisfy their periodic nature, can be written as $e^{-j\beta_m z}$ where β_m is given by

$$\beta_m = \beta_0 + \frac{2\pi m}{h} \qquad --2.2.1$$

and where m can have any integral value including zero. Since the angular dependence of the fields can be written as $e^{jn\theta}$ as in the sheath helix case, the differential equation to be satisfied for the radial dependence f(r) is

$$r\frac{\partial^2 f}{\partial r^2} + r\frac{\partial f}{\partial r} - \left[(\beta_m^2 - k^2)r^2 + n^2\right]f = 0 \qquad --2.2.2$$

The solution to this equation for E_z is

$$E_z^{i,e} = \sum_{m,n} E_{zmn}^{i,e} = e^{-j\beta_0 z} \sum_{m,n} A_{m,n}^{i,e} \frac{I_n(\gamma_m r)}{K_n} e^{jn\theta} e^{-j\frac{2\pi m}{h}z} \qquad --2.2.3$$

where the superscripts refer to the internal and external regions as before and

$$\gamma_m^2 = \beta_m^2 - k^2 \qquad --2.2.4$$

A further application of Floquet's Theorem to the angular coordinate instead of the axial coordinate enables this solution to be simplified. Let $z = z' + z_j$ and $\theta = \theta' + \phi$ where ϕ is the angle through which the helix must be rotated after a translation of z to make/

make it coincide with itself. i.e. $\phi = \frac{2\pi z}{h}$.

Substituting these values in Equation 2.2.3., E_z becomes

$$E_z^{i,e} = \sum_{m,n} E_{zmn}^{i,e} = e^{-j\beta_0 z'} e^{-j\beta_0 z} \sum_{m,n} A_{m,n}^{i,e} \frac{I_n}{K_n}(\gamma_m r) e^{-j(m-n)\frac{2\pi z}{h}} e^{jn\theta'} e^{-j\frac{2\pi m}{h}z'} \quad -- \quad 2.2.5$$

Since the above translation and rotation have resulted in the helix coinciding with its original position, Equation 2.2.5. must be of the same form as Equation 2.2.3. If this is to be true for all z, then (m-n) = 0. Accordingly Equation 2.2.3. can be written as

$$E_z^{i,e} = \sum_m E_{zm}^{i,e} = e^{-j\beta_0 z} \sum_m A_m^{i,e} \frac{I_m}{K_m}(\gamma_m r) e^{jn\theta} e^{-j\frac{2\pi m}{h}z} \quad -- \quad 2.2.6$$

Similarly

$$H_z^{i,e} = \sum_m H_{zm}^{i,e} = e^{-j\beta_0 z} \sum_m B_m^{i,e} \frac{I_m}{K_m}(\gamma_m r) e^{jn\theta} e^{-j\frac{2\pi mz}{h}} \quad -- \quad 2.2.7$$

The boundary conditions for the tape helix require continuity of the tangential electric field and a total surface current density equal to the discontinuity in tangential magnetic field. Formally these conditions are that where r = a,

$$E_z^i = E_z^e \quad -- \quad 2.2.8$$

$$E_\theta^i = E_\theta^e \quad -- \quad 2.2.9$$

$$J_\theta = H_z^i - H_z^e \quad -- \quad 2.2.10$$

$$J_z = H_\theta^e - H_\theta^i \quad -- \quad 2.2.11$$

where

$$J_\theta = e^{-j\beta_0 z} \sum_m j_{\theta m} e^{jn\theta} e^{-j\frac{2\pi mz}{h}} \quad -- \quad 2.2.12$$

and

$$J_z = e^{-j\beta_0 z} \sum_m j_{zm} e^{jn\theta} e^{-j\frac{2\pi mz}{h}} \quad -- \quad 2.2.13$$

In equations 2.2.12 and 2.2.13 $j_{\theta m}$ and j_{zm} are the total surface current densities associated with the mth space or Hartree harmonics, i.e. the component of the total wave travelling with phase constant β_m.

The solution to the tape helix problem follows from the application of Equations 2.2.8 through 2.2.11 to the formal expressions for E_z and H_z in Equations 2.2.6 and 2.2.7, together with the expressions for the other field quantities which can be derived from these. These are not written out explicitly here since they may be derived very simply by comparison with equations 2.1.14 through 2.1.21.

Since however this procedure involves difficulties with the solution of the resulting determinant, the following further approximations are introduced at this stage:-

(a) The current is assumed to flow only along the tape, and does not vary in amplitude or phase across its width.

(b) Since (a) is an approximation, the tangential electric field can not be zero everywhere along the tape surface and so it is arbitrarily equated to zero along the centreline of the tape.

Mathematically, denoting the directions along and perpendicular to the tape by the subscripts

11/

ll and $\perp$

$$J_\perp = 0 \qquad -- 2.2.14$$

$$J_{ll} = \begin{cases} J e^{-j\beta_0 \frac{h\theta}{2\pi}} , & \frac{h\theta}{2\pi} < z < \frac{h\theta}{2\pi} + \delta \\ 0 , \text{ elsewhere} \end{cases} \qquad -- 2.2.15$$

Also $$J_{ll} = e^{-j\beta_0 z} \sum_m j_{llm} e^{jm\theta} e^{-j\frac{2\pi m z}{h}} \qquad -- 2.2.16$$

where $$j_{llm} = J e^{j\frac{\beta_m \delta}{2}} \frac{\sin \frac{\beta_m \delta}{2}}{\frac{\beta_m \delta}{2}} \qquad -- 2.2.17$$

To apply approximation (b) requires the use of

$$E_{llm} = E_{zm} \sin\psi + E_{\theta m} \cos\psi \qquad -- 2.2.18$$

where E_{zm} and $E_{\theta m}$ are found from the Boundary Conditions in the following way :

$$A_m^i I_m(\gamma_m a) - A_m^e K_m(\gamma_m a) = 0 \qquad -2.2.19.$$

$$-\frac{m\beta_m}{\gamma_m^2 a} A_m^i I_m(\gamma_m a) - j\frac{\omega\mu}{\gamma_m} B_m^i I_m'(\gamma_m a) + \frac{m\beta_m}{\gamma_m^2 a} A_m^e K_m(\gamma_m a) + j\frac{\omega\mu}{\gamma_m} B_m^e K_m'(\gamma_m a) = 0 \qquad -2.2.20.$$

$$j\frac{\omega\varepsilon}{\gamma_m} A_m^e K_m'(\gamma_m a) - \frac{m\beta_m}{\gamma_m^2 a} B_m^e K_m(\gamma_m a) - j\frac{\omega\varepsilon}{\gamma_m} A_m^i I_m'(\gamma_m a) + \frac{m\beta_m}{\gamma_m^2 a} B_m^i I_m(\gamma_m a) = j_{zm} \qquad -2.2.21$$

$$B_m^i I_m(\gamma_m a) - B_m^e K_m(\gamma_m a) = j_{\theta m} \qquad -2.2.22$$

Then using

$$I_m(\gamma_m a) = a \qquad j\frac{\omega\mu}{\gamma_m} K_m'(\gamma_m a) = f$$

$$-K_m(\gamma_m a) = b \qquad j\frac{\omega\varepsilon}{\gamma_m} K_m'(\gamma_m a) = g$$

$$-\frac{m\beta_m}{\gamma_m^2 a} I_m(\gamma_m a) = c \qquad -j\frac{\omega\varepsilon}{\gamma_m} I_m'(\gamma_m a) = h \qquad -2.2.23$$

$$-j\frac{\omega\mu}{\gamma_m} I_m'(\gamma_m a) = d \qquad j_{\theta m} = \delta$$

$$\frac{m\beta_m}{\gamma_m^2 a} K_m(\gamma_m a) = e \qquad j_{zm} = \tau$$

$$A_m^i = \frac{\Delta_2}{\Delta_1} \qquad --2.2.24$$

and $$B_m^i = \frac{\Delta_3}{\Delta_1} \qquad --2.2.25$$

where $\Delta_1 =$

$$\begin{vmatrix} a & 0 & b & 0 \\ c & d & e & f \\ h & -c & g & -e \\ 0 & a & 0 & b \end{vmatrix} \qquad --2.2.26$$

$\Delta_2 =$

$$\begin{vmatrix} 0 & 0 & b & 0 \\ 0 & d & e & f \\ \gamma & -c & g & -e \\ \delta & a & 0 & b \end{vmatrix} \qquad --2.2.27$$

$\Delta_3 =$

$$\begin{vmatrix} a & 0 & b & 0 \\ c & 0 & e & f \\ h & \gamma & g & -e \\ 0 & \delta & 0 & b \end{vmatrix} \qquad --2.2.28$$

Simplifying the determinants gives

$$A_m^i = \frac{j\omega\mu}{k^2} \gamma_m^2 a K_m(\gamma_m a)\left[j z_m - \frac{m\beta_m}{\gamma_m^2 a} j\theta_m\right]$$

and $\qquad --2.2.29$

$$B_m^i = -\gamma_m a K_m'(\gamma_m a) j\theta_m \qquad --2.2.30$$

Then from Equation 2.2.18 after some simplification

$$E_{\parallel m}\big|_{r=a} = j\frac{e^{-j\beta_0 z}\sin^2\psi}{\omega\varepsilon a}\left\{\left[\gamma_m^2 a^2 - 2m\beta_m a\cot\psi + \frac{m^2\beta_m^2 a^2\cot^2\psi}{\gamma_m^2 a^2}\right] I_m(\gamma_m a)\,K_m(\gamma_m a) + k^2 a^2\cot^2\psi\, I_m'(\gamma_m a)\,K_m'(\gamma_m a)\right\} e^{jm\theta} e^{-j\frac{2\pi m z}{h}} f_{\parallel m} \quad -- 2.2.31$$

Since

$$E_{\parallel}\big|_{r=a} = \sum_m E_{\parallel m}\big|_{r=a}$$

$$E_{\parallel}\big|_{r=a} = j\frac{e^{-j\beta_0 z}\sin^2\psi}{\omega\varepsilon a}\sum_m\left\{\left[\gamma_m^2 a^2 - 2m\beta_m a\cot\psi + \frac{m^2\beta_m^2 a^2\cot^2\psi}{\gamma_m^2 a^2}\right] I_m(\gamma_m a)\,K_m(\gamma_m a) + k^2 a^2\cot^2\psi\, I_m'(\gamma_m a)\,K_m'(\gamma_m a)\right\} e^{jm\theta} e^{-j\frac{2\pi m z}{h}} f_{\parallel m} \quad -- 2.2.32$$

Setting this expression equal to zero along the centre line of the tape at $z = \frac{h\theta}{2\pi} + \frac{\delta}{2}$ and using Equation 2.2.17 gives finally

$$0 = \sum_m\left\{\left[\gamma_m^2 a^2 - 2m\beta_m a\cot\psi + \frac{m^2\beta_m^2 a^2\cot^2\psi}{\gamma_m^2 a^2}\right] I_m(\gamma_m a)\,K_m(\gamma_m a) + k^2 a^2\cot^2\psi\, I_m'(\gamma_m a)\,K_m'(\gamma_m a)\right\}\frac{\sin\frac{\beta_m\delta'}{2}}{\frac{\beta_m\delta'}{2}} \quad -- 2.2.33$$

CHAPTER III

The Simple Helical Aerial

A comparison will be made in this chapter between the numerical values of phase velocity calculated for the infinite helix and the values of phase velocity corresponding to the Hansen-Woodyard condition, which it is known from experiment are always satisfied for the simple helical aerial[19]. If the phase velocity exceeds that for the Hansen-Woodyard condition the width of the main lobe will be increased, while if it is lower the sidelobe level will be increased. Consideration will be given to two widely different values of pitch angle, to assess better the applicability of the theory to practical aerials.

3.1. The Bandwidth of a Medium-Pitch Helical Aerial.

A pitch angle of $\psi = 13^{\circ}$ has been chosen here for two reasons,

(a) accurate experimental values of phase velocity for this pitch angle and for a specific length of $1.6\lambda_0$ are available,[9,19]

and (b) it is known that an angle of about this size gives the largest bandwidth for a helix $1.6\lambda_0$ long[19].

In predicting the bandwidth of such an aerial use will be made of the Array Factor

$$\frac{\sin \frac{n\psi'}{2}}{\sin \frac{\psi'}{2}}$$ where

$$\psi' = \beta d \cos\phi - \alpha \quad --3.1.1\,(a)$$

with β the free-space phase constant, α the phase change between successive elements, d their distance apart and ϕ the angle measured from the line of the array.

This may conveniently be rewritten as

$$\psi' = 2\pi C_\lambda \tan\psi \cos\phi - \frac{L_\lambda}{v/c} \cdot 2\pi \quad --3.1.1\,(b)$$

where C_λ is the circumference in free space wavelengths of the imaginary cylinder on which the helix is wound, L_λ is the corresponding length of one turn, and v is the phase velocity along the conductor.

Figure 3.1.1. illustrates the array factor for an array of 50 isotropic elements. Only the part of this pattern to the right of the point $\phi = 0^\circ$ is traced out; this point is a function of the phase velocity v along the conductor. Point A represents the point $\phi = 0^\circ$ for the Hansen-Woodyard phase condition, and point B is the point $\phi = 0^\circ$ where the sidelobe level has increased to 45% of the main beam. This sidelobe level will be arbitrarily taken to represent the upper allowable frequency of operation for the aerial.

It will be noted that in moving from A to B ψ' has increased from 3.6° $(= \frac{\pi}{50})$ to 4.6° (= 0.080 radians). Substituting these values in Equation 3.1.1. and taking $C_\lambda = 1.0$, enables/

FIG 3.1.1

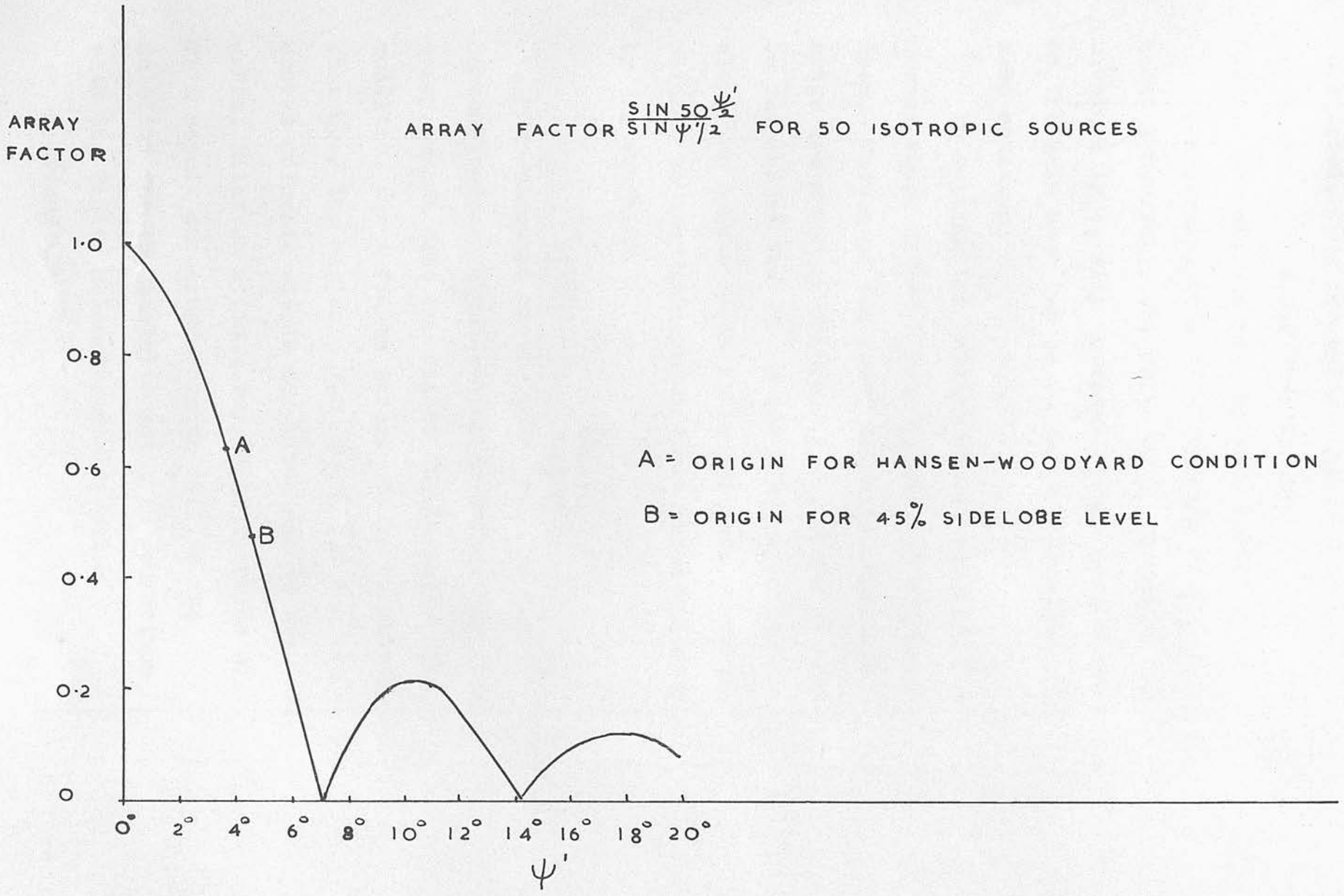
ARRAY FACTOR $\frac{\sin 50\frac{\psi'}{2}}{\sin\psi'/2}$ FOR 50 ISOTROPIC SOURCES
ARRAY FACTOR
1·0
0·8
0·6
0·4
0·2
0
A
B
0°
2°
4°
6°
8°
10°
12°
14°
16°
18°
20°
ψ'
A = ORIGIN FOR HANSEN-WOODYARD CONDITION
B = ORIGIN FOR 45% SIDELOBE LEVEL

enables the two corresponding values of v to be calculated. The percentage change in v as A moves along the array factor curve to B is only 0.22%. Use will be made of this result later.

Conversely, if v as a function of C_λ, is known accurately, the value of C_λ for which the sidelobe level will be equal to any percentage of the main beam can be calculated from the same equation.

In solving the characteristic equation the normal range of $ka(=C_\lambda)$ from 0.7 to 1.3 has been used. Values of the phase velocity over this range are shown in Figure 3.1.2., where it must be remembered that it is the phase velocity along the conductor which is plotted. This is related to the fundamental axial phase velocity by the equation

$$v_{\text{conductor}} = \frac{v_{\text{axial}}}{\sin \psi} \qquad 3.1.2.$$

Superimposed on the same graph is the Hansen-Woodyard condition for an infinitely long array, which also represents the in-phase fidd condition for a finite array. It is noteworthy that over the region $0.7 < ka < 1.0$ the two curves coincide within the thickness of the curve, although a) is always slightly below b). This result encourages one to utilise the solution for the infinite helix in connection with the finite helical aerial problem.

However/

FIG 3.1.2

CONDUCTOR PHASE VELOCITY VS CIRCUMFERENCE IN WAVELENGTHS

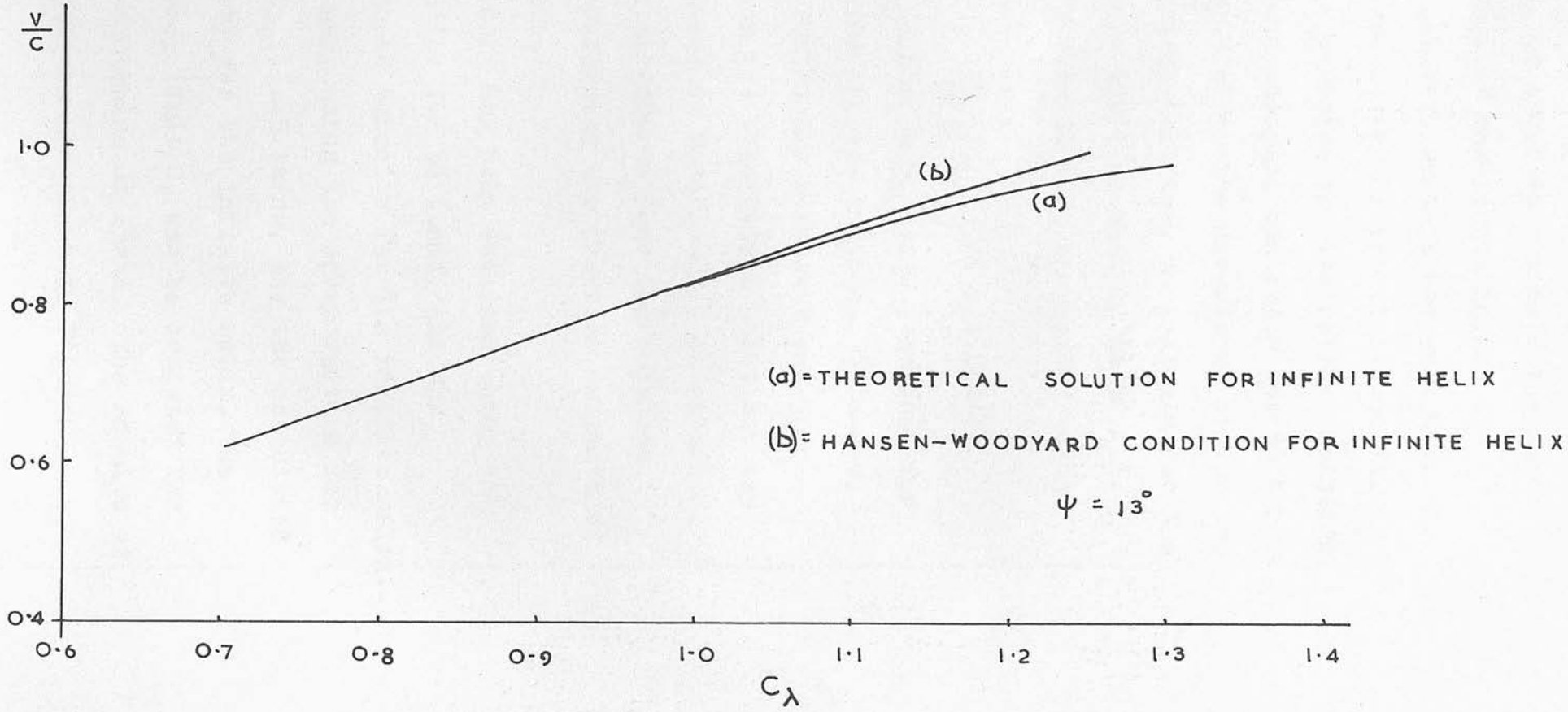

However, in order to estimate the upper frequency limit of the finite helix, the theoretical solution must be compared with the Hansen-Woodyard curve for the finite helix. Figure 3.1.3. compares the theoretical solution with the Hansen-Woodyard condition for 50 turns. Using the point where the divergence of the two curves becomes significant, an estimate for the upper frequency limit is that C_λ is $\simeq$ 1.1. This can be evaluated more accurately using Equation 3.1.1. i.e.

$$2\pi\left(C_\lambda \tan\psi - \frac{L_\lambda}{v/c}\right) = -(2\pi + 0.080)$$

It is noted that $L_\lambda = C_\lambda \sec\psi$, so that for $\psi = 13^\circ$ there are two unknowns, C_λ and v. Using the relationship between v and C_λ resulting from the theoretical solution, the desired solution of Equation 3.1.1 is obtained. For the case considered here the solution is $C_\lambda = 1.10$, confirming the previous estimate of the same value.

This result has been obtained using only the array factor for 50 turns, and the calculated phase velocity for the infinite helix. In the same way, using the array factors for 3, 5, 10, 15 .....45 turns, and the calculated phase velocity for the infinite helix, the upper frequency limit C_λ can be computed for each of these numbers of turns. The results of these computations are shown in Figure 3.1.4.

as/

FIG 3.1.3

CONDUCTOR PHASE VELOCITY VS CIRCUMFERENCE IN WAVELENGTHS

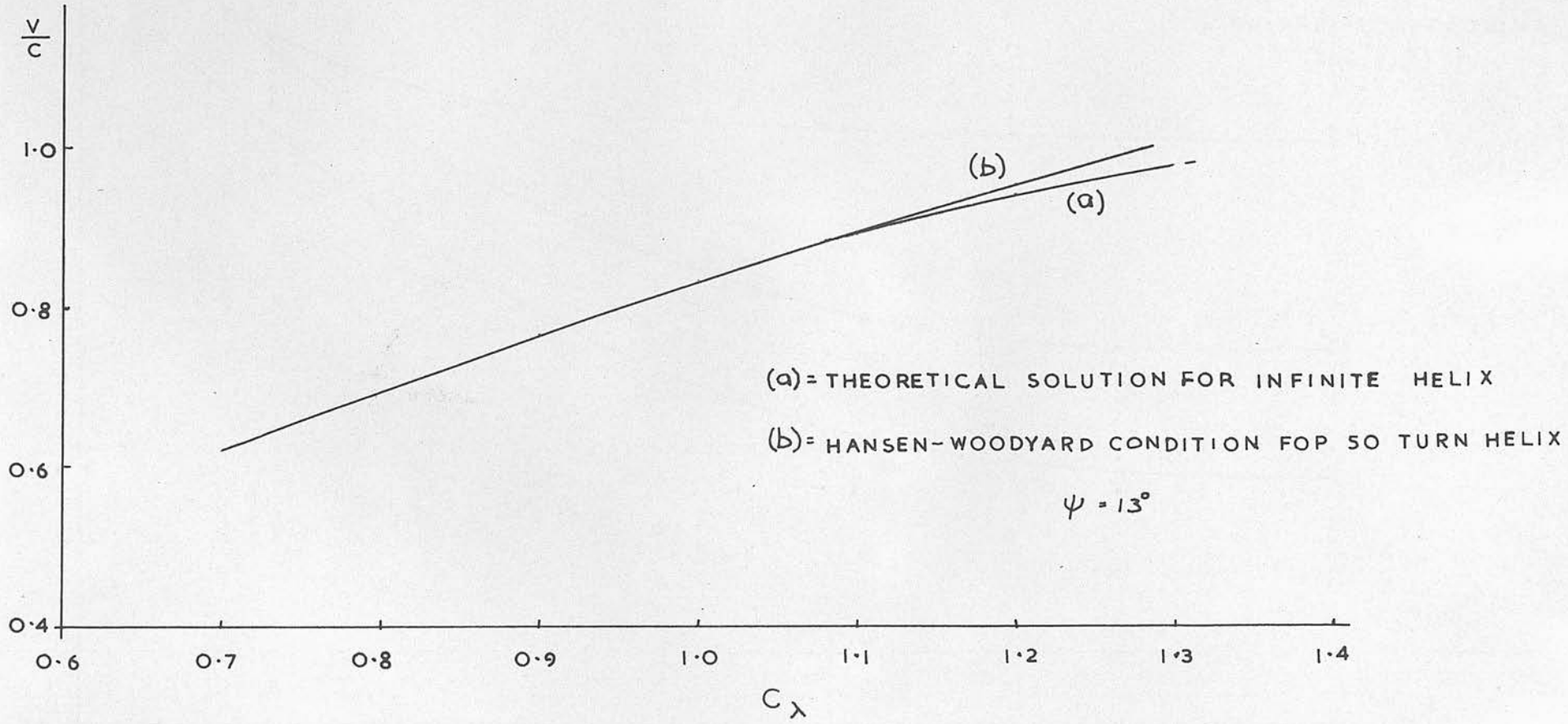

UPPER FREQUENCY LIMIT VS NUMBER OF TURNS FOR $\psi = 13^\circ$

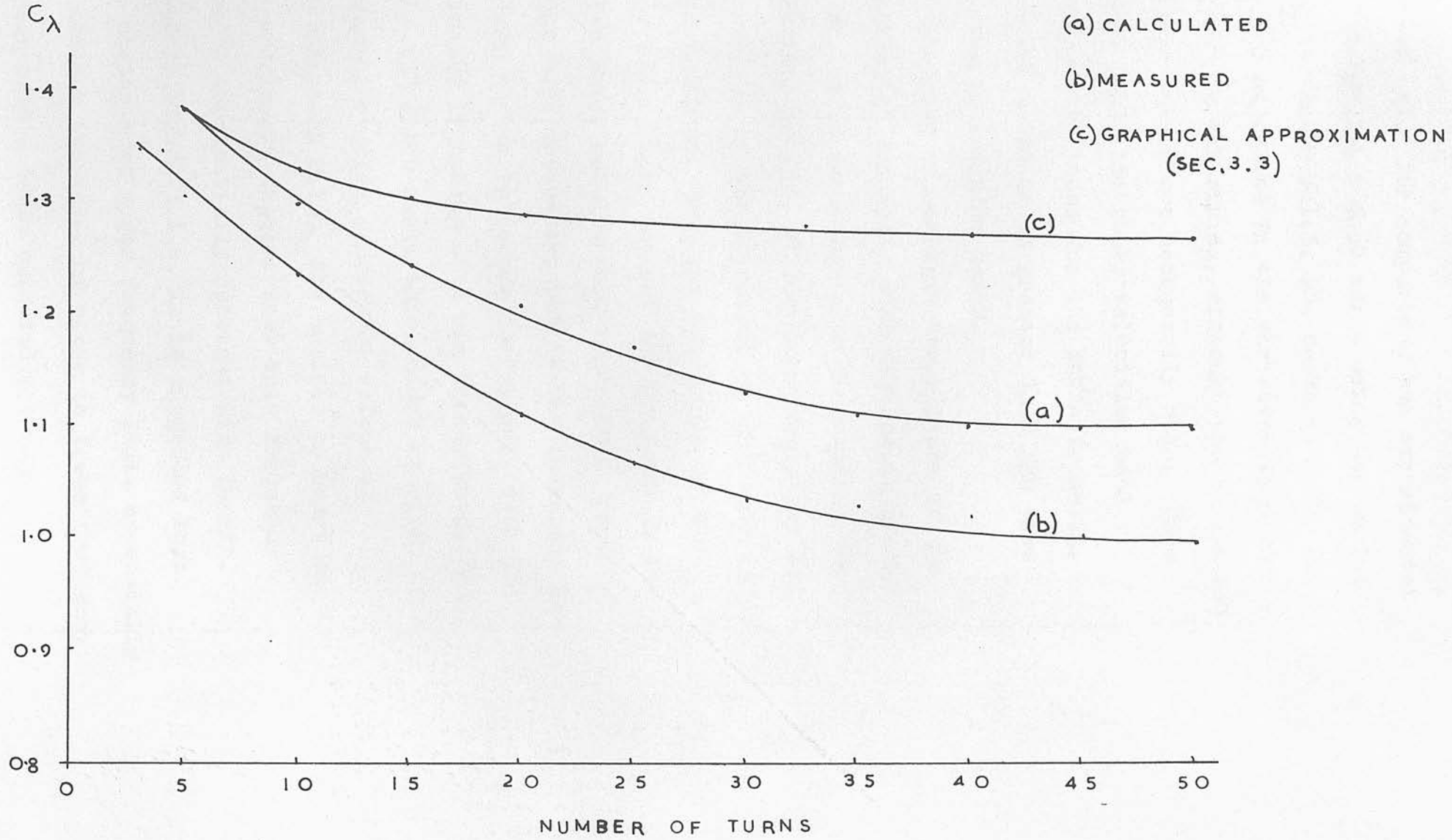

as curve (a). For comparison the experimental results for $3 \leqslant n \leqslant 50$ turns using the aerial shown in Figure 3.1.5. are shown as curve (b).

The agreement in the variation with number of turns is satisfying, although the calculated absolute values are necessarily high. This follows since the phase velocities used correspond to those for the infinite helix, which are known to be greater than the ones applying to a finite helix.

In order to complete the picture of the variation of bandwidth with the length of the aerial, it is necessary also to consider the variation, if any, of the lower frequency limit. The physics of the situation in this case is quite different from the limitation at the upper end. There the pattern break-up is due to the phase velocity not increasing rapidly enough with frequency, but at the lower end the pattern begins to become useful only with the effective launching of a new transmission mode. For a 13° pitch angle this occurs at $0.77C_{\lambda}$ for an infinite helix. Measured values of approximately $0.75C_{\lambda}$ for helices as short as 0.7 wavelength suggest that this frequency remains substantially constant with length. Hence in Figure 3.1.4. it is suggested that the ordinate of upper frequency limit essentially determines the ratio of upper to lower frequency limits with a scale conversion factor

of/

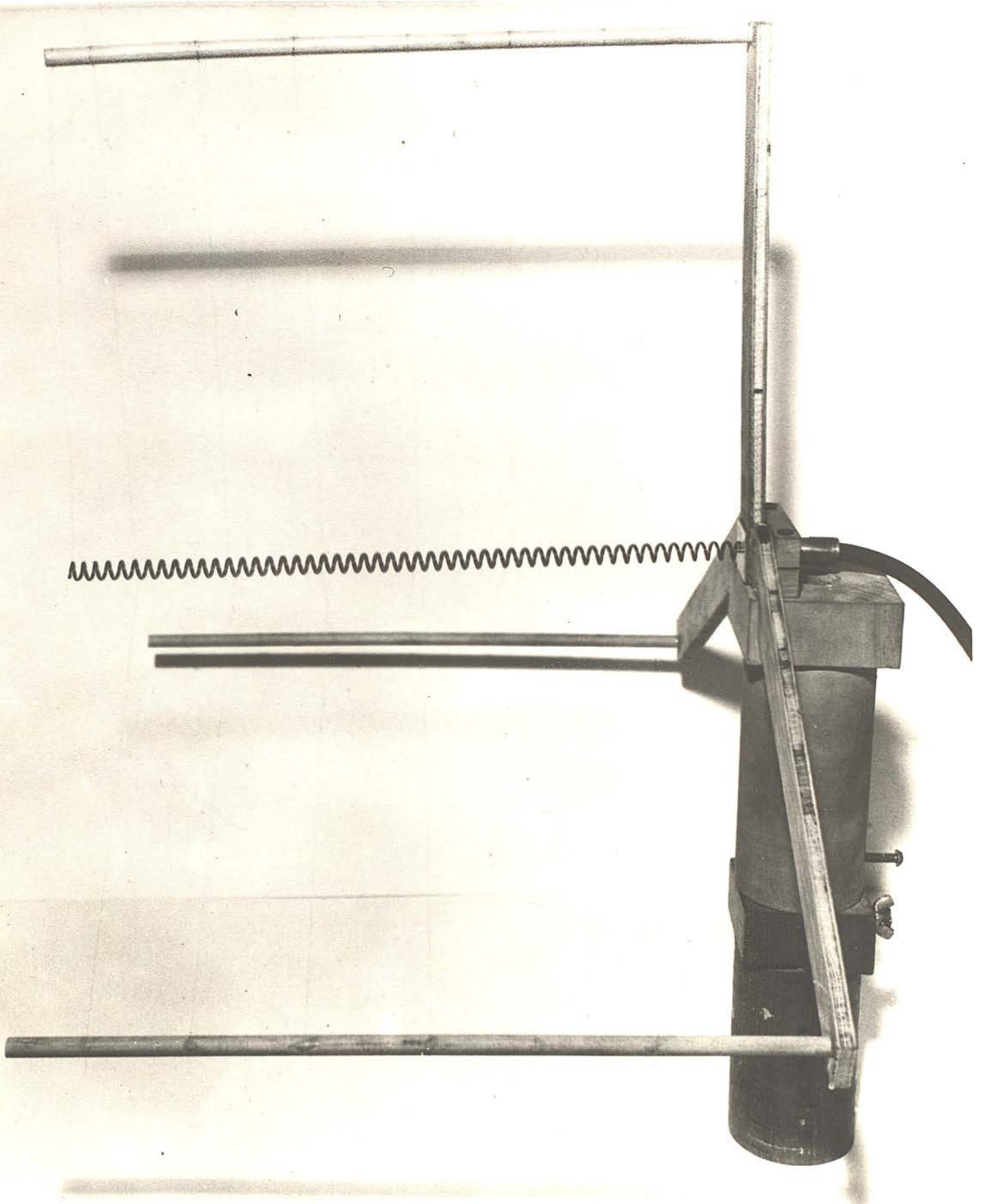

FIG 3.1.5

of $\frac{1.0}{0.77}$ or 1.3. This result corrects the earlier, universally held idea that the useful frequency range of a helical aerial centres about the frequency corresponding to $C_\lambda = 1.0$. According to the results reported here, however, it should rather be considered as existing above $C_\lambda = 0.77$ for the 13° pitch angle case. The value of $0.77C_\lambda$ is a fixed lower limit while the upper limit varies with length.

In obtaining the experimental results for Figure 3.1.4. (b) it was necessary to take patterns of E_θ, E_φ and Axial Ratio for $3 \leq n \leq 50$ turns. A selction of these patterns is shown in Figures 3.1.6. through 3.1.10. The most important of these are the ones for large n, since it is believed that these represent the patterns of the longest helices which have as yet been tested. In all cases it can be seen that both the patterns and the axial ratios are good.

The variation of half-power beamwidth with length of the aerial is shown in Figure 3.1.11 for the E_θ and E_φ patterns. These curves are based on the experimental measurements shown in the previous figures, and agree closely with the values which may be predicted from Hansen-Woodyard conditions. The constant frequency to which the curves are applicable is $0.92C_\lambda$.

At still higher frequencies corresponding to/

FIG 3.1.6

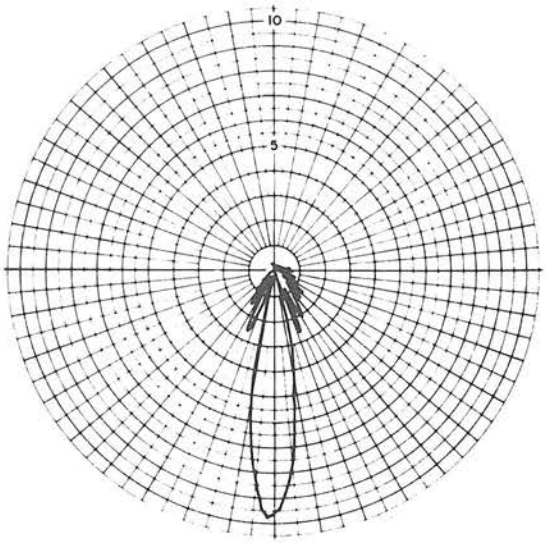

E_θ pattern for 50 turn, 13 ^{o} helix; f=8 Kmc/s.

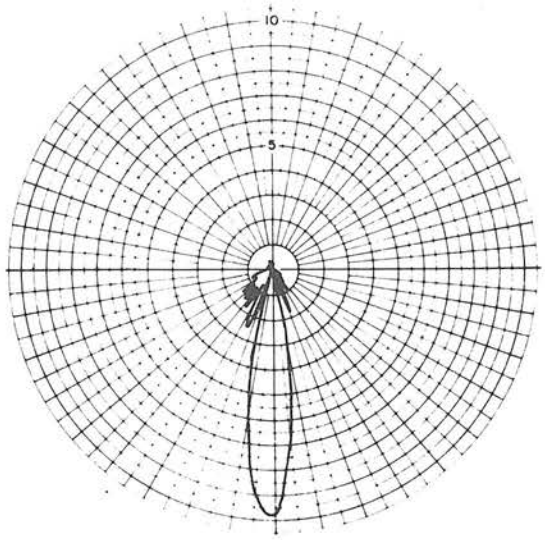

E_ϕ pattern for 50 turn, 13^o helix; f=8 Kmc/s.

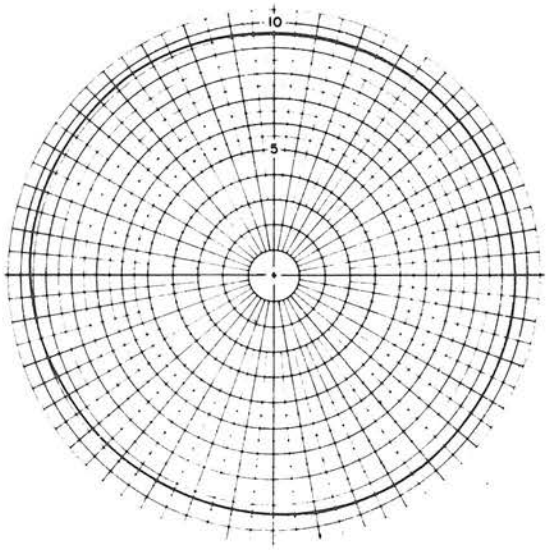

Polarization pattern for 50 turn, 13^o helix; f = 8 Kmc/s.

FIG 3.1.7

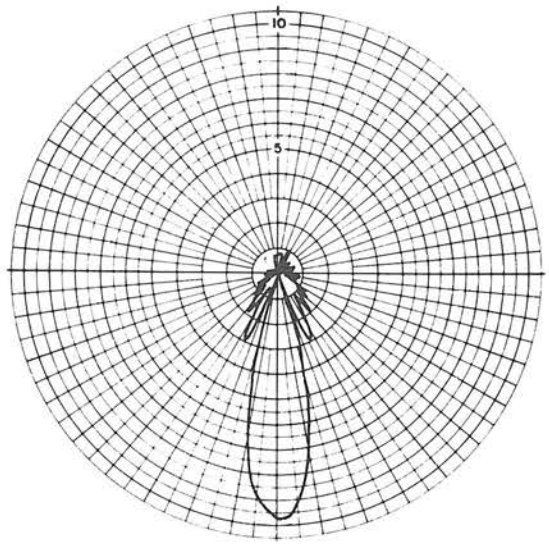

E_θ pattern for 40 turn, 13^o helix; f=8 Kmc/s.

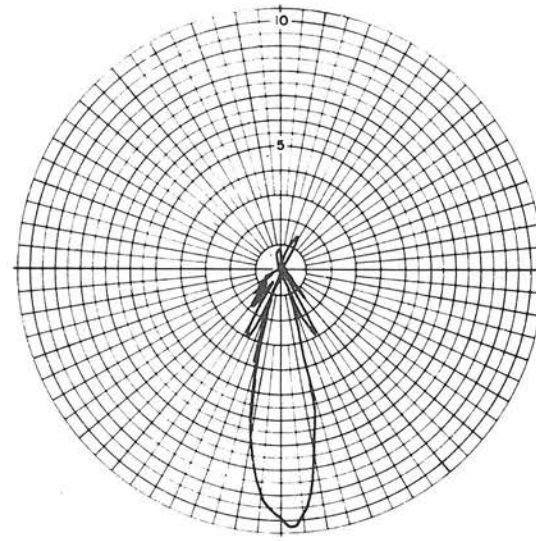

E_ϕ pattern for 40 turn, 13^o helix; f=8 Kmc/s.

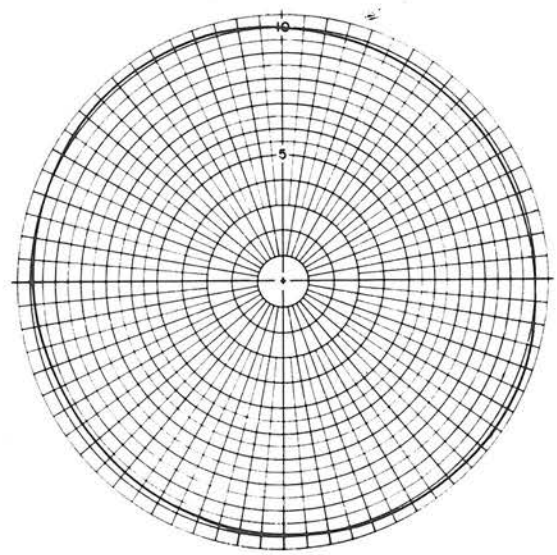

Polarization pattern for 40 turn, 13^o helix; f = 8 Kmc/s.

FIG 3.1.8

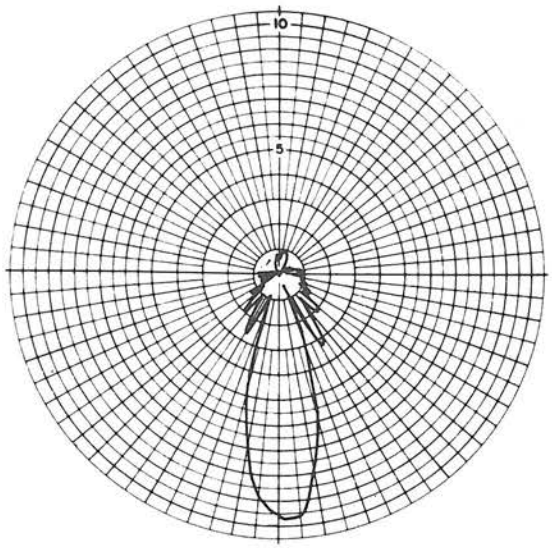

E_θ pattern for 30 turn,
13° helix; f=8 Kmc/s.

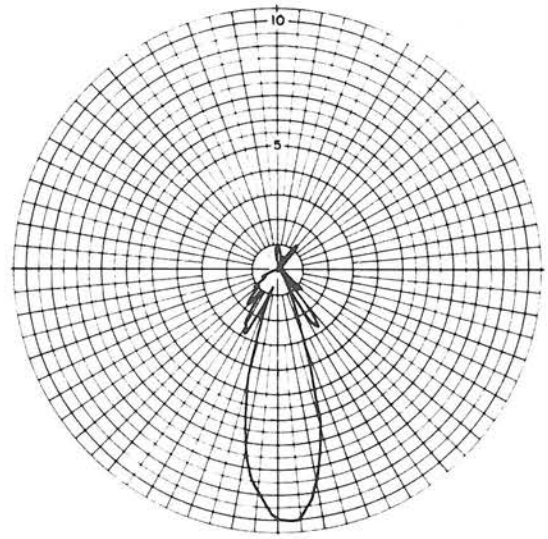

E_ϕ pattern for 30 turn,
13° helix; f=8 Kmc/s.

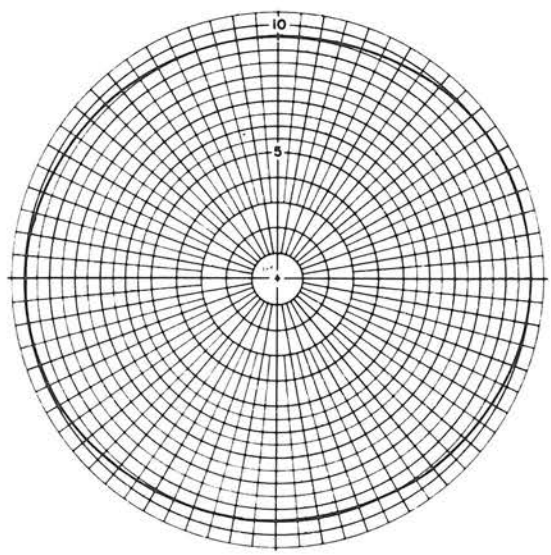

Polarization pattern for 30 turn,
13° helix; f = 8 Kmc/s.

FIG 3.1.9

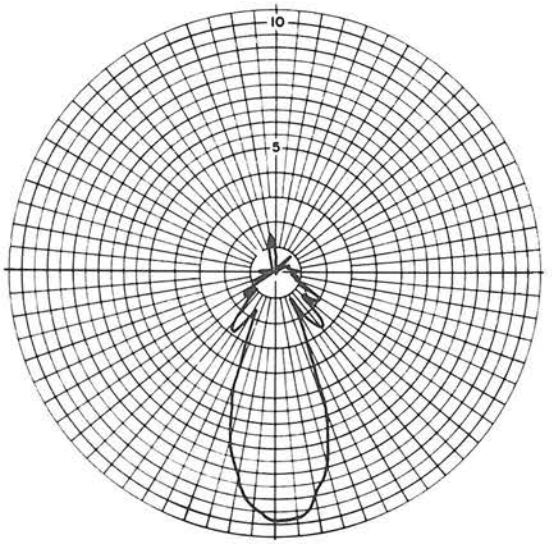

E_θ pattern for 20 turn,
13° helix; f=8 Kmc/s.

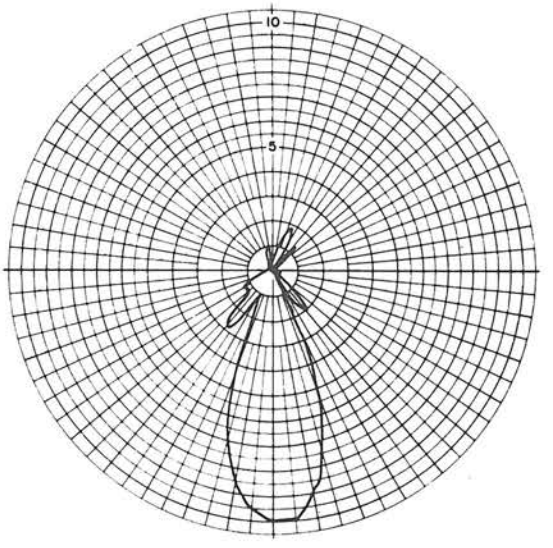

E_ϕ pattern for 20 turn,
13° helix; f=8 Kmc/s.

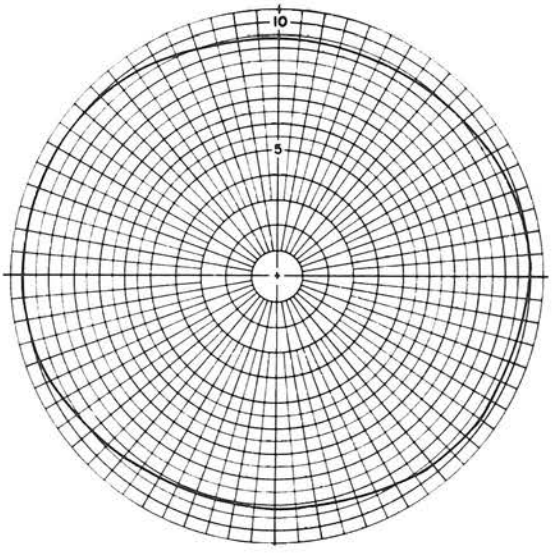

Polarization pattern for 20 turn,
13° helix; f = 8 Kmc/s.

FIG 3.1.10

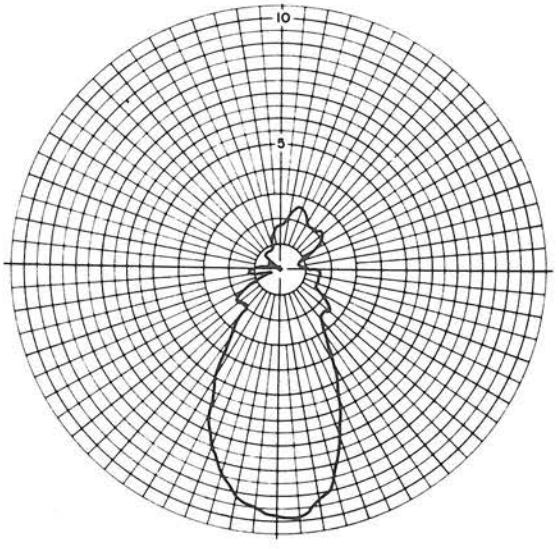

E_θ pattern for 10 turn, 13° helix; f=8 Kmc/s.

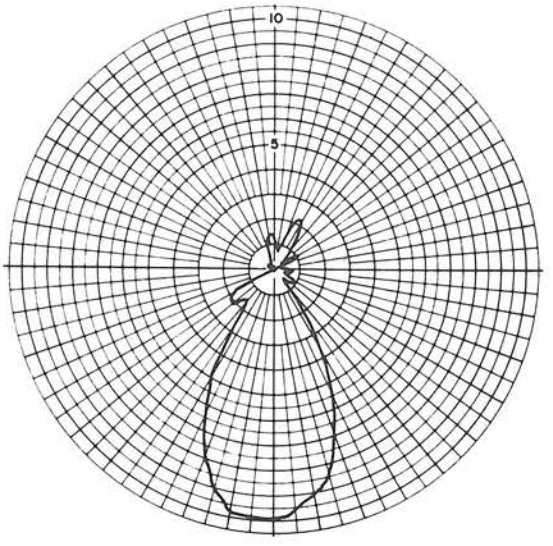

E_ϕ pattern for 10 turn, 13° helix; f=8 Kmc/s.

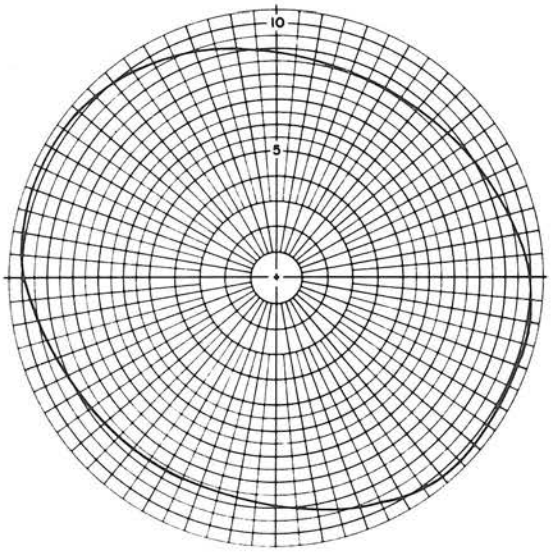

Polarization pattern for 10 turn, 13° helix; f = 8 Kmc/s.

FIG 3.1.11

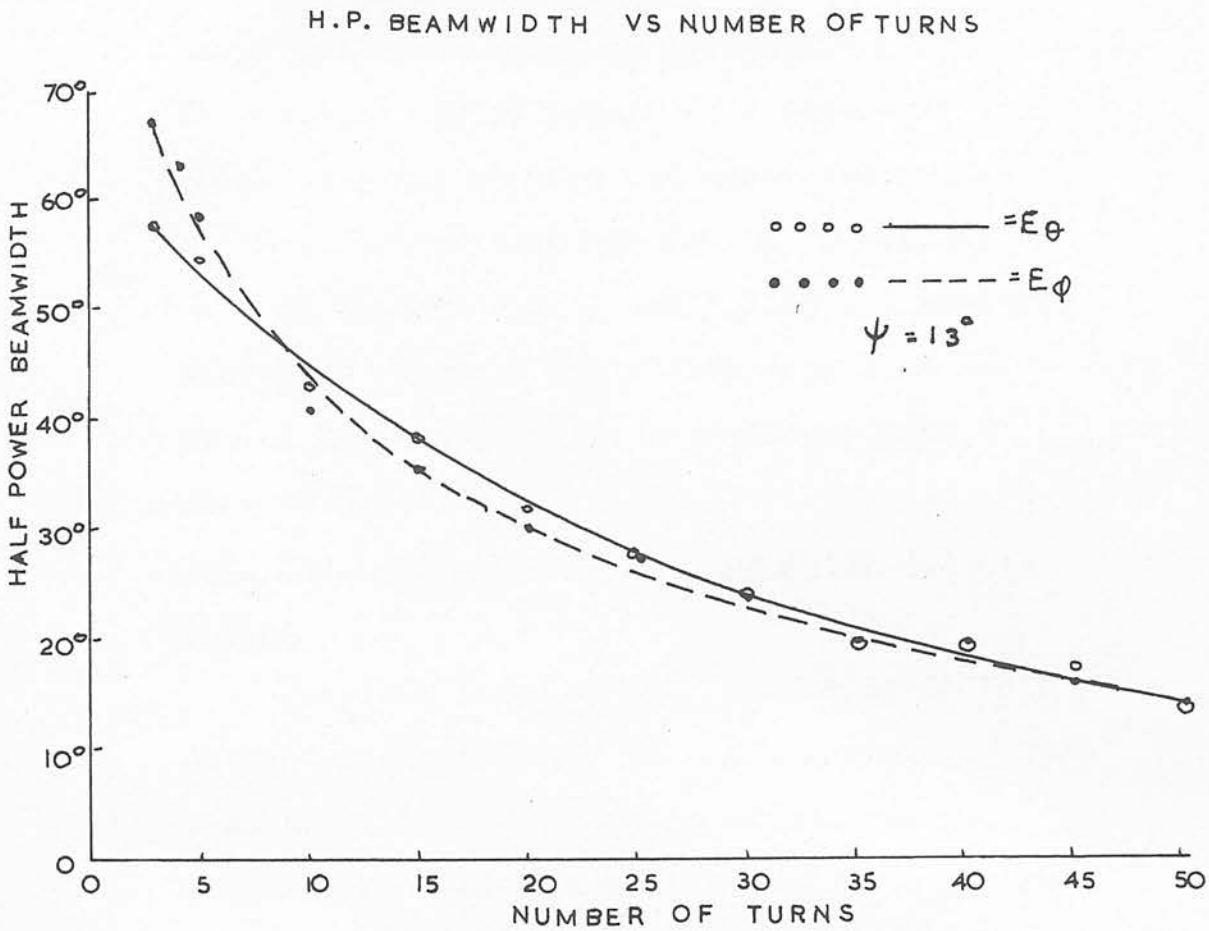

FIG 3.1.12

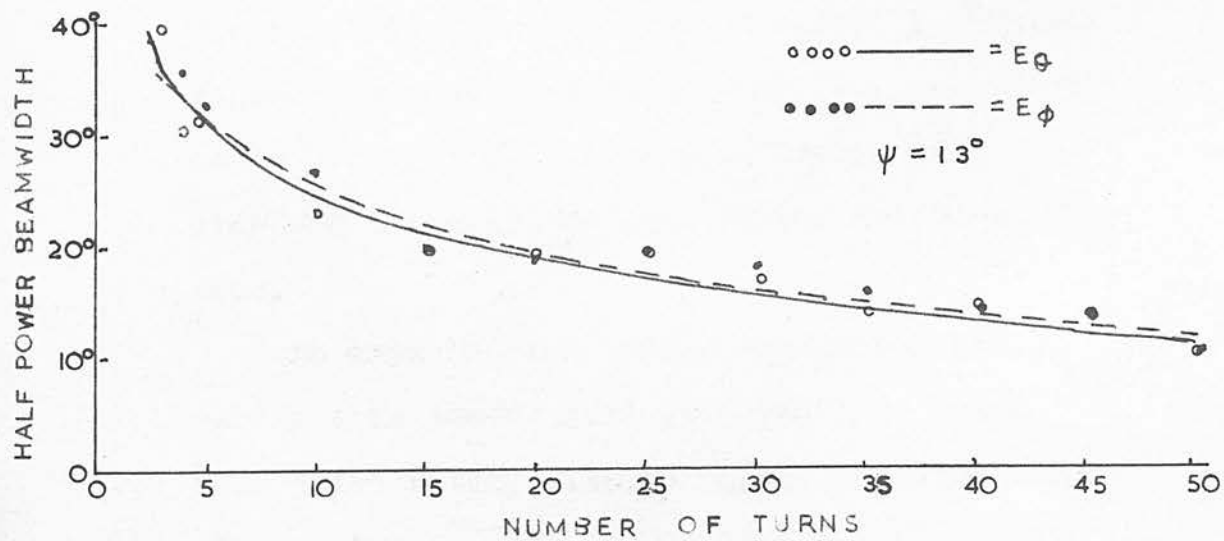

to the extreme upper bandwidth, the larger sidelobes are accompanied by a smaller half-power beamwidth which is plotted in Figure 3.1.12. This occurs as the result of a reduction in phase velocity so that the array factor is shifted further into the imaginary region.

In figures 3.1.13 and 3.1.14 the measured variation of axial ratio with length of the aerial is shown for the frequencies used in Figures 3.1.11 and 3.1.12.

3.2. The Bandwidth of a Narrow-Pitch Helical Aerial

Previous information[19] available on this subject indicated that at a pitch angle of less than about 5^{o} the bandwidth of the helical aerial decreased to zero. Examination of the approach used by the author suggested that not only was this an unlikely result, but that the frequency of operation of such a narrow-pitch aerial should be looked for at the lower end of the normal band and not at its centre. Specifically for a 181 turn helix of 1.8^{o} pitch angle, the upper frequency limit was estimated to be $0.87C_{\lambda}$, for the same criterion of sidelobe level as was used in the medium-pitch case.

An experimental model constructed to verify this theory gave good patterns and a good axial ratio, with an upper frequency limit of/

FIG 3.1.13

VOLTAGE AXIAL RATIO VS NUMBER OF TURNS

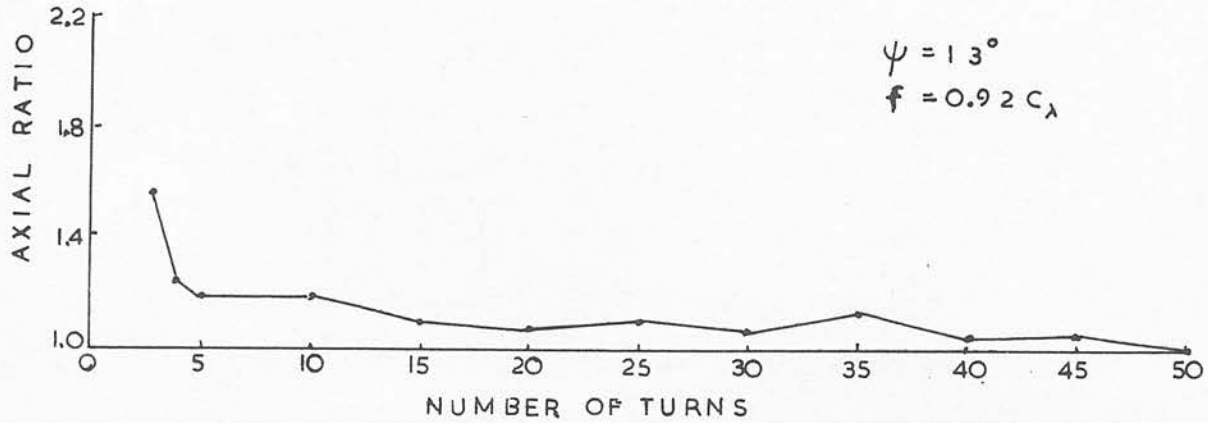

FIG 3.1.14

VOLTAGE AXIAL RATIO AT UPPER FREQUENCY LIMITS VS NUMBER OF TURNS

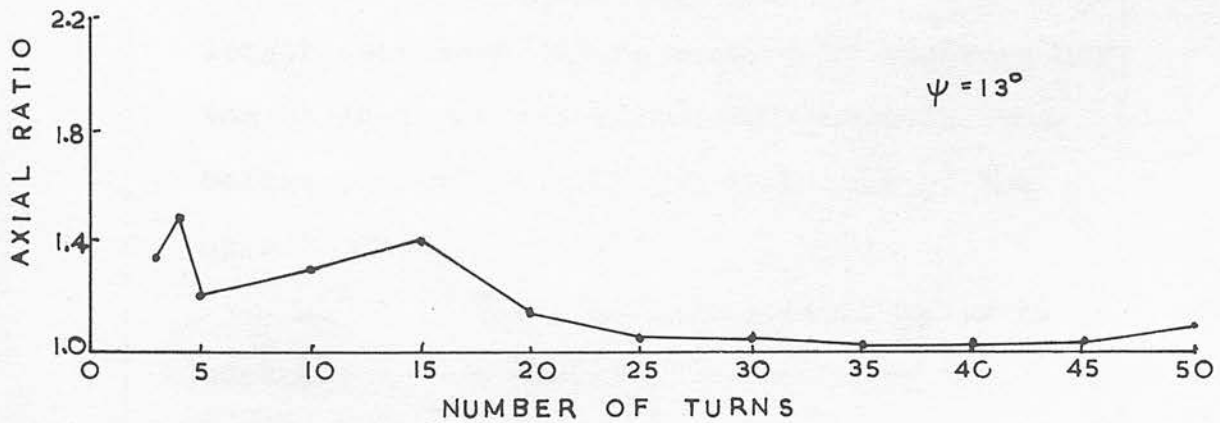

of about $0.81C_\lambda$, compared with $1.1C_\lambda$ for a 13° pitch helix of the same total length. Three of the patterns obtained are shown in Figure 3.2.1. It will be noted that the agreement with theory is of the same order as for the medium-pitch aerial, as far as the upper frequency limit is concerned.

It was found experimentally that the patterns obtained with helical aerials of length two wavelengths or less, were not in general very satisfactory. It appears that it may be more difficult to excite the surface wave on a short narrow-pitch helix than on a medium-pitch helix of the same length. This may be due to the axial phase velocity being less for $\psi = 1.8^\circ$ than for $\psi = 13^\circ$, so that a greater length of helix is necessary to bring about this reduction of velocity. Some evidence exists which suggests that the over-all length necessary may be reduced by starting off the helical winding with a medium-pitch turn before proceeding with the remainder of the narrow pitch.

No claim that the narrow pitch helix is superior to the medium-pitch helix in radiation pattern seems to be proper, nor is it expected that there will be any advantage in impedance characteristics. Nevertheless the elimination of this gap in the lower pitch-angle range is satisfying/

FIG 3.2.1

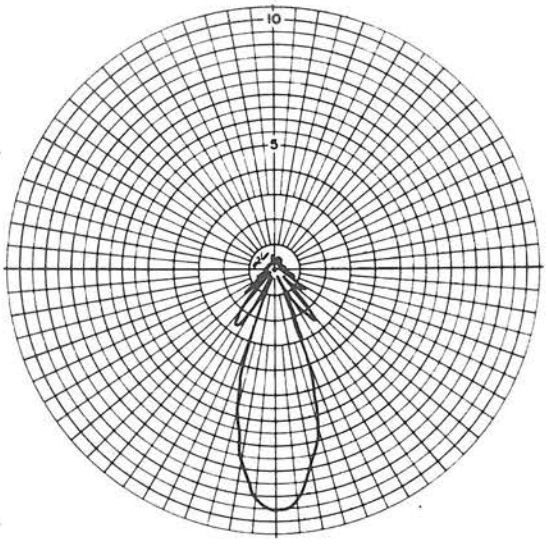

E_θ pattern for 181 turn,
1.8° helix; f=8 Kmc/s.

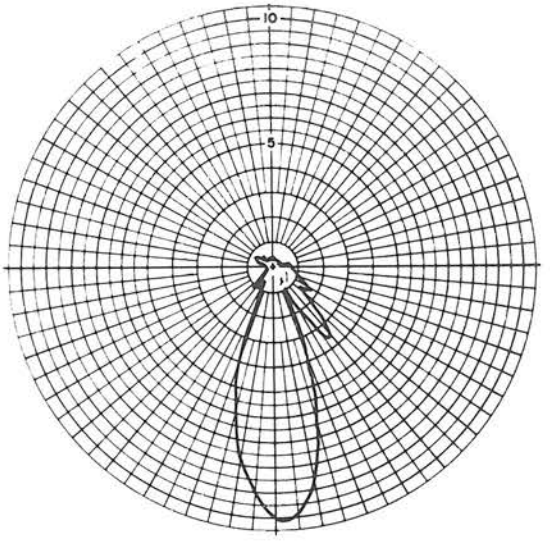

E_ϕ pattern for 181 turn,
1.8° helix; f=8 Kmc/s.

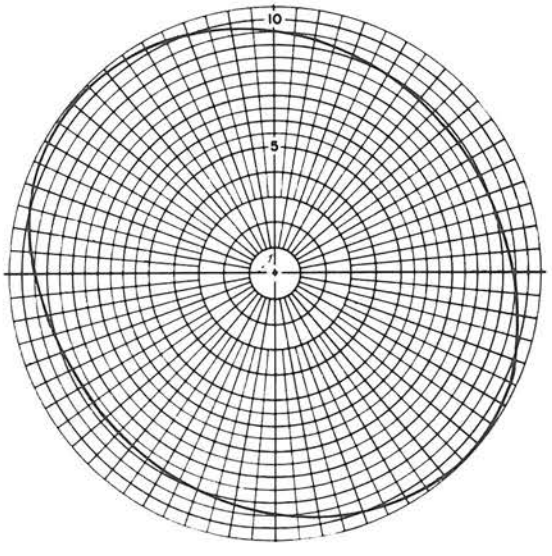

Polarization pattern for 181 turn,
1.8° helix, f = 8 Kmc/s.

satisfying, since from a theoretical viewpoint there was no valid reason for it to exist. It is now believed that a satisfactory pattern may be obtained for any pitch angle up to the value where the deterioration is due to the pattern of the array factor. This occurs at approximately 20^{o}.

3.3. Estimation of Bandwidth of Helical Aerial Using Approximate Graphical Solution.

The solution to the characteristic equation for the infinite helix with $\psi = 13^{o}$ has been given as curve (a) in Figures 3.1.2. and 3.1.3. An alternative way of presenting the same information is to show the solution on the same graph as the pass-band region, as illustrated in Figure 3.3.1 . This has an advantage in that it shows clearly the degree of approximation in an approximate graphical solution suggested by Sensiper[14] which takes the form of the two straight lines AB and BC. AB lies along the edge of the forbidden region m = -1, and BC is that portion of the line $\frac{ka}{\cot\psi} = \frac{\beta_0 a}{\cot\psi} \cdot \sin\psi$ that lies between the m = -1 and m = -2 forbidden regions.

It will be seen that the approximate graphical solution always gives a value of phase velocity along the axis of the aerial which is too high. Nevertheless it offers a quick method of estimating the upper frequency/

SOLUTIONS OF CHARACTERISTIC EQUATION FOP $\psi = 13^{\circ}$

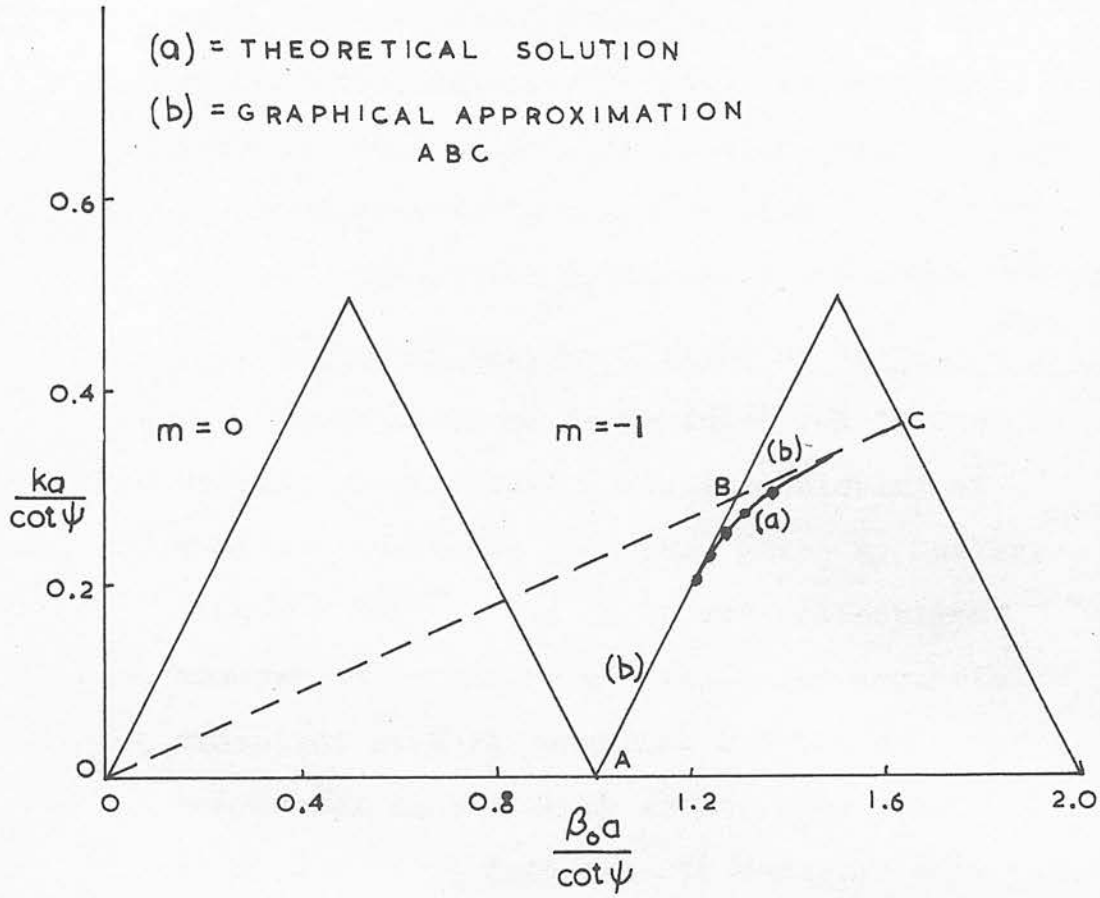

FIG 3.3.1

frequency limit along BC, the solution obtained being shown as curve (c) in Figure 3.1.4. along with the more exact computed value and the experimental value. It should be mentioned, perhaps, that this approximation involves only a few minutes work, compared with the several days of computation required by the other method.

3.4. Radiation Pattern Testing of Helical Aerial

The conditions to be fulfilled in the testing of microwave aerials consisting of vertical apertures have been given by Cutler, King and Kock[30]. As it is not self-evident however, that the requirements for accurate radiation pattern recording are the same for a horizontal linear array as for a vertical aperture, it is desirable to consider this case explicitly.

The distance requirements for a given small variation of phase across the 'aperture' of the aerial are of course the same. The effect of the ground reflected wave can be considered as follows:

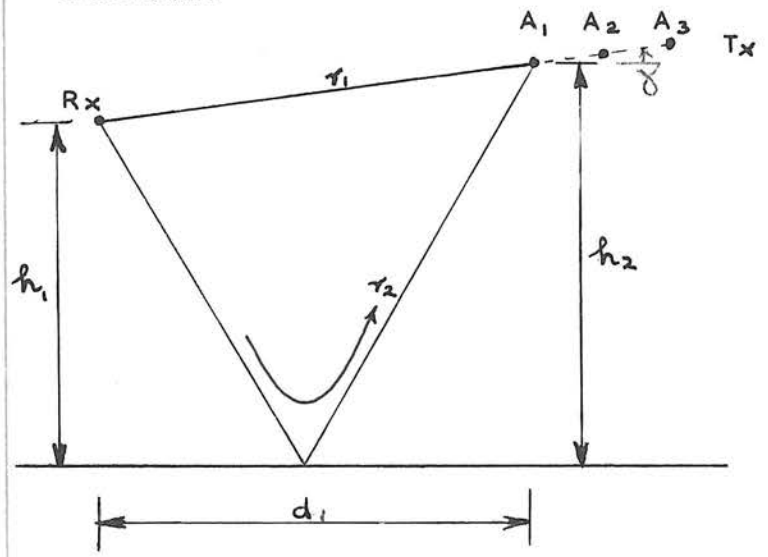

Fig. 3.4.1.

Let the aerial under test be considered the transmitting aerial, which will be assumed to consist of n isotropic sources A_1, A_2 ..... A_{n+1} in the form of a linear array. Let the spacing between these sources be d', and the heights above ground of the receiving and transmitting aerials be h_1 and h_m, $m \geq 2$. It will be assumed that the phase shift at the ground reflection is 180°. Assuming that the field at the receiving aerial due to the direct ray from source A_1 is E sin ωt, then the field due to the ground reflected ray can be written approximately as

$$E_r = E \sin\left(\omega t - 180^\circ - \frac{\beta 2 h_1 h_2}{d_1}\right) \quad -3.4.1$$

where β is the phase shift per unit length and d_1 is the ground distance between the receiving aerial and source A_1, as shown in Fig 3.4.1. The total field due to source A_1 is then

$$E_{t_1} = 2E \sin \frac{\beta h_1 h_2}{d_1} \sin\left(\omega t - 90^\circ - \frac{\beta h_1 h_2}{d_1}\right) \quad -3.4.2$$

Similarly if the field due to the direct ray from source A_2 is E sin $(\omega t - \psi)$ where

$$\psi = \beta d' \cos\phi - \alpha \quad -3.4.3$$

in the usual notation, then the field due to the ground reflected ray can be written approximately as

$$E_r = E \sin\left(\omega t - \psi - 180^\circ - \frac{\beta 2 h_1 h_3}{(d_1 + d' \cos\phi \cos\gamma)}\right) \quad -3.4.4$$

The total field due to source A_2 is thus

$$E_{t_2} = 2E \sin \frac{\beta h_1 h_3}{(d_1 + d' \cos\phi \cos\gamma)} \sin\left(\omega t - \psi - 90^\circ - \frac{\beta h_1 h_3}{d_1 + d' \cos\phi \cos\gamma}\right) \quad -3.4.5$$

If $d' \cos\phi \cos\gamma \ll d_1$, this can be written as

and $(h_3 - h_2) \ll \lambda$

$$E_{t_2} \simeq 2E \sin\frac{\beta h_1 h_2}{d_1} \sin\left(\omega t - \psi - 90^\circ - \frac{\beta h_1 h_2}{d_1}\right) \quad \text{--- 3.4.6}$$

Hence to this approximation E_{t_1} and E_{t_2} are equal in magnitude and separated in phase by the same angle ψ which is the phase difference between the direct rays. Consequently the radiation pattern for the two sources A_1 and A_2 as a function of ϕ is the same for the total fields as it is for the direct rays. The presence of ground reflections therefore does not cause error in the radiation pattern. This result may readily be extended to include all n sources, provided

$$\left.\begin{aligned} nd' \cos\phi\cos\gamma &\ll d_1 \\ \text{and } h_{n+1} - h_2 &\ll \lambda \end{aligned}\right\} \qquad 3.4.7.$$

It will be noted that the variation of field strength with height for any source, due to the interference between direct and ground reflected rays, is of the form $\sin\frac{\beta h_1 h_n}{d_1}$. Since in its operation as a receiving aerial the height will normally be adjusted for maximum signal, corresponding to $\frac{\beta h_1 h_n}{d_1}$ equal to $(2n+1)\frac{\pi}{2}$, n = 0, 1, 2, ..., it is worthwhile noting that if the height is optimum in this sense for element A_1, it will also be optimum for all the elements A_2, A_3 .....A_n provided

$$\left.\begin{aligned} 2nd'\cos\gamma &\ll d_1 \\ \text{and } 2(h_{n+1} - h_2) &\ll \lambda \end{aligned}\right\} \qquad 3.4.8.$$

The factor 2 arises since the aerial will normally rotate about its ground plane for the end-fire helix, making the total length of operation in a radiation pattern test equal to 2nd'.

Care/

Care has to be taken in the testing of the helical aerial when the second aerial used in the radiation pattern test is fed by means of a coaxial cable. If this is the case it is essential to make use of a balance-to-balance converting device to prevent currents from flowing on the outside of the coaxial cable. If these are allowed to flow then either the E_θ or the E_φ pattern will be a combination of the two patterns, and the axial ratio measurement will also be in error.

3.5. Input Impedance of Helical Aerial

The viewpoint adopted by the author in this study of the helical aerial is that the only characteristic of this type of aerial per se is its radiation pattern. The impedance is not a characteristic of the aerial but of the particular means adopted for launching the wave along it. The same argument applies likewise to all end-fire travelling wave aerials such as the Yagi-Uda aerial or the dielectric rod aerial, in so far as reflection from the far end does not reach as far back as the feed point.

In the case of the Yagi-Uda aerial the impedance is normally taken to be that associated with a dipole-plus-reflector type of launching device, but it must be understood that this is only a convention. The essential feature of the Yagi-Uda aerial is its array of director elements,

and/

and these may be equally well excited by a waveguide as by a dipole-plus-reflector launching device.

Similarly, the impedance of a helical aerial is generally understood to be that associated with a plane reflector type of launching mechanism. This,however, is surely not the only way in which the desired surface wave can be launched, though it is a very good one. It is of course true that there is a unique impedance associated with the forward travelling wave on a helical aerial, but it is quite wrong to confuse this, as has been done by Watkins[21], with the input impedance of the aerial. This will be discussed in the next section.

3.5.1. Impedance of Simple Tape Helix

It is necessary to calculate the average power Wav in the forward travelling wave along the helix[21,14]

$$W_{av} = \tfrac{1}{2} Re \int_0^{\infty} \int_0^{2\pi} \left(E_r H_\theta^{\times} - E_\theta H_r^{\times} \right) r \, d\theta \, dr \quad -- 3.5.1$$

$$= \tfrac{1}{2} Re \sum_{m,n} \int_0^{\infty} \int_0^{2\pi} \left(E_{rm} H_{\theta n}^{\times} - E_{\theta m} H_{rn}^{\times} \right) r \, d\theta \, dr \quad -- 3.5.2$$

For $m \neq n$, $\int_0^{2\pi} E_{rm} H_{\theta r}^{\times} \, d\theta = 0$ -- 3.5.3

so that Equation 3.5.2. becomes

$$W_{av} = \tfrac{1}{2} Re \sum_m \int_0^{\infty} \left(E_{rm} H_{\theta m}^{\times} - E_{\theta m} H_{rm}^{\times} \right) 2\pi r \, dr \quad -- 3.5.4$$

From the modified forms of Equations 1.14 to 1.21. which are applicable to the tape helix, and from Equations 2.29 and 2.30 which express the constants A_m and B_m in terms of the surface current density, there/

there follows after some simplification,

$$E^{i}_{rm} = -\frac{\omega\mu a \sin\psi}{\gamma_m a}\left[\frac{\beta_m a}{k^2 a^2} K_m(\gamma_m a)(\gamma_m^2 a^2 - m\beta_m a \cot\psi) I_m'(\gamma_m r) - \frac{ma}{r}\cot\psi\left[K_m'(\gamma_m a) I_m(\gamma_m r)\right]\right] j_{11m} \quad -3.5.5$$

$$E^{i}_{\theta m} = j\omega\mu a \sin\psi\left[-\frac{m\beta_m a^2}{r}\frac{(\gamma_m^2 a^2 - m\beta_m a\cot\psi)}{\gamma_m^2 a^2 - k^2 a^2} K_m(\gamma_m a) I_m(\gamma_m r) + K_m'(\gamma_m a)\cot\psi\, I_m'(\gamma_m r)\right] j_{11m} \quad -3.5.6$$

$$H^{i}_{\theta m} = -\frac{\sin\psi}{\gamma_m a}\left[(\gamma_m^2 a^2 - m\beta_m a\cot\psi) K_m(\gamma_m a) I_m'(\gamma_m r) - \frac{m\beta_m a^2}{r}\cot\psi\, K_m'(\gamma_m a) I_m(\gamma_m r)\right] j_{11m} \quad -3.5.7$$

$$H^{i}_{rm} = \left[\frac{j\gamma_m a}{r}(\gamma_m^2 a^2 - m\beta_m a\cot\psi)\frac{K_m(\gamma_m a)}{\gamma_m^2 a^2} I_m(\gamma_m r) - j\beta_m a\cot\psi\, K_m'(\gamma_m a) I_m'(\gamma_m r)\right]\sin\psi\, j_{11m} \quad -3.5.8$$

The expressions for E^{e}_{rm}, $E^{e}_{\theta m}$, $H^{e}_{\theta m}$ and H^{e}_{rm} are identical with Equations 3.5.5. to 3.5.8. with the modified Bessel Functions I_m and K_m interchanged. Re-writing Equation 3.5.4. in terms of the internal and external regions of the helix there results

$$W_{av} = \tfrac{1}{2} Re \sum_m \left[\int_0^a \left(E^{i}_{rm} H^{i\times}_{\theta m} - E^{i}_{\theta m} H^{i\times}_{rm}\right) + \int_a^\infty \left(E^{e}_{rm} H^{e\times}_{\theta m} - E^{e}_{\theta m} H^{e\times}_{rm}\right)\right] 2\pi r\, dr \quad -3.5.9$$

Performing the necessary integrations with respect to r gives finally [14]

$$W_{av} = \frac{\pi a^2 \sin^2\psi}{\omega\varepsilon a}\sum_m I_m(\gamma_m a) K_m(\gamma_m a)\left[\beta_m a\left\{\frac{q_m^2}{\gamma_m^3 a^3}\left[\tfrac{1}{2}\left(\frac{I_m'(\gamma_m a)}{I_m(\gamma_m a)} + \frac{K_m'(\gamma_m a)}{K_m(\gamma_m a)}\right) + \frac{1}{\gamma_m a}\right] + \frac{k^2 a^2 \cot^2\psi}{\gamma_m a}\left[-\frac{1}{\gamma_m a}\frac{K_m'(\gamma_m a) I_m'(\gamma_m a)}{K_m(\gamma_m a) I_m(\gamma_m a)} + \tfrac{1}{2}\left(1 + \frac{m^2}{\gamma_m^2 a^2}\right)\left(\frac{I_m'(\gamma_m a)}{I_m(\gamma_m a)} + \frac{K_m'(\gamma_m a)}{K_m(\gamma_m a)}\right)\right]\right\} + \frac{m q_m \cot\psi}{\gamma_m^4 a^4}\left(\beta_m^2 a^2 + k^2 a^2\right)\right]\left|j_{11m}\right|^2 \quad -3.5.10$$

where

$$q_m = \gamma_m^2 a^2 - m\beta_m a \cot\psi$$

Since it is the -1 space harmonic/axially which is responsible for the end-fire helical aerial operation, and since the ratio of the power carried by this harmonic to the power carried by any other harmonic approaches infinity[21] when it is so operating, the above equation may be re-written as

$$W_{av\,-1} \simeq \frac{\pi a^2 \sin^2\psi}{\omega\varepsilon a} I_{-1}(\gamma_{-1}a) K_{-1}(\gamma_{-1}a)\Bigg[\beta_{-1}a\Bigg\{\frac{q_{-1}^2}{\gamma_{-1}^3 a^3}\Bigg[\frac{1}{2}\Big(\frac{I_{-1}'(\gamma_{-1}a)}{I_{-1}(\gamma_{-1}a)} + \frac{K_{-1}'(\gamma_{-1}a)}{K_{-1}(\gamma_{-1}a)}\Big) + \frac{1}{\gamma_{-1}a}\Bigg] + \frac{k^2 a^2 \cot^2\psi}{\gamma_{-1}a}\Bigg[-\frac{1}{\gamma_{-1}a}\frac{K_{-1}'(\gamma_{-1}a) I_{-1}'(\gamma_{-1}a)}{K_{-1}(\gamma_{-1}a) I_{-1}(\gamma_{-1}a)} + \frac{1}{2}\Big(1 + \frac{1}{\gamma_{-1}^2 a^2}\Big)\Big(\frac{I_{-1}'(\gamma_{-1}a)}{I_{-1}(\gamma_{-1}a)} + \frac{K_{-1}'(\gamma_{-1}a)}{K_{-1}(\gamma_{-1}a)}\Big)\Bigg]\Bigg\} + \Bigg[-\frac{q_{-1}\cot\psi}{\gamma_{-1}^4 a^4}\Big(\beta_{-1}^2 a^2 + k^2 a^2\Big)\Bigg]\Bigg]\Big|j_{11-1}\Big|^2 \quad -- \quad 3.5.11$$

Substituting for the total current I along the helical tape, and using the numerical values previously obtained in Section 3.1., the curve for input resistance as a function of C_λ is finally obtained as shown in Fig. 3.5.1.

It is immediately evident as might have been predicted that these calculated values are quite different from the measured values[5,19] of input impedance for the helical aerial. The measured values must necessarily be dependent on the proximity of the ground plane to the first turn of the helix, and the correct approach if theoretical/

INPUT IMPEDANCE OF FORWARD TRAVELLING WAVE.

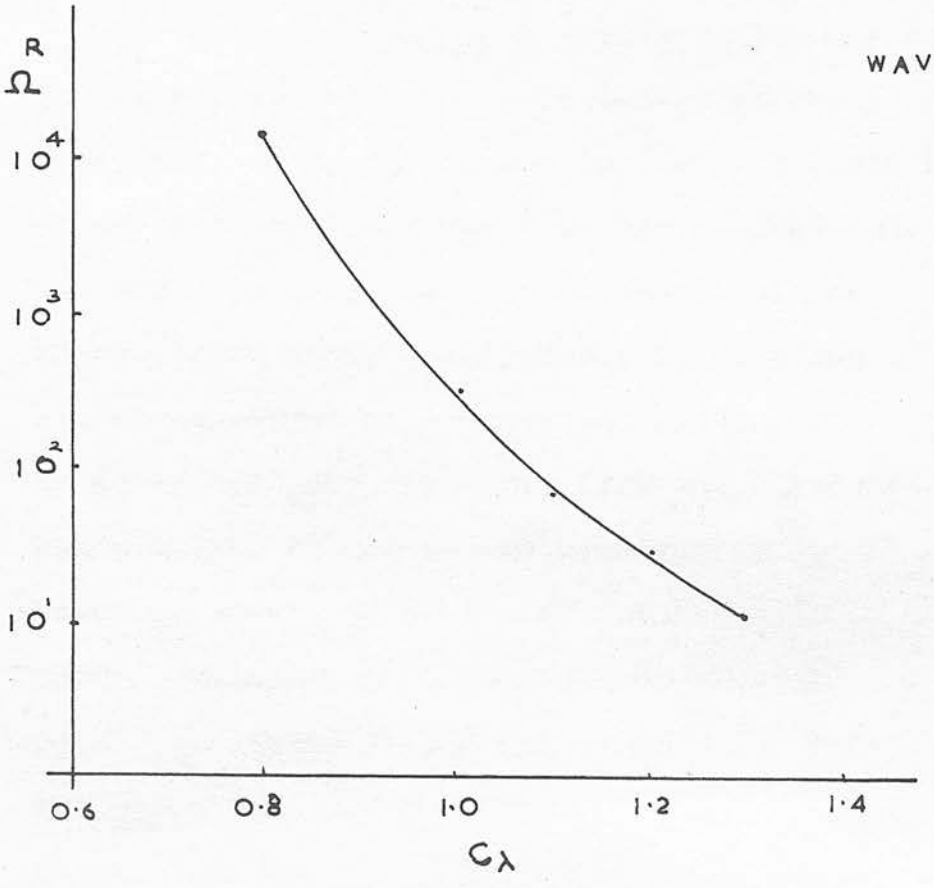

FIG 3.5.1

theoretical results are desired would seem to be that used by Schelkunoff.

Nevertheless although the waveguide approach is not suitable for the calculation of input impedance, it does indicate that at the lower end of the pattern bandwidth when the desired mode has begun to propagate, the input impedance changes from being highly reactive to being almost non-reactive. Hence the pattern bandwidth is not completely separable from the impedance bandwidth as is maintained by Reynolds[32]. However, at the upper end of the aerial's useful frequency band they are completely separate. There the pattern breaks up because the phase velocity along the conductor does not increase sufficiently rapidly with frequency, while the input impedance shows no marked change because the travelling wave continues to be propagated until the influence of a new mode becomes marked at a much higher frequency.

3.6. Effect of Ground Plane on Radiation Pattern

In all the theoretical work which has been carried out on radiation from helical aerials [19,39,40] it has been assumed that the effect of the ground plane on the radiation pattern is negligible. Since the backward radiation from the helical conductor is small it is of course plausible to assume that the currents flowing in the ground plane are likewise small, and that there is therefore justification for this simplification. The following approximate analysis was undertaken when experiments showed that under either of the two following conditions

(a) the ground plane consisted of radial conductors only

(b) the ground plane diameter was many wavelengths,

the radiation pattern was profoundly affected.

Referring to Figure 3.6.1., a travelling wave of current of constant amplitude is assumed to flow,

$$I = I_o e^{-j\beta s} \qquad 3.6.1.$$

where s is the distance measured along the conductor.

Since the phase constant β along the conductor is related to the free space phase constant k by a reduction factor p, and s is proportional to the angle u and the length of 1 turn L, this equation may be written

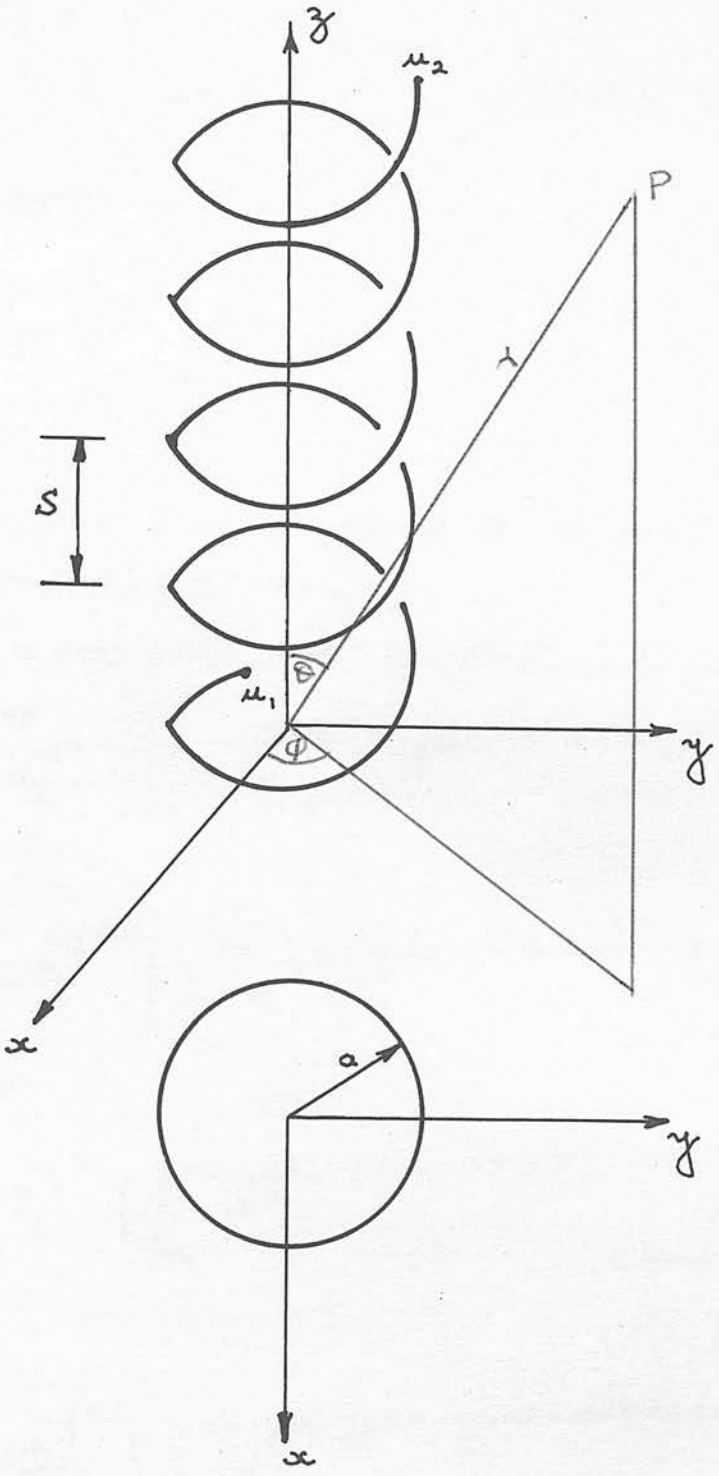

FIG 3.6.1 CO-ORDINATE SYSTEMS FOR HELIX

$$I = I_0 e^{-j\frac{k}{h}\frac{u}{2\pi}L} \quad -- \quad 3.6.2$$

Also referring to Figure 3.6.1.

$$x_1 = a\cos u \quad -- \quad 3.6.3$$

$$y_1 = a\sin u \quad -- \quad 3.6.4$$

$$z_1 = \frac{u}{2\pi} S \quad -- \quad 3.6.5$$

where the subscript 1 refers to the physical helix, of which S is the pitch.

The x component of vector potential is defined as

$$A_{x_1} = \frac{\mu_0}{4\pi}\frac{e^{-jkR}}{R}\iiint J_x(x,y,z)\, e^{+jk[x_1\cos\phi\sin\theta + y_1\sin\phi\sin\theta + z_1\cos\theta]}\, dx\,dy\,dz \quad -- \quad 3.6.6.$$

i.e.

$$A_{x_1} = \frac{\mu_0 I_0}{4\pi}\frac{e^{-jkR}}{R}\left[\int_{u_1}^{u_2} e^{-jk\left[\frac{L}{2\pi}hu - a\cos u\sin\theta\cos\phi - a\sin u\sin\phi\sin\theta - \frac{S}{2\pi}u\cos\theta\right]} \times(-a\sin u)\,du\right] \quad -- \quad 3.6.7$$

Similarly

$$A_{y_1} = \frac{\mu_0 I_0}{4\pi}\frac{e^{-jkR}}{R}\left[\int_{u_1}^{u_2} e^{-jk\left[\frac{L}{2\pi}hu - a\cos u\sin\theta\cos\phi - a\sin u\sin\phi\sin\theta - \frac{S}{2\pi}u\cos\theta\right]} \times(a\cos u)\,du\right] \quad -- \quad 3.6.8$$

and

$$A_{z_1} = \frac{\mu_0 I_0}{4\pi}\frac{e^{-jkR}}{R}\left[\int_{u_1}^{u_2} e^{-jk\left[\frac{L}{2\pi}hu - a\cos u\sin\theta\cos\phi - a\sin u\sin\phi\sin\theta - \frac{S}{2\pi}\cos\theta\right]} \times\frac{S}{2\pi}\,du\right] \quad -- \quad 3.6.9$$

Let

$$\frac{\mu_0 I_0 a}{4\pi} = K \quad ; \quad z = ka\sin\theta \quad ; \quad H_1 = \frac{k}{2\pi}\left(\frac{L}{h} - S\cos\theta\right) \quad -- \quad 3.6.10\ (a),(b),(c)$$

Then expanding in Bessel Function form and simplifying

$$A_{x_1} \propto \left\{ \sum_{n=0}^{\infty} (2-\delta_{0n})(j)^n J_n(z) \left[e^{-j n\phi} \left(\frac{e^{-j(H_1+1-n)u}}{H_1+1-n} - \frac{e^{-j(H_1-1-n)u}}{H_1-1-n} \right) \right.\right.$$

$$\left.\left. + e^{+j n\phi} \left(\frac{e^{-j(H_1+1+n)u}}{H_1+1+n} - \frac{e^{-j(H_1-1+n)}}{H_1-1+n} \right) \right]_{u_1}^{u_2} \right\}$$

where δ_{0n} is the Kronecker Delta — — — — 3.6.11

Similarly

$$A_{y_1} \propto \left\{ \sum_{n=0}^{\infty} (2-\delta_{0n})(j)^{n+1} J_n(z) \left[e^{-j n\phi} \left(\frac{e^{-j(H_1+1-n)u}}{H_1+1-n} + \frac{e^{-j(H_1-1-n)u}}{H_1-1-n} \right) \right.\right.$$

$$\left.\left. + e^{+j n\phi} \left(\frac{e^{-j(H_1+1+n)u}}{H_1+1+n} + \frac{e^{-j(H_1-1+n)u}}{H_1-1+n} \right) \right]_{u_1}^{u_2} \right\}$$

— — — — 3.6.12

and

$$A_{z_1} \propto \left\{ \sum_{n=0}^{\infty} (2-\delta_{0n})(j)^{n+1} J_n(z) \left[e^{-j n\phi} \frac{e^{-j(H_1-n)u}}{H_1-n} \right.\right.$$

$$\left.\left. + e^{+j n\phi} \frac{e^{-j(H_1+n)u}}{H_1+n} \right]_{u_1}^{u_2} \right\} \text{ — — } 3.6.13$$

For the image helix

$$I = -I_0 e^{j\beta s \cos 2\psi} \quad \text{— —} \quad 3.6.14$$

Re-writing this in the same way as for the original helix gives

$$I = -I_0 e^{j \frac{\beta}{\pi} \frac{u}{2\pi} L \cos 2\psi} \quad \text{— —} \quad 3.6.15$$

Since further

$$x_2 = a \cos u \quad \text{— —} \quad 3.6.16$$

$$y_2 = a \sin u \quad \text{— —} \quad 3.6.17$$

$$z_2 = -\frac{u}{2\pi} S \quad \text{— —} \quad 3.6.18$$

where the subscript 2 refers to the image helix, then

$$A_{x2} = \frac{-\mu_0 I_0}{4\pi} \frac{e^{-j\beta R}}{R} \left[\int_{u_1}^{u_2} e^{-j\beta \left[-\frac{L}{h} \frac{\cos 2\psi}{2\pi} \cdot u - a\cos u \sin\theta \cos\phi - a \sin u \sin\phi \sin\theta + \frac{S}{2\pi} u \cos\theta \right]} \times (-a \sin u)\, du \right] \quad - - - \quad 3.6.19$$

Similar expressions hold for A_{y2} and A_{z2}
Using Equations 3.6.10 (a) and (b) and further defining

$$H_2 = \frac{\beta}{2\pi} \left(\frac{L}{h} \cos 2\psi - S \cos\theta \right) \quad - - \quad 3.6.20$$

gives

$$A_{x2} \propto - \left\{ \sum_{n=0}^{\infty} (2 - \delta_{0n}) (j)^n J_n(z) \left[e^{-j n\phi} \left(\frac{e^{-j(-H_2+1-n)u}}{-H_2+1-n} - \frac{e^{-j(-H_2-1-n)u}}{-H_2-1-n} \right) + e^{j n\phi} \left(\frac{e^{-j(-H_2+1+n)u}}{-H_2+1+n} - \frac{e^{-j(-H_2-1+n)u}}{-H_2-1+n} \right) \right]_{u_1}^{u_2} \right\}$$

$$- - - \quad 3.6.21$$

It is possible to simplify the analysis at this stage by restricting it to the case where ψ is a small angle, so that $\cos 2\psi \simeq 1$. The other extreme case where $\psi \simeq 90^\circ$ is of no interest since in this case the helix approaches a straight wire, for which it is known there is no axial radiation.

Using this approximation makes H_1 equal to H_2. Then for an integral number of turns with $u_2 = -u$, $= N\pi$, where N = 1,2,3 ....., Equations 3.6.7.- 9 become for H = 1

$$A_{x_1} \propto (j)\, N\Pi\, e^{-j\phi}\left[J_2(z)\, e^{-j\phi} + J_0(z)\, e^{j\phi}\right] \quad -- 3.6.22$$

$$A_{y_1} \propto (j)^2\, N\Pi\, e^{-j\phi}\left[J_2(z)\, e^{-j\phi} - J_0(z)\, e^{j\phi}\right] \quad -- 3.6.23$$

$$A_{z_1} \propto (j)\, \frac{NS}{a}\, e^{-j\phi}\, J_1(z) \quad -- 3.6.24$$

Similarly Equation 3.6.21 becomes

$$A_{x_2} \propto (-j)\, N\Pi\, e^{-j\phi}\left[J_0(z)\, e^{j\phi} + J_2(z)\, e^{-j\phi}\right] \quad -- 3.6.25$$

$$= -A_{x_1} \quad -- 3.6.26$$

Also

$$A_{y_2} = -A_{y_1} \quad -- 3.6.27$$

$$A_{z_2} = +A_{z_1} \quad -- 3.6.28$$

From the rectangular components of vector potential the magnetic field components H_r, H_θ and H_ϕ in the radiation field may be derived, since

$$H_r = \frac{1}{R\sin\theta}\left[\frac{\partial}{\partial\theta}(A_\phi \sin\theta) - \frac{\partial A_\theta}{\partial\phi}\right] \quad -- 3.6.29$$

$$H_\theta = \frac{1}{R}\left[\frac{1}{\sin\theta}\frac{\partial A_r}{\partial\phi} - \frac{\partial}{\partial R}(R A_\phi)\right] \quad -- 3.6.30$$

$$H_\phi = \frac{1}{R}\left[\frac{\partial}{\partial R}(R A_\theta) - \frac{\partial A_r}{\partial\theta}\right] \quad -- 3.6.31$$

where

$$A_r = A_x \sin\theta\cos\phi + A_y \sin\theta\sin\phi + A_z\cos\theta \quad -- 3.6.32$$

$$A_\theta = A_x \cos\theta\cos\phi + A_y \cos\theta\sin\phi - A_z\sin\theta \quad -- 3.6.33$$

$$A_\phi = -A_x \sin\phi + A_y\cos\phi \quad -- 3.6.34$$

Carrying through the algebra gives

$$\left.\begin{aligned} H_{r\,total} &= 2H_{r_1} \\ H_{\theta\,total} &= 0 \\ H_{\phi\,total} &= 2H_{\phi_1} \end{aligned}\right\} \quad \text{at } \theta = \pm 90^\circ \quad -- 3.6.35$$

Hence

$$i_r = K\,\frac{2}{R}\,e^{-j\beta R}\,\frac{\sqrt{N}}{a}\,J_1(z)\,e^{-j\varphi}\left(-k-\frac{1}{R}\right) \quad --3.6.36$$

$$i_\varphi = K\,2\,\frac{e^{-j\beta R}}{R^2}\,\frac{\sqrt{N}}{a}\,J_1(z)\,e^{-j\varphi} \quad --3.6.37$$

This analysis shows the presence of both circumferential and radial currents far out in the plane of the ground screen, and it is reasonable to presume that these will also flow close in to the helix. The assumption has been made of a travelling wave of current on the aerial, and if the ground screen does not permit the flow of circumferential currents, it would appear that subject to the approximation $\cos 2\psi \simeq 1$ the travelling wave cannot be supported.

Although this approximation appears to the author to be a very severe one, it is interesting that experiment supports the deduction that no travelling wave is launched when the ground plane consists of radial conductors alone. Figures 3.6.2. and 3.6.3. show the E_θ and E_φ radiation patterns for this case. These are in approximate accordance with the patterns for a circular loop of the same dimensions, carrying a standing wave of current[41].

When the ground plane allows both radial and circumferential currents to flow, then because of the phase factor $e^{-j\varphi}$ these must flow in the same sense at diametrically opposite points.

E_θ PATTERN FOR $3\frac{1}{4}$ TURN HELIX WITH 4 RADIAL WIRE GROUND SCREEN

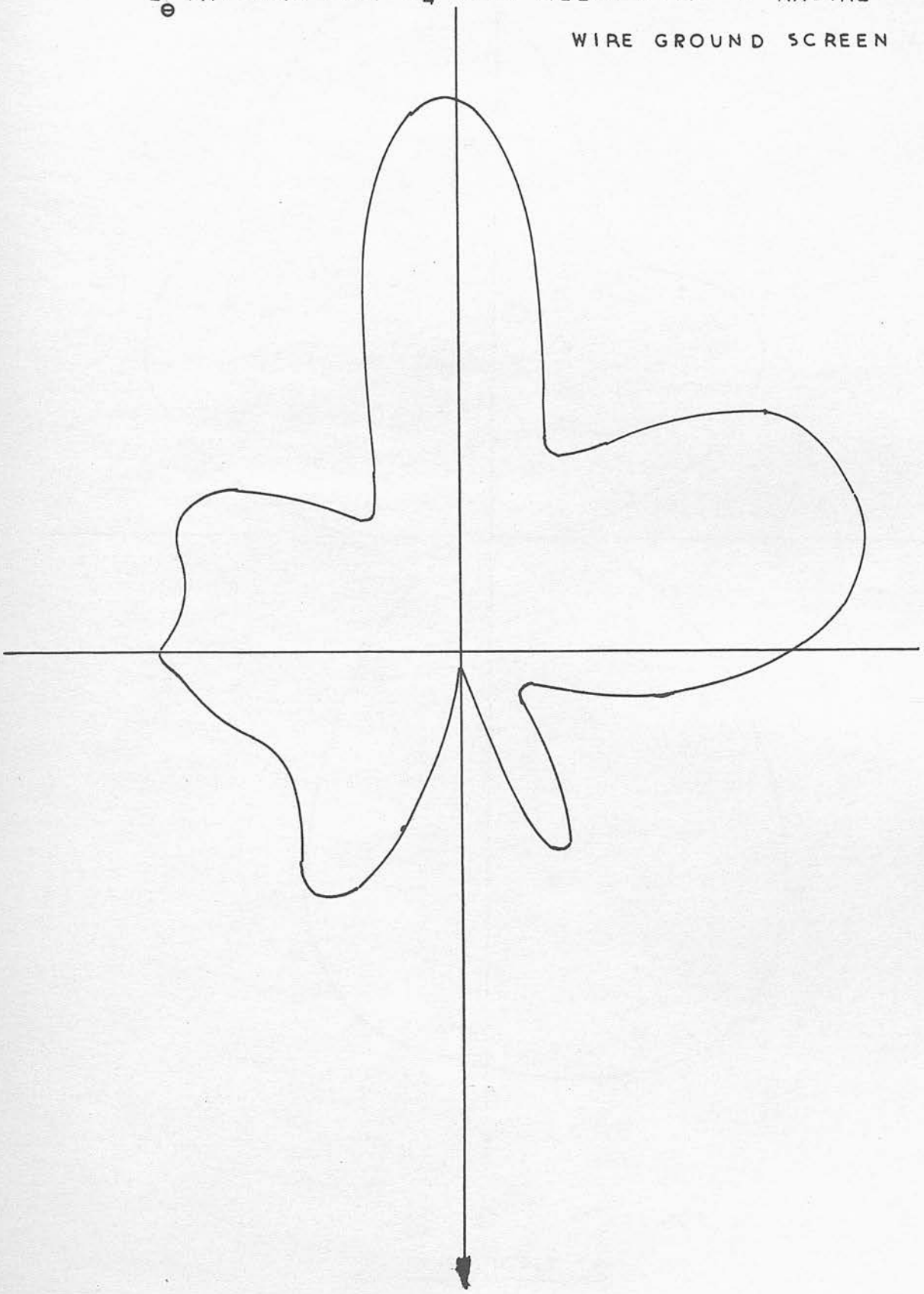

FIG 3.6.2

E_ϕ PATTERN FOR $3\frac{1}{4}$ TURN HELIX WITH 4 RADIAL WIRE GROUND SCREEN

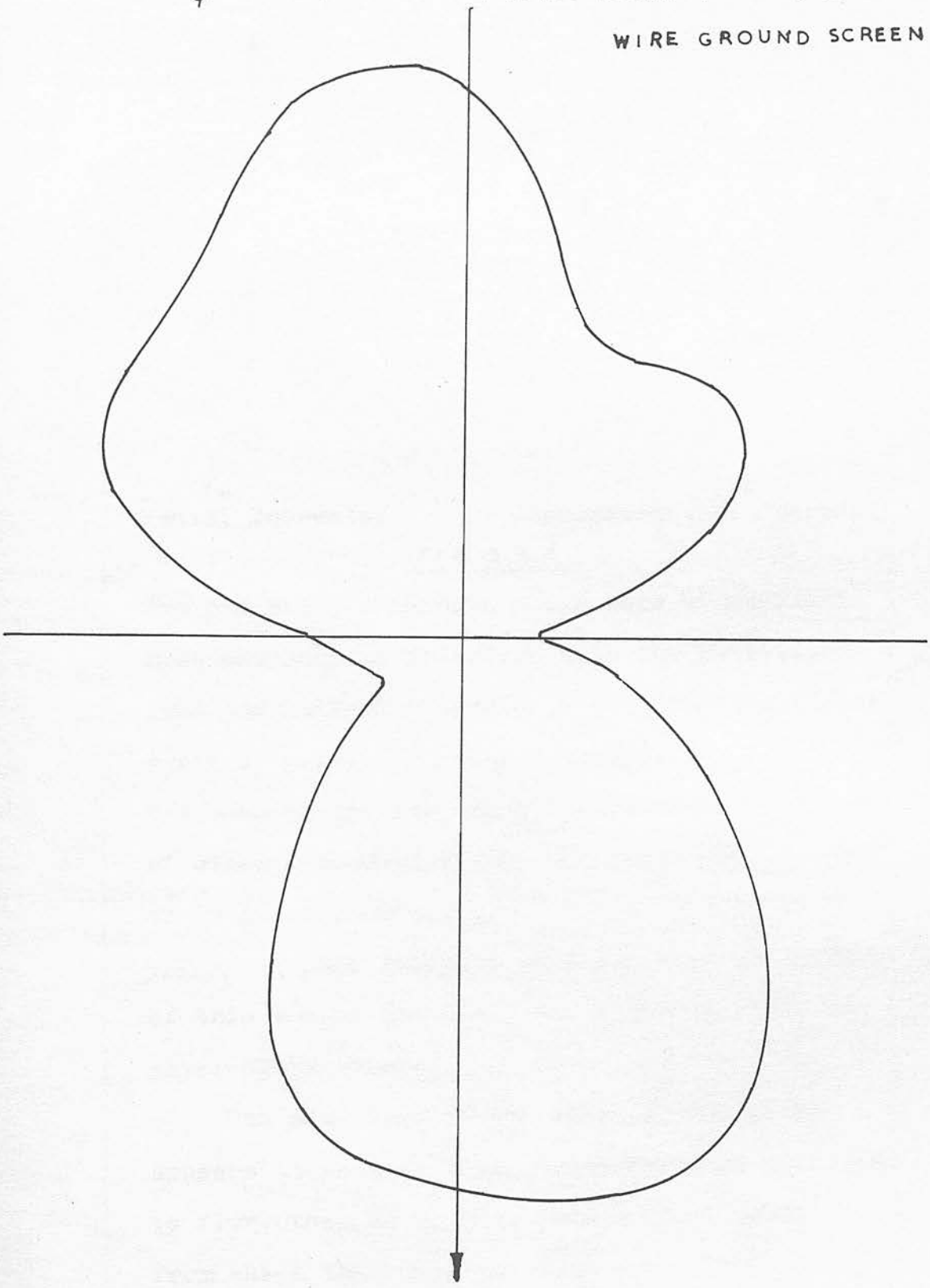

FIG 3.6.3

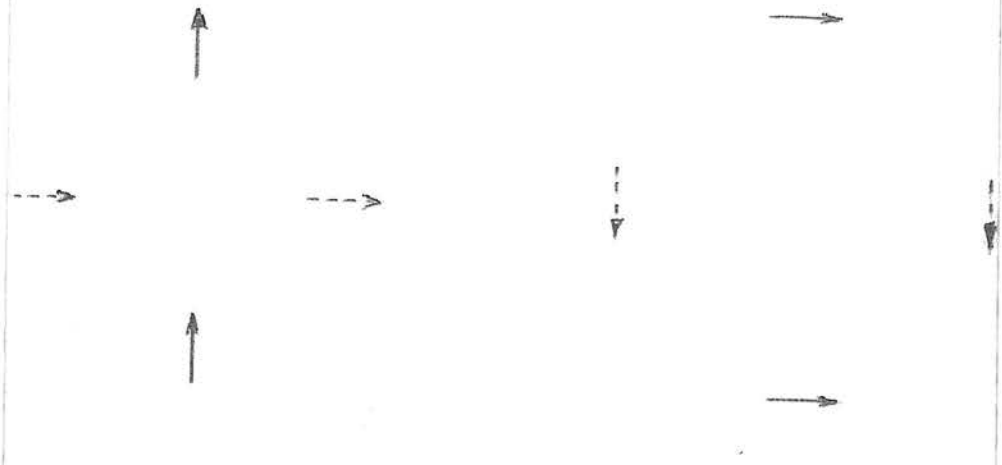

(a) Radial Currents

(b) Circumferential Currents

FIG 3.6.4

The radiation from both these sets of currents must necessarily interfere with the radiation from the helical conductor along the axis of the aerial. But it is clear that while at some frequencies the two radiations will be in phase, at other frequencies they may be in anti-phase, or in phase quadrature. Figures 3.6.5. to 3.6.7. are included to illustrate the effect of this vector addition, for a ground plane 10 wavelengths square.

The advantage of the small ground plane appears to be that while these currents continue to flow, they do so only over a small area, from which the radiation does not affect the field due to the helical conductor. Figure 3.6.8. shows for comparison a field pattern for and identical helix with a ground plane 1 wavelength square.

FIG 3.6.5

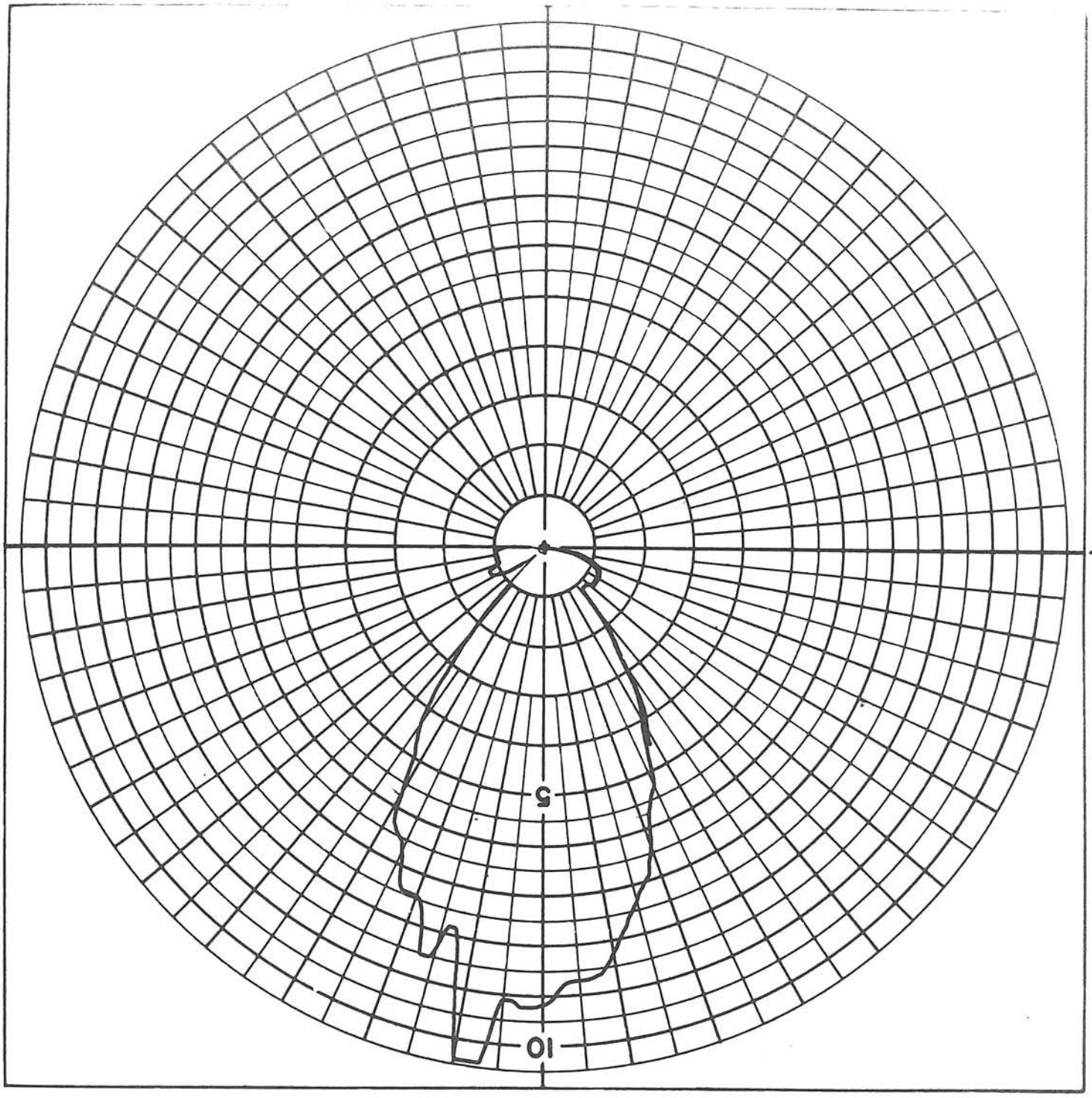

PATTERN I FOR $7\frac{1}{2}$ TURN HELIX WITH LARGE GROUND PLANE

FIG 3.6.6

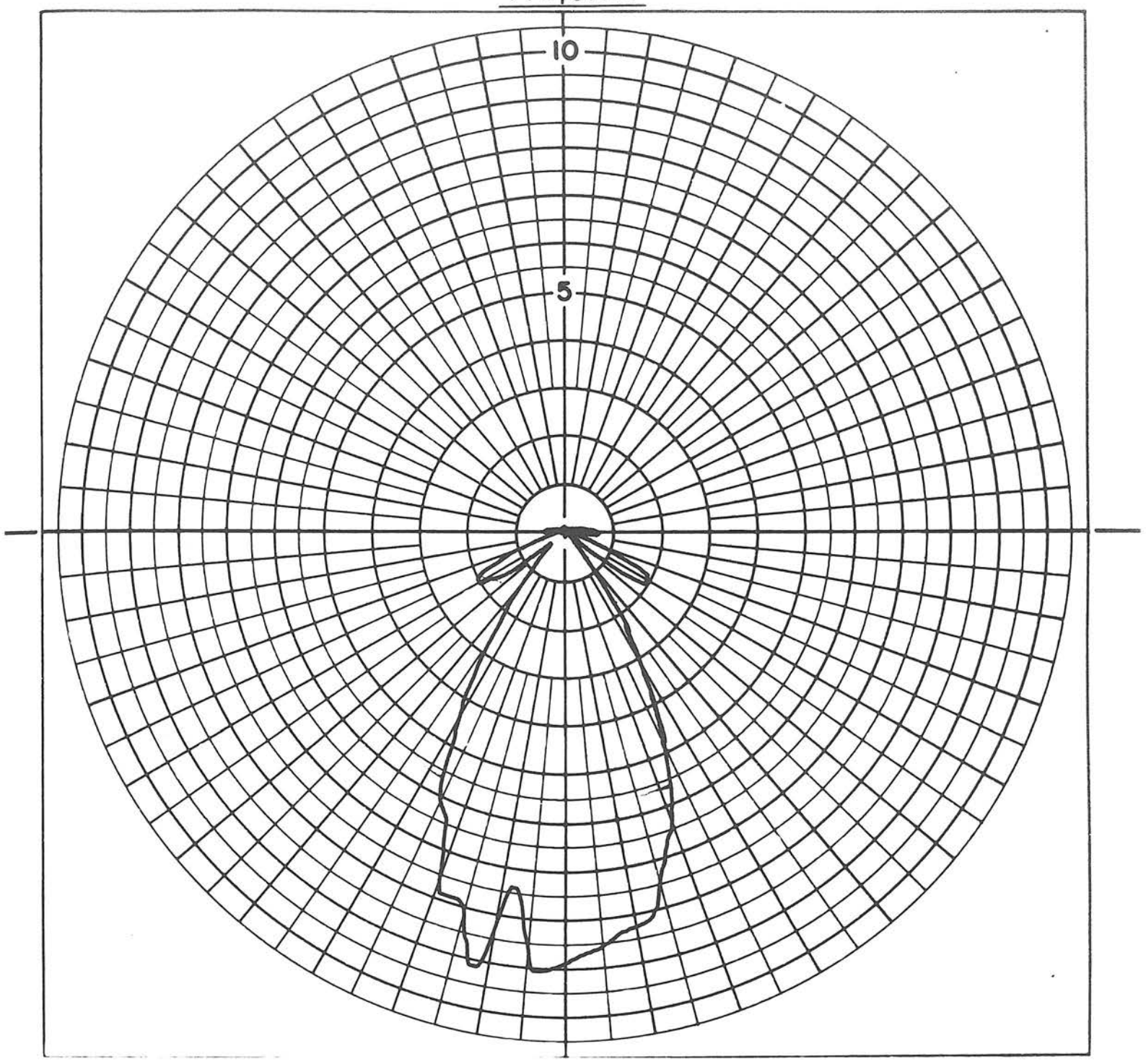

PATTERN 2 FOR $7\frac{1}{2}$ TURN HELIX WITH LARGE

GROUND PLANE

FIG 3.6-7

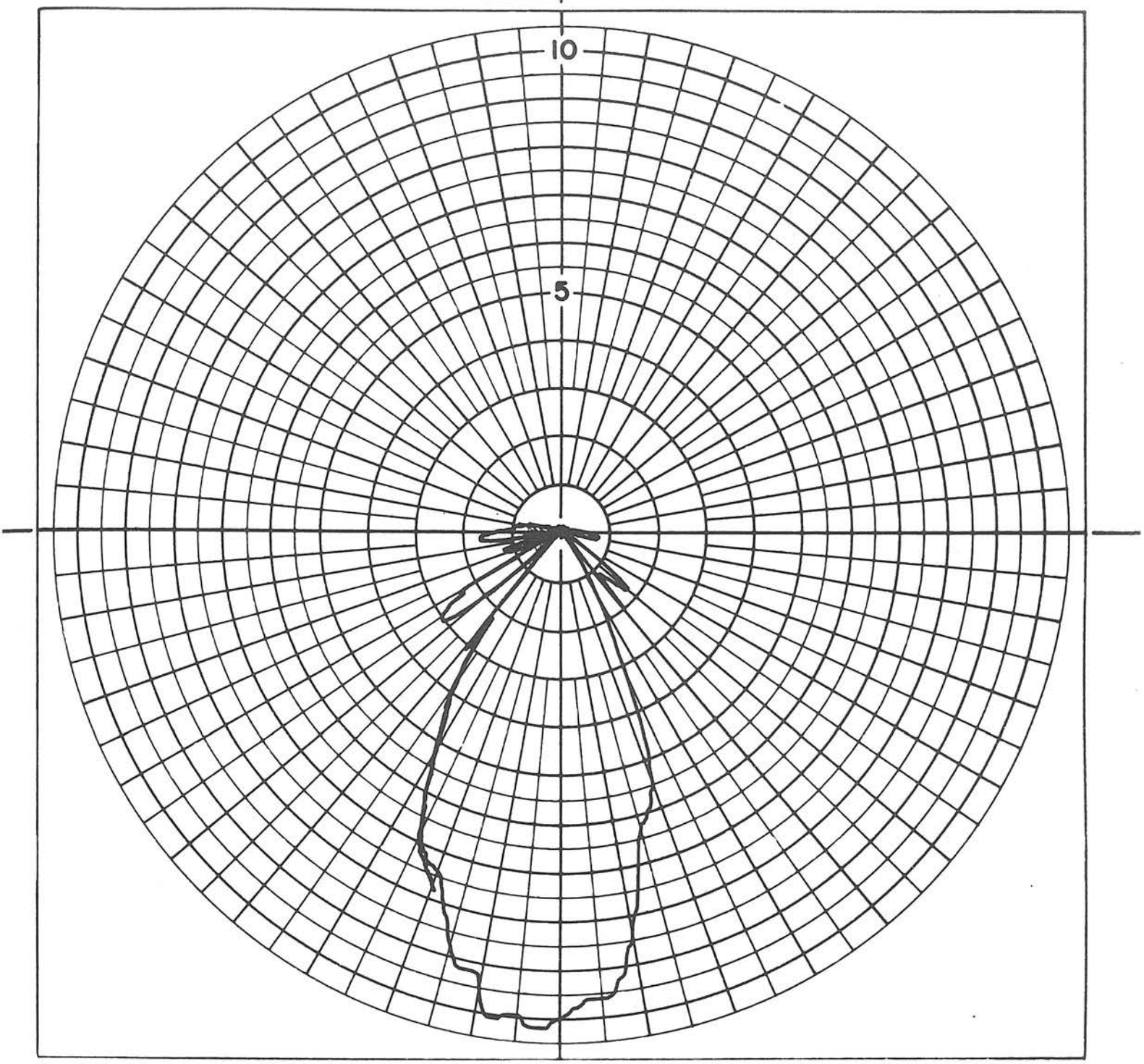

PATTERN 3 FOR $7\frac{1}{2}$ TURN HELIX WITH LARGE GROUND PLANE

FIG 3.6.8

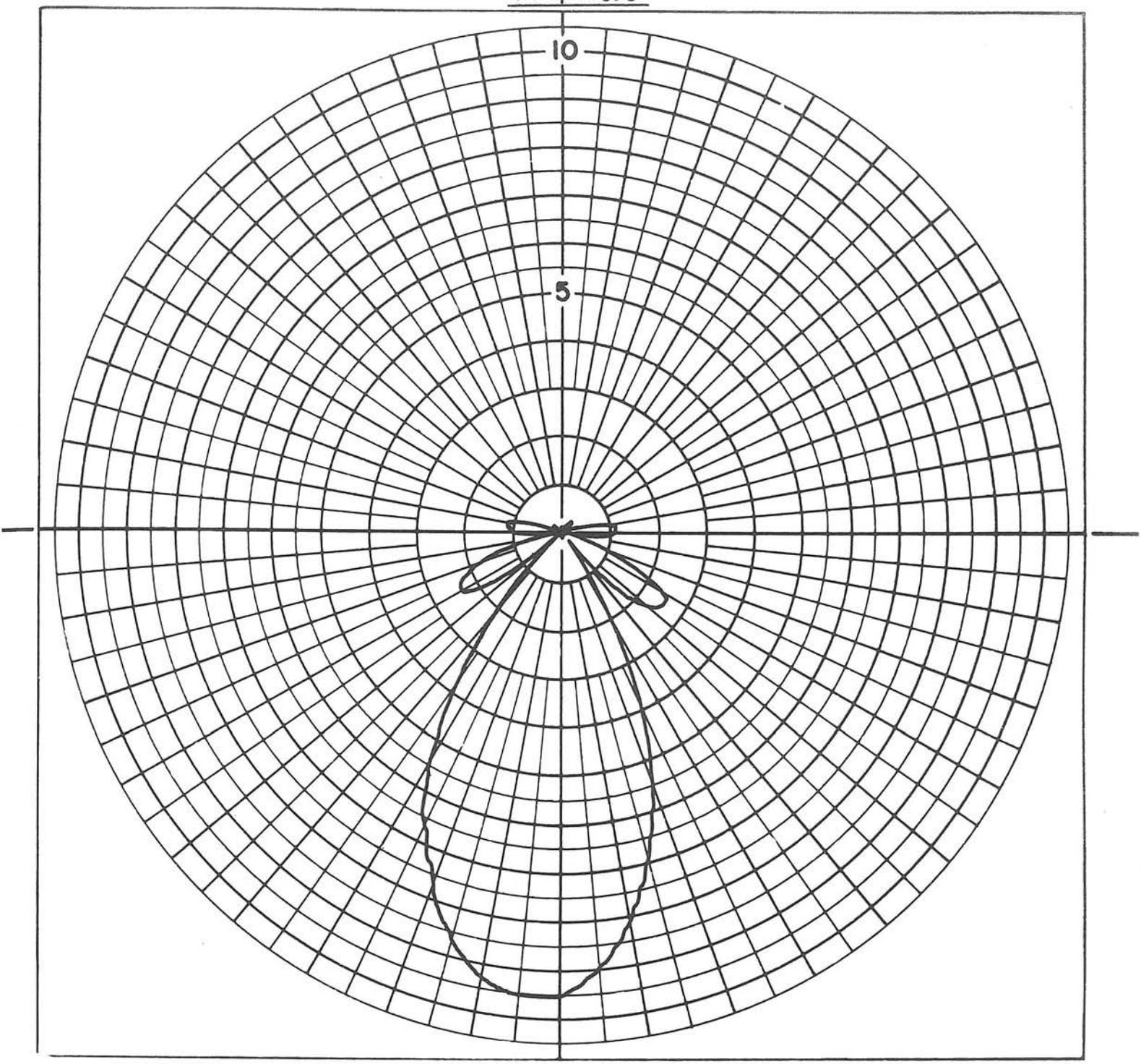

PATTERN FOR $7\frac{1}{2}$ TURN HELIX WITH SMALL GROUND PLANE

3.7. Comparison Between Tape Helix and Sheath Helix Results

The numerical results which have been derived from the waveguide approach in preceding sections of this Chapter, have been based on the Tape Helix model. In calculating the transmission phase velocity for this model either the fundamental wave assumed to be travelling along the helical conductor can be used, or the -1 space harmonic travelling axially. Both these approaches give identical results as will now be shown.

Let the phase shift between adjacent elements in the linear array be denoted by α with the subscript 0 or -1, according as the fundamental or the - 1 space harmonic is being considered. Then

$$\alpha_o = \frac{L}{\lambda_o} 2\pi \qquad 3.7.1.$$

where L is the length of 1 helical turn and λ_o is the fundamental wavelength. Denoting the axial velocity of the fundamental by v_o, the conductor phase velocity for the fundamental is $\frac{v_o}{\sin\psi}$ so that

$$\alpha_o = \frac{L f}{\left(\frac{v_o}{\sin\psi}\right)} \cdot 2\pi \quad -- \quad 3.7.2(a)$$

$$= \frac{2\pi d f}{v_o} \quad -- \quad 3.7.2.(b)$$

where d is the spacing between turns.

Similarly $\alpha_{-1} = \frac{2\pi d f}{v_{-1}}$ — — 3.7.3

where v_{-1} is the axial phase velocity of the -1 space harmonic. This is related to the fundamental axial phase velocity v_o by the equation:

$$\frac{v_{-1}}{v_0} = \frac{\beta_0 a}{\beta_0 a - \cot\psi} \quad \text{— —} \quad 3.7.4$$

so that α_{-1} eventually simplifies to

$$\alpha_{-1} = \frac{2\pi d f}{v_0} - 2\pi \quad \text{— —} \quad 3.7.5$$

which is the same as Equation 3.7.2.(b) apart from a difference of 2π which is not significant.

Both ways of looking at the phase shift between adjacent elements are valid. The approach using the -1 space harmonic considers an axial wave along the helix, while the fundamental mode approach is based on the wave following the helical conductor It should be noted explicitly however that while the conductor phase velocity (fundamental) increases with frequency, the axial phase velocity (-1 space harmonic) decreases. This follows since in the region of interest $\cot\psi > \beta_0 a$ so that $\beta_{-1} a$ is negative and hence v_{-1} is negative. Considerable confusion is therefore possible unless the direction to which the phase velocity refers is given.

It is of interest to compare the numerical values of say axial phase velocity derived from the Tape Helix model with the corresponding values derived from the Sheath Model. The computation in this case is much simpler and the results are shown for the -1 mode in Figure 3.7.1., along with those for the -1 space harmonic of the Tape Helix. Using these results for the Sheath Helix, the upper frequency limit of an aerial of this kind can

FIG 3.7.1

COMPARISON OF PHASE VELOCITIES FOR TAPE HELIX -1 SPACE HARMONIC AND SHEATH HELIX -1 MODE ; $\psi = 13^{\circ}$

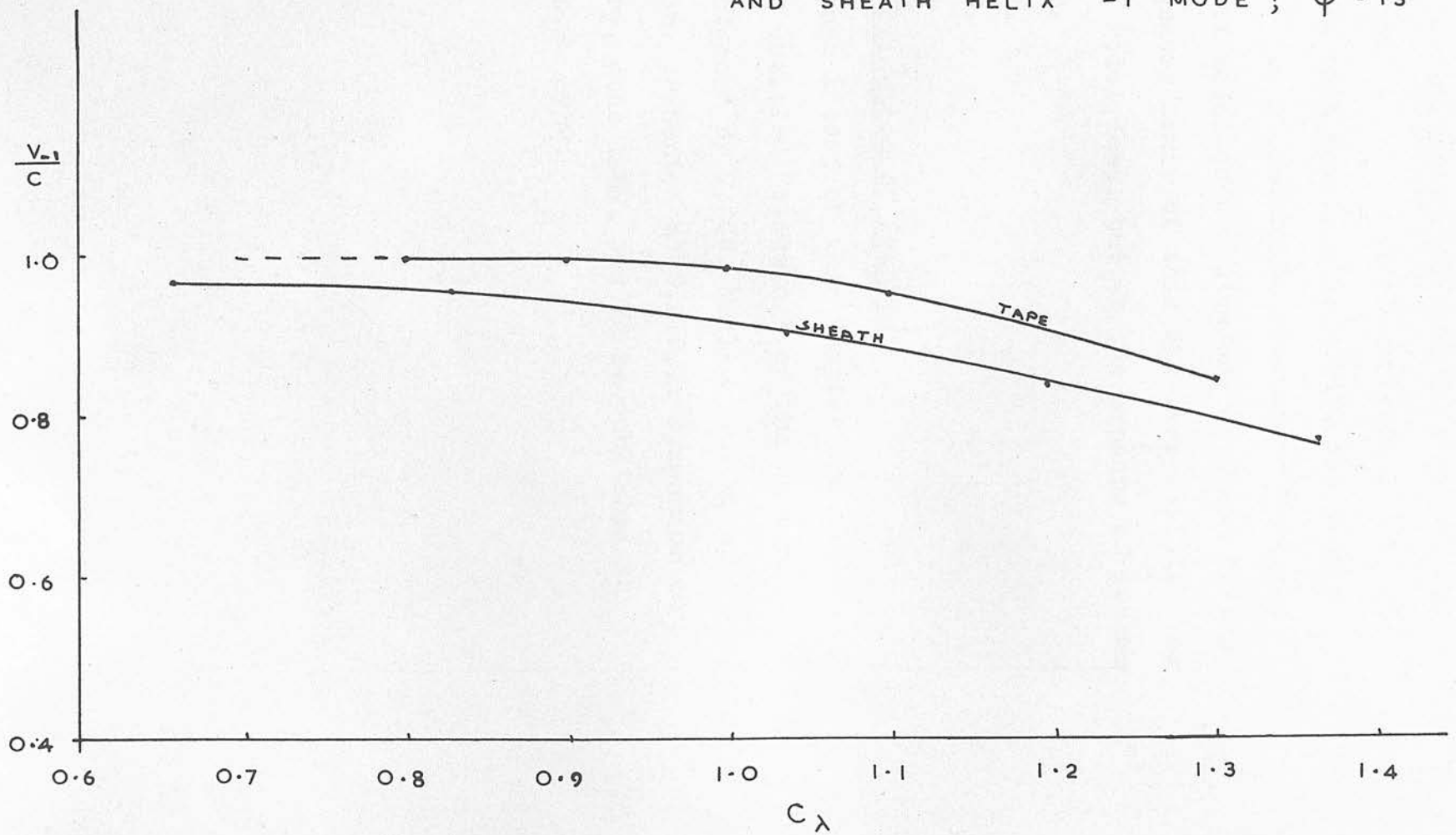

be calculated as was done in Section 3.1. for the Tape Helix. The variation of this limit with aerial length is shown in Figure 3.7.2. along with the corresponding result for the Tape Helix, and the experimentally determined variation. It can be seen that both models give accuracies of the same order, but it should be remembered that the Sheath Helix model cannot give any estimate of the lower frequency limit of this end-fire aerial. The Tape Helix model does, but at the expense of greater complexity.

Note on Publication of Results

Sections 1 to 3 of this Chapter are included in a paper entitled "Bandwidth of the Uniform Helical Antenna" by T.S.M. Maclean and R. G. Kouyoumjian, presented at U.R.S.I. Symposium on E.M. Theory, June 1959, and to be published in Trans. I.R.E. 1959.

FIG 3.7.2

UPPER FREQUENCY LIMIT VS NUMBER OF TURNS FOR $\psi = 13^\circ$

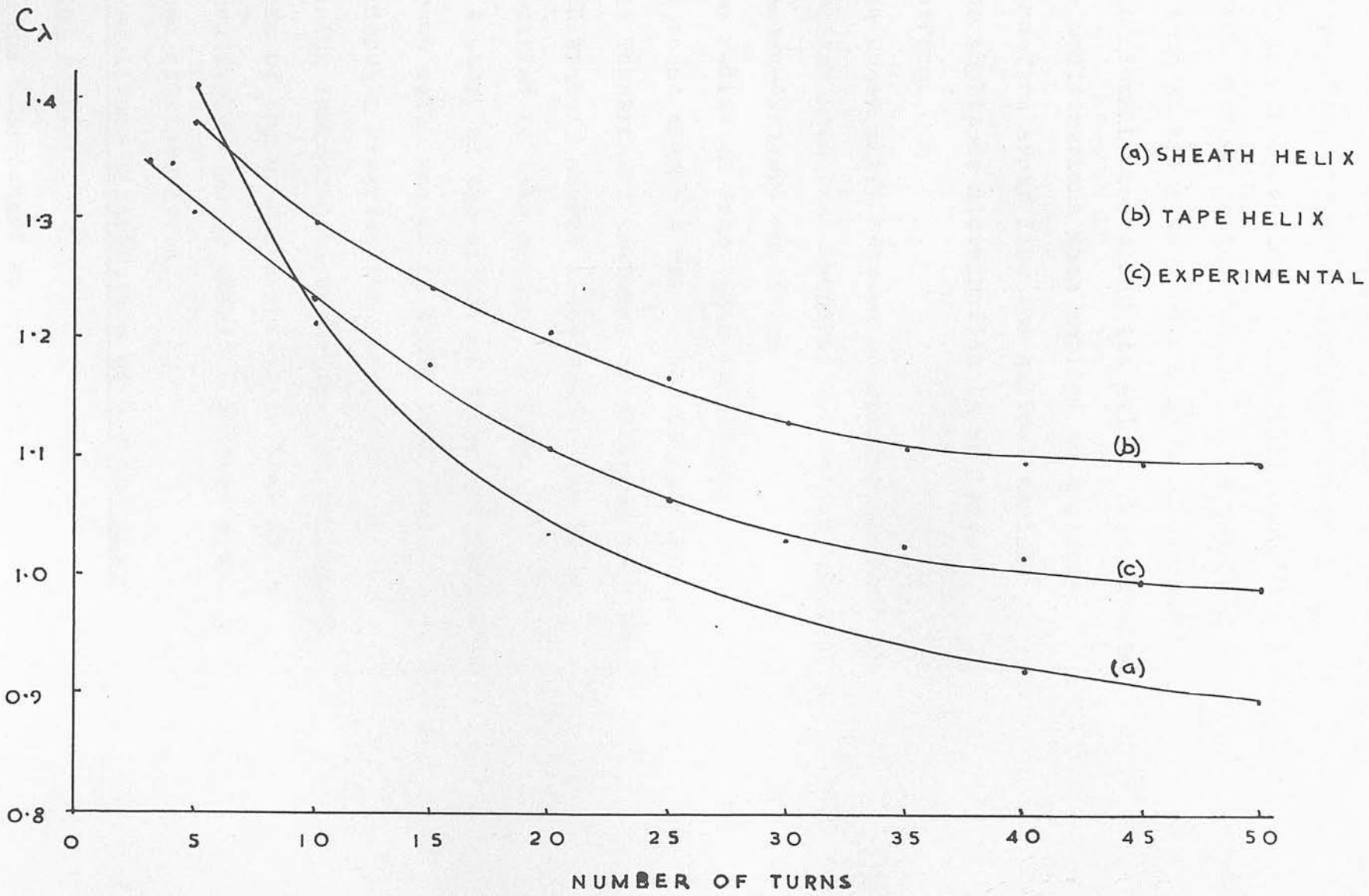

CHAPTER IV

Modulated Helical Aerial

A study of the modulated helical aerial was begun with the object of applying linear array theory to its operation. It is well known[24] that the optimum pattern which can be obtained from such an array is produced by a Tchebycheff source distribution along its axis. This entails three modifications when applied to a singly fed end-fire array like the helical aerial,

1. The amplitude distribution is no longer uniform.
2. The phase shift between successive elements is greater than that required for satisfying the Hansen-Woodyard condition
3. The radiation from turns connecting the adjacent elements has to be superimposed on the Tchebycheff pattern, or alternatively the Tchebycheff source distribution has to be modified to take account of them.

A study of the effect of these modifications has been made, and it is shown that they considerably restrict the possibility of obtaining increased directivity. An incidental outcome of the study, however, is that it is comparatively easy to obtain a pattern with reduced sidelobe level.

4.1. Amplitude Distribution of Sources Along Helical Axis.

The Tchebycheff source distribution for a

linear array is a function of the sidelobe level with respect to the main beam, and this ratio will be denoted by R (>1). For the case considered here of an element spacing of $0.1824\lambda_o$ at the operating frequency - corresponding to $C_\lambda = 1.0$ for a pitch angle of 13^o - the distribution along a 6 element array for various values of R is given by:-

R	CURRENT AMPLITUDE DISTRIBUTION						PHASE SHIFT α
3	1	3·617	6·234	6·234	3·617	1	177·8°
10	1	3·772	6·616	6·616	3·772	1	173·7°
35	1	3·975	7·136	7·136	3·975	1	168·16°
400	1	4·391	8·247	8·247	4·391	1	155·99°
1400	1	4·567	8·739	8·739	4·567	1	148·56°

The Array Factors for the cases R = 3 and R = 10 are shown in Figure 4.1.1. and for comparison the Array Factor for the Hansen-Woodyard condition is shown superimposed. It is clear that a considerable improvement in directivity and side-lobe level over the Hansen-Woodyard case is possible, by means of the additional degree of freedom available. The exact amount of improvement in directivity is necessarily fixed by the allowable side-lobe level and conversely. However, it must be remembered that the sharper the beam width which is desired, the smaller is the tolerance which can be allowed in the individual sources[24].

In applying the above theory to the case of the/

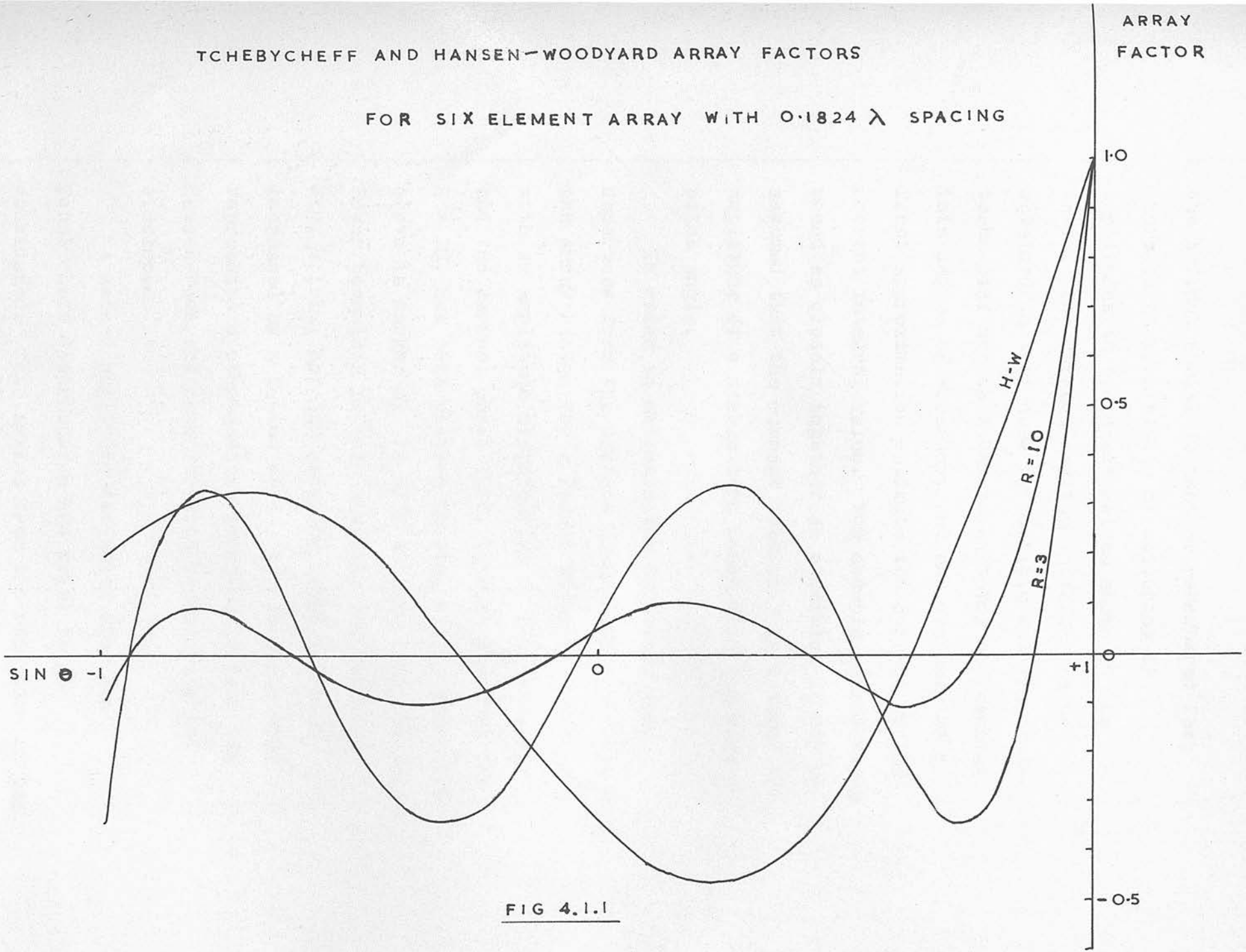
TCHEBYCHEFF AND HANSEN–WOODYARD ARRAY FACTORS
FOR SIX ELEMENT ARRAY WITH 0·1824 λ SPACING
ARRAY FACTOR
1·0
0·5
0
-0·5
H-W
R=10
R=3
SIN θ
-1
0
+1

FIG 4.1.1

the helical aerial it must be remembered that there is no possibility of tailoring the amplitudes to the exact values shown in the table. The current amplitudes which can be obtained in this case by multiple coiling of the terms will not be known to anything approaching this degree of accuracy, and one can only as a first approximation estimate the current to the nearest integral value. For example, for 4 turns wound as closely together as possible, it may be assumed that the current "element" is 4 times the amplitude of a single turn wound with the same pitch angle.

In order to estimate the effect of this departure from the correct Tchebycheff distribution the Array Factor for a linear array of 6 elements with an amplitude distribution of 1-4-7-7-4-1, and the correct phase shift between elements for R = 10, has been plotted in Fig. 4.1.2. where the curve is marked A. It will be seen that the Half-Power beamwidth is only slightly less than in Fig. 4.1.1., but the sidelobe level has been increased by a factor of 3. Nevertheless this represents a considerable improvement over the Hansen-Woodyard case for both directivity and sidelobes.

A second amplitude deviation from the Tchebycheff distribution has still to be considered. This arises from the radiation of the medium pitch turn connecting the main radiating elements/

FIG 4.1.2

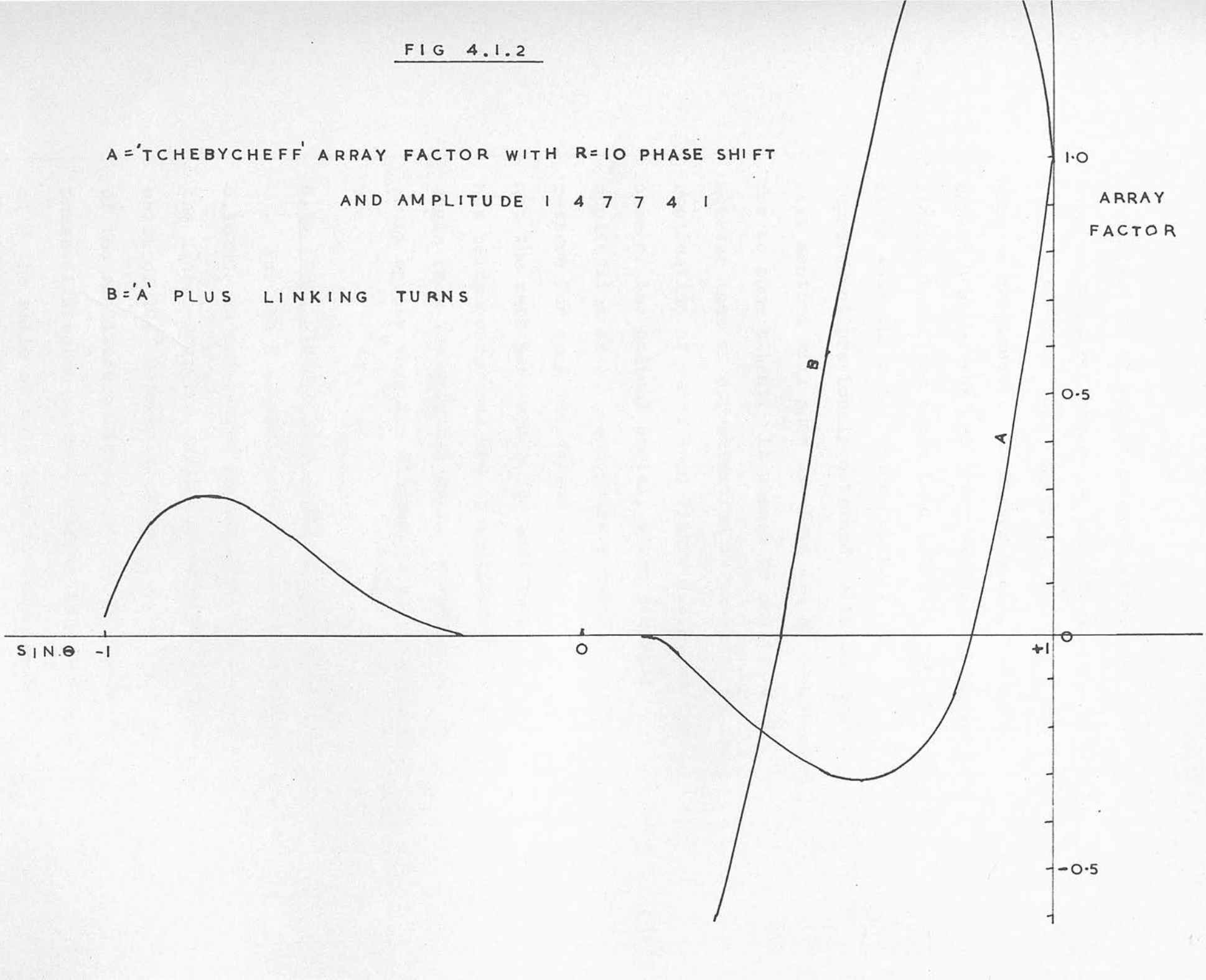
A = 'TCHEBYCHEFF' ARRAY FACTOR WITH R=10 PHASE SHIFT
AND AMPLITUDE 1 4 7 7 4 1
B = 'A' PLUS LINKING TURNS
1·0
ARRAY
FACTOR
0·5
B
A
SIN.Θ -1
0
+1
0
-0·5

elements. If it should prove possible to suppress this radiation, no problem arises, but since this is at least doubtful, the deviation must be considered. In Figure 4.1.2. the curve marked B shows the new Array Factor when these linking turns are taken into account. It is clear that their influence destroys the improvement previously obtained, although the next section will show how this can be compensated for to some extent. It should be mentioned however that an approximation is involved in the application of Curve B in Figure 4.1.2. to the case of the helical aerial, since a direct application of it presupposes a constant unit pattern for each individual element. This is not the case here since the additional elements now being considered are of a different pitch angle from the original ones. Nevertheless it would appear that the diagram is of considerable use.

4.2. Phase Distribution Along Helical Axis

For the 6 element array with a spacing of $0.1824C_{\lambda}$ as considered in the previous section, the Hansen-Woodyard condition requires a phase shift of 101^{o} between sources. As in the case of the amplitude distribution the Tchebycheff phase difference between sources is a function of R the ratio of main beam to sidelobe level, as shown in the preceding table.

From/

From this table it can be seen that in all cases the wave travelling along the helical conductor must be slowed down to a value substantially below the phase velocity required for the Hansen-Woodyard condition. In order to determine how much difference this makes to the Array Factor, Figure 4.2.1. shows for an amplitude distribution of 1-4-7-7-4-1 what effect slowing the wave down from the Hansen-Woodyard value to the Tchebycheff value for R = 10, has on the pattern, Figure 4.2.2. shows the same variation for an amplitude distribution of 1-3-6-6-3-1

In figure 4.2.3. the result is shown for 1-4-7-7-4-1 distribution when the linking turns are taken into account. It can be seen that a value of 140° gives a slightly narrower beam and substantially lower sidelobes than the Hansen-Woodyard Array Factor. It may also be estimated that a phase shift of about 145° would be the most which could be tolerated for sidelobes no larger than those of the Hansen-Woodyard case.

4.3. Position Variation of Elements Along Helical Axis.[43]

The improvement in the directivity of a Hansen-Woodyard type of pattern over the conventional end-fire pattern results from a control of phase along the line of the array. The still further improvement of the Tchebycheff pattern results from a second degree of freedom being/

FIG 4.2.1

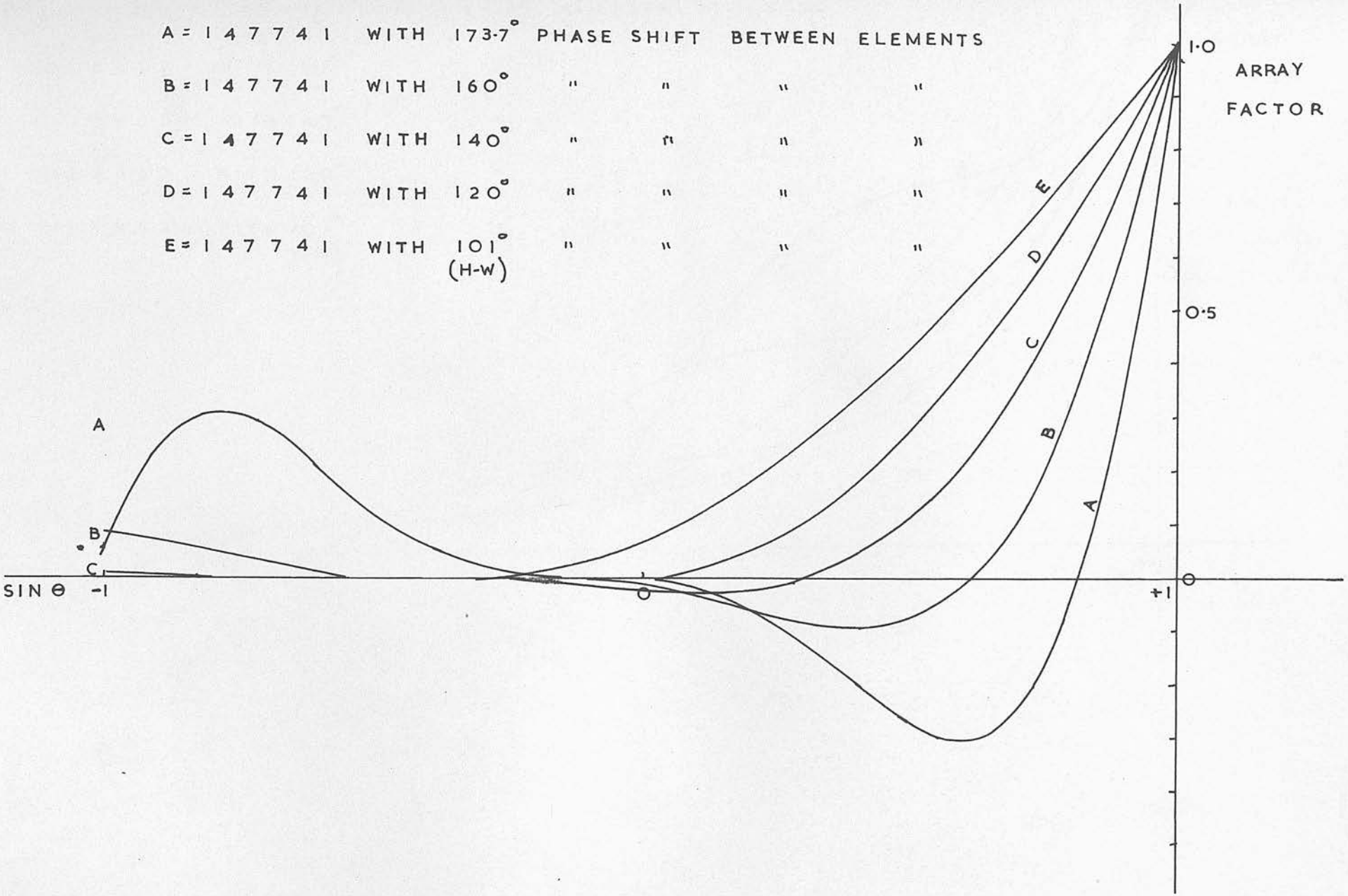
A = 1 4 7 7 4 1 WITH 173·7° PHASE SHIFT BETWEEN ELEMENTS
B = 1 4 7 7 4 1 WITH 160° " " " "
C = 1 4 7 7 4 1 WITH 140° " " " "
D = 1 4 7 7 4 1 WITH 120° " " " "
E = 1 4 7 7 4 1 WITH 101° (H-W) " " " "
1·0
ARRAY FACTOR
0·5
E
D
C
B
A
A
B
C
SIN θ -1
0
+1
0

FIG 4.2.2

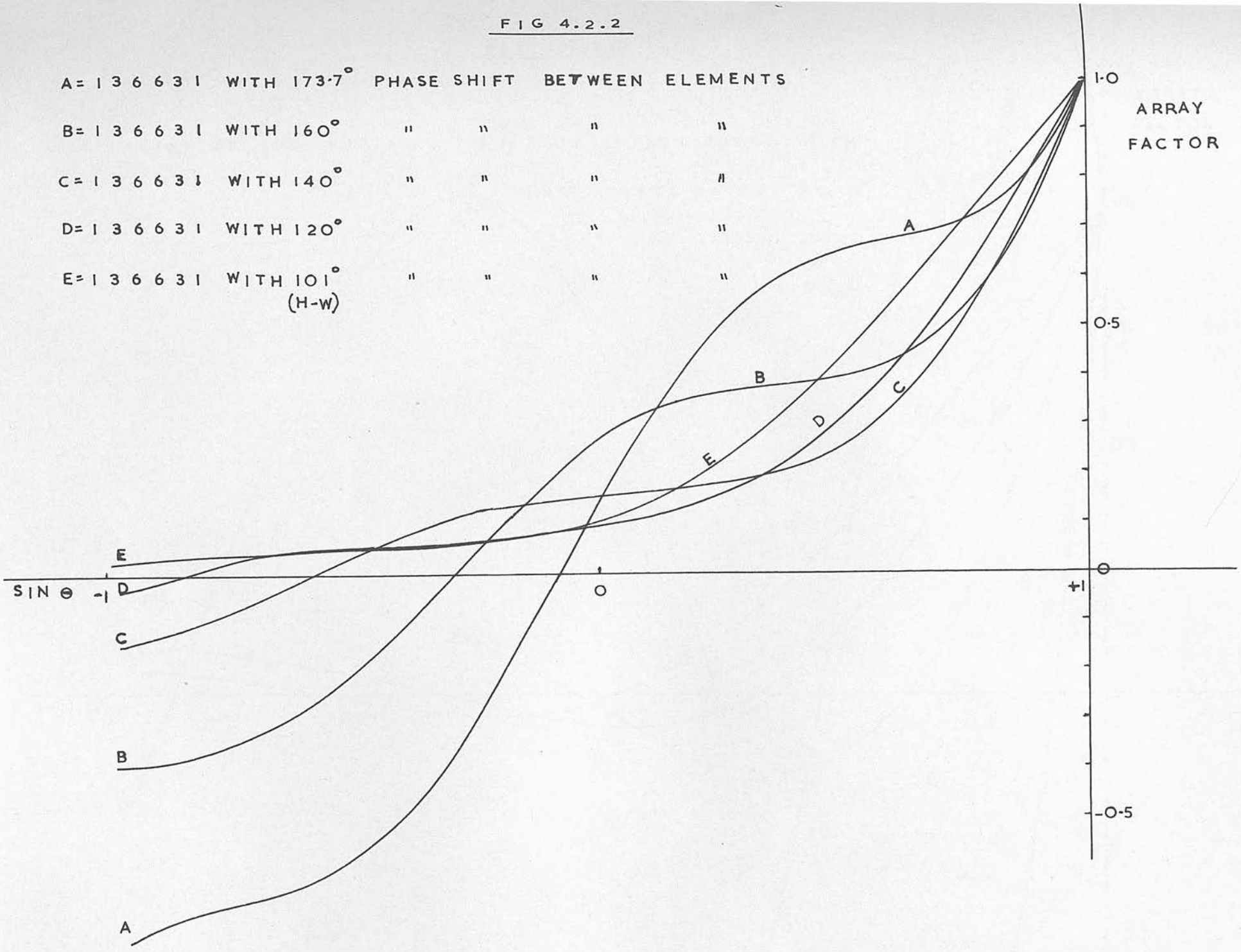
A= 1 3 6 6 3 1 WITH 173·7° PHASE SHIFT BETWEEN ELEMENTS
B= 1 3 6 6 3 1 WITH 160° " " " "
C= 1 3 6 6 3 1 WITH 140° " " " "
D= 1 3 6 6 3 1 WITH 120° " " " "
E= 1 3 6 6 3 1 WITH 101° " " " "
(H-W)
1·0
ARRAY
FACTOR
0·5
-0·5
SIN Θ
-1
0
+1
A
B
C
D
E

FIG 4.2.3

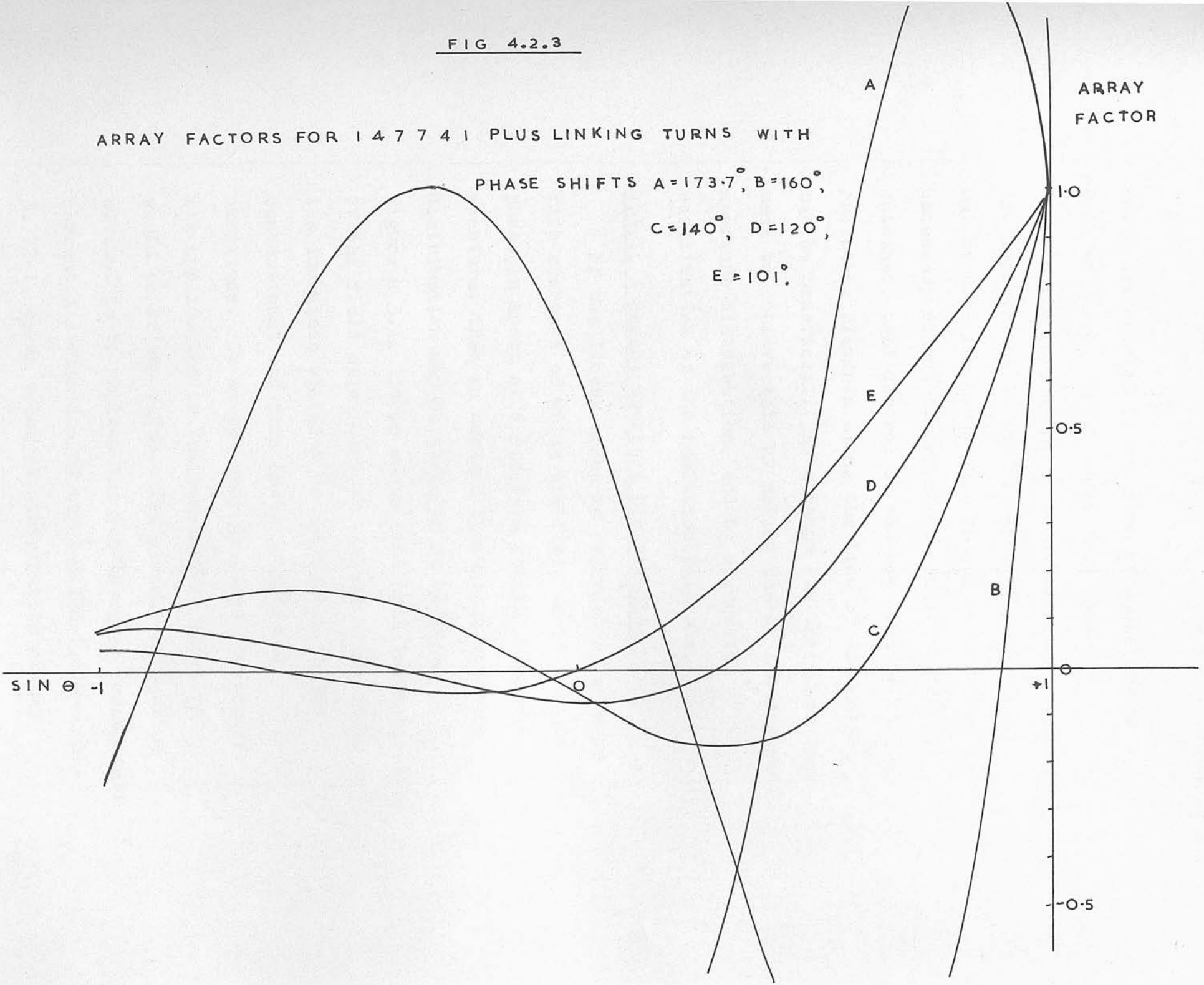
ARRAY FACTORS FOR 1 4 7 7 4 1 PLUS LINKING TURNS WITH
PHASE SHIFTS A = 173·7°, B = 160°,
C = 140°, D = 120°,
E = 101°.
A
B
C
D
E
ARRAY FACTOR
1·0
0·5
-0·5
SIN θ -1
0
+1

being avaialable, in the form of amplitude as well as phase. While it is true that the introduction of any more variables cannot produce any improvement in the Tchebycheff pattern, it may be that for cases such as the helix where the necessary source distribution cannot be exactly obtained, that control of the position of the radiating elements along the line of the array may be beneficial. An attempt has therefore been made to achieve this by making use of the apparent aperture distribution, and by algebraic equalisation of the radiation patterns.

4.3.1. Apparent Aperture Distribution

If the linear array is regarded as an end-fire aperture of which the field amplitude and phase is known at 6 discrete points along the aperture, then an assumed fictitious aperture distribution may be sketched in as shown in Figure 4.3.1. It is known that this generalisation of the field at a point to represent the field in its immediate vicinity is applicable to the conventional end-fire array of uniform amplitude. It is not easy to judge however if its application to the non-uniform aperture would be of any value. The purpose of such an attempt is to replace the non-integral Tchebycheff current distribution of say 1-3.772-6.616-6.616-3.772-1, by an integral distribution of say 1-4-7-7-4-1 at the points along the aperture

where/

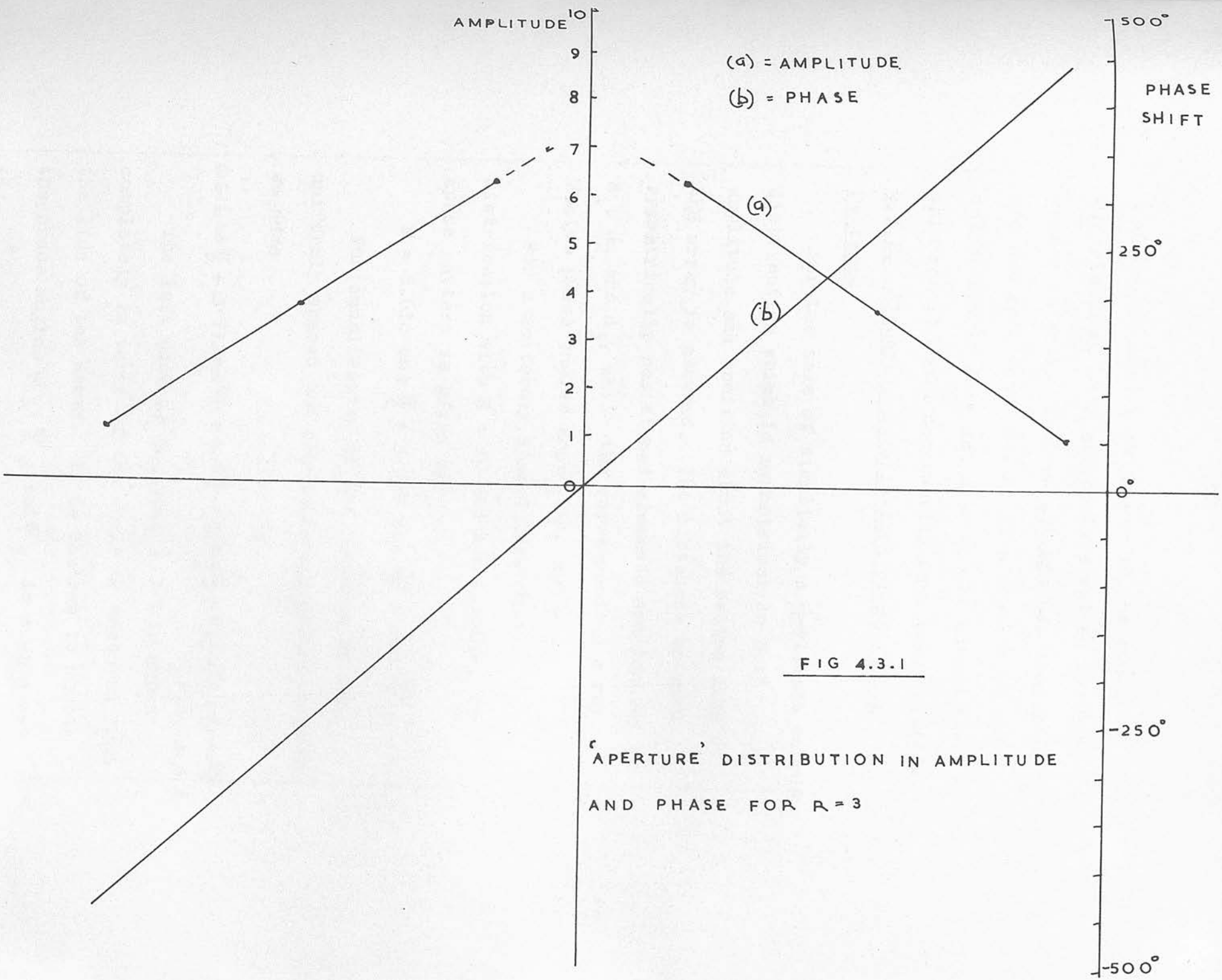

FIG 4.3.1

'APERTURE' DISTRIBUTION IN AMPLITUDE AND PHASE FOR R = 3

where these ordinates appear in the field distribution, with appropriate values of phase chosen as well. Such an attempt has been made and has been found not go give results of any value, but it does not seem to the author that this result could necessarily have been foreseen.

4.3.2. Algebraic Equalisation of Radiation Patterns

For the sake of simplicity a 6-element source distribution which is symmetrical in both amplitude and position about the centre line of the array is assumed. The distances between symmetrically positioned elements are denoted by d_1, d_2 and d_3, while the corresponding Array Factor phase angles are ψ_1, ψ_2 and ψ_3.

For a uniformly spaced Tchebycheff distribution with $\tilde{R}$ = 10 and d = 0.1824λ, the space pattern is given by

$$E = 6.616 \cos\frac{\psi}{2} + 3.772 \cos\frac{3\psi}{2} + \cos\frac{5\psi}{2} \quad -- 4.3.1$$

For equalisation of the patterns of the uniformly spaced and non-uniformly spaced sources we have

$$6.616\cos\frac{\psi}{2} + 3.772\cos\frac{3\psi}{2} + \cos\frac{5\psi}{2} = E_1\cos\frac{\psi_1}{2} + E_2\cos\frac{\psi_2}{2} + E_3\cos\frac{\psi_3}{2} \quad -- 4.3.2$$

The left side of Equation 4.3.2 is known completely in terms of the angle Φ measured from the line of the array. It is desired to choose the phase angles ψ_1, ψ_2 and ψ_3 in such a way as/

as to make the equality valid when integral values of E_1, E_2 and E_3 are used. In addition it would be desirable if possible to make the lengths of the two arrays equal so that

$$\frac{\Psi_3}{2} = \frac{5\Psi}{2} \qquad --4.3.3$$

It will further be assumed here that the integral values of E are $E_1 = 7$, $E_2 = 4$ and $E_1 = 1$.

The space pattern corresponding to the left side of Equation 4.3.2 can be written in terms of the sources as

$$F(\phi) = \sum_{m=0}^{M} A_m e^{j\beta \frac{d_m}{2} \cos\phi} \qquad --4.3.4$$

where A_m is the complex current of element m, and d_m is the spacing between the symmetrically positioned sources carrying this current.

By using θ as the complement of ϕ this can be re-written as

$$F(\theta) = \sum_{m=0}^{M} A_m e^{j\beta d} \qquad ---4.3.5$$

$$= \sum_{m=0}^{M} A_m \sum_{n=-\infty}^{+\infty} e^{jn\theta} J_n\left(\frac{\beta d_m}{2}\right) --4.3.6$$

which by comparison with the Fourier Series expansion of the space pattern

$$F(\theta) = \sum_{n=-\infty}^{+\infty} f_n e^{jn\theta} \qquad ---4.3.7$$

gives $$f_n = \sum_{m=0}^{M} A_m J_n\left(\frac{\beta d_m}{2}\right) \qquad ---4.3.8$$

Since the Fourier Coefficients f_n can thus be evaluated for the known complex currents A_m and distances d_m in the Tchebycheff Array, the problem of synthesising the new array reduces to finding/

finding the corresponding values of A_m and d_m there. Thus

$$f_0 = 2\times6.616\, J_0\left(\frac{2\pi}{\lambda}\,\frac{0.1824\lambda}{2}\right) + 2\times3.772\, J_0\left(\frac{2\pi}{\lambda}\,\frac{0.5472\lambda}{2}\right) + 2\, J_0\left(\frac{2\pi}{\lambda}\,\frac{0.912\lambda}{2}\right) \quad -- 4.3.9.$$

$$= 14.68$$

$$f_2 = 2\times6.616\, J_2(0.573) + 2\times3.772\, J_2(1.719) + 2J_2(2.865) \quad -- 4.3.10$$

$$= 3.65$$

Similarly

$$f_4 = 0.381\,, \quad f_6 = 0.0127 \qquad -- 4.3.11 \qquad -- 4.3.12$$

and

$$f_{2n+1} = 0 \quad \text{since} \quad J_{-n}(x) = J_n(x).(-)^n \quad -- 4.3.13$$

Thus for the new array

$$14.68 = 2\times7\, J_0\left(\frac{\beta d_1}{2}\right) + 2\times4\, J_0\left(\frac{\beta d_2}{2}\right) + 2J_0(2.865) -- \quad -- 4.3.14$$

$$3.65 = 2\times7\, J_2\left(\frac{\beta d_1}{2}\right) + 2\times4\, J_2\left(\frac{\beta d_2}{2}\right) + 2J_2(2.865) -- \quad -- 4.3.15$$

$$0.381 = 2\times7\, J_4\left(\frac{\beta d_1}{2}\right) + 2\times4\, J_4\left(\frac{\beta d_2}{2}\right) + 2J_4(2.865) -- \quad -- 4.3.16$$

$$0.0127 = 2\times7\, J_6\left(\frac{\beta d_1}{2}\right) + 2\times4\, J_6\left(\frac{\beta d_2}{2}\right) + 2J_6(2.865) -- \quad -- 4.3.17$$

It is found that even when Equations 4.3.16 and 4.3.17 are neglected because they represent smaller contributions to the total field, it is not possible to find values of d_1 and d_2 which satisfy the remaining two equations. Hence it is unlikely that position variation of the inner elements can compensate for the change in currents from non-integral to integral values, when the total length of the arrays is kept contant. Further analysis without this restriction could of course be made, but has not been thought worthwhile here.

4.4. Experimental Results

The preceding sections have shown how much easier it is to obtain reduced sidelobe level with a modulated helix of the type discussed, than to obtain increased directivity. Experimental confirmation of the reduced sidelobes is given in Figures 4.4.1 - 4.4.3., where at the frequency corresponding approximately to $0.79C_{\lambda}$ good patterns and axial ratio are obtained. It is of interest and significance that the narrow band of acceptable radiation pattern and axial ratio is the same band as that of the narrowest pitch turns used in the winding. In this connection it must be remembered that as outlined in Chapter III lower pitch angles can be used than was previously thought possible.

Since this type of aerial was completely new it seemed desirable to obtain confirmation of the travelling wave nature of the fields along the helix by measurement of the conductor current distribution, as well as of the radiation pattern. The helix shown in Figure 4.4.4. was used for these tests, in which the current was measured by means of a loop probe connected to a crystal detector, type 1N23B, followed by a high-gain tuned A.F. amplifier.

The construction of the loop probe presented two difficulties which do not appear to be mentioned in the literature. Both these difficulites/

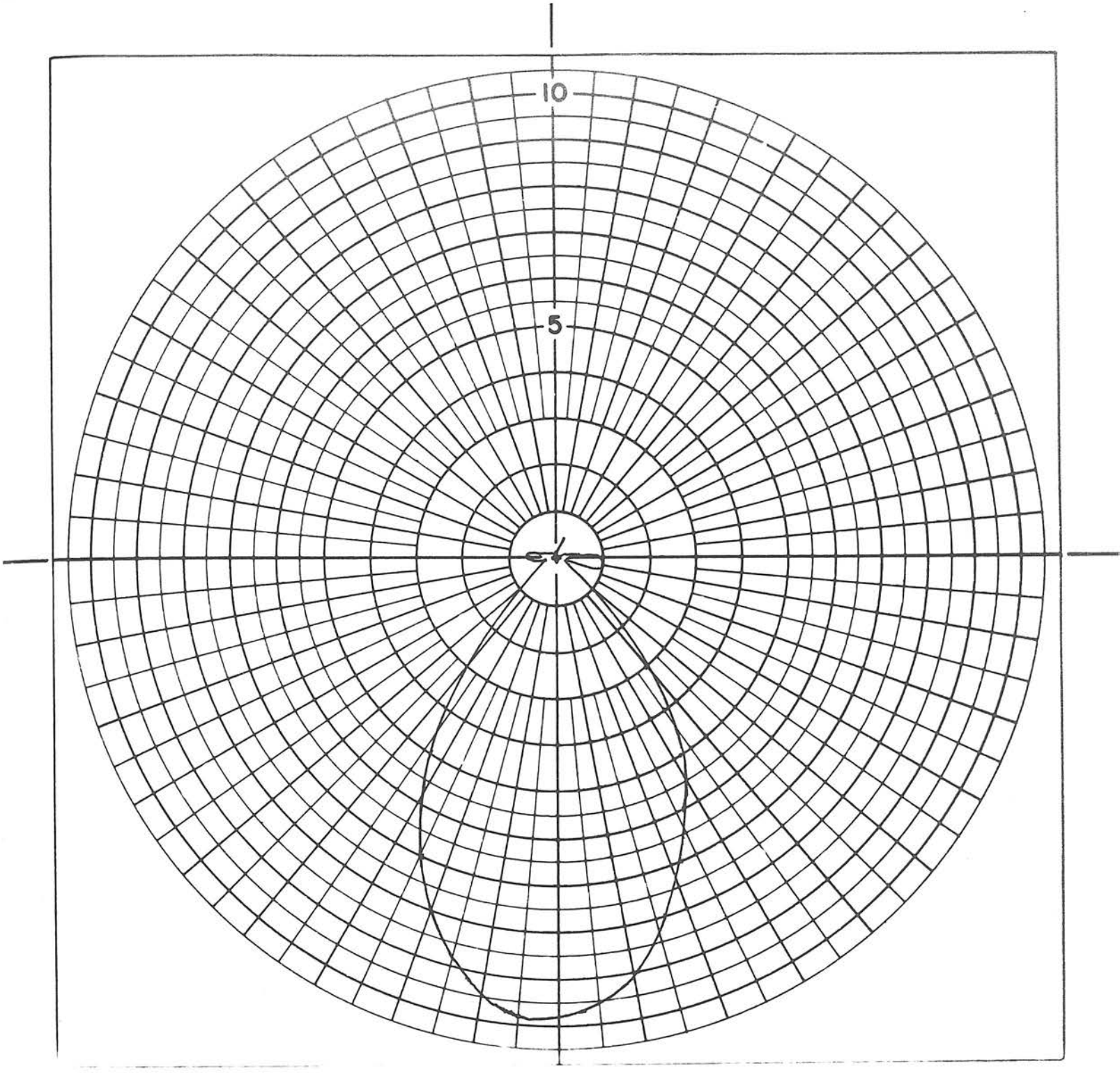

FIG 4.4.1 E_θ PATTERN FOR MODULATED HELIX 0·9λ LONG

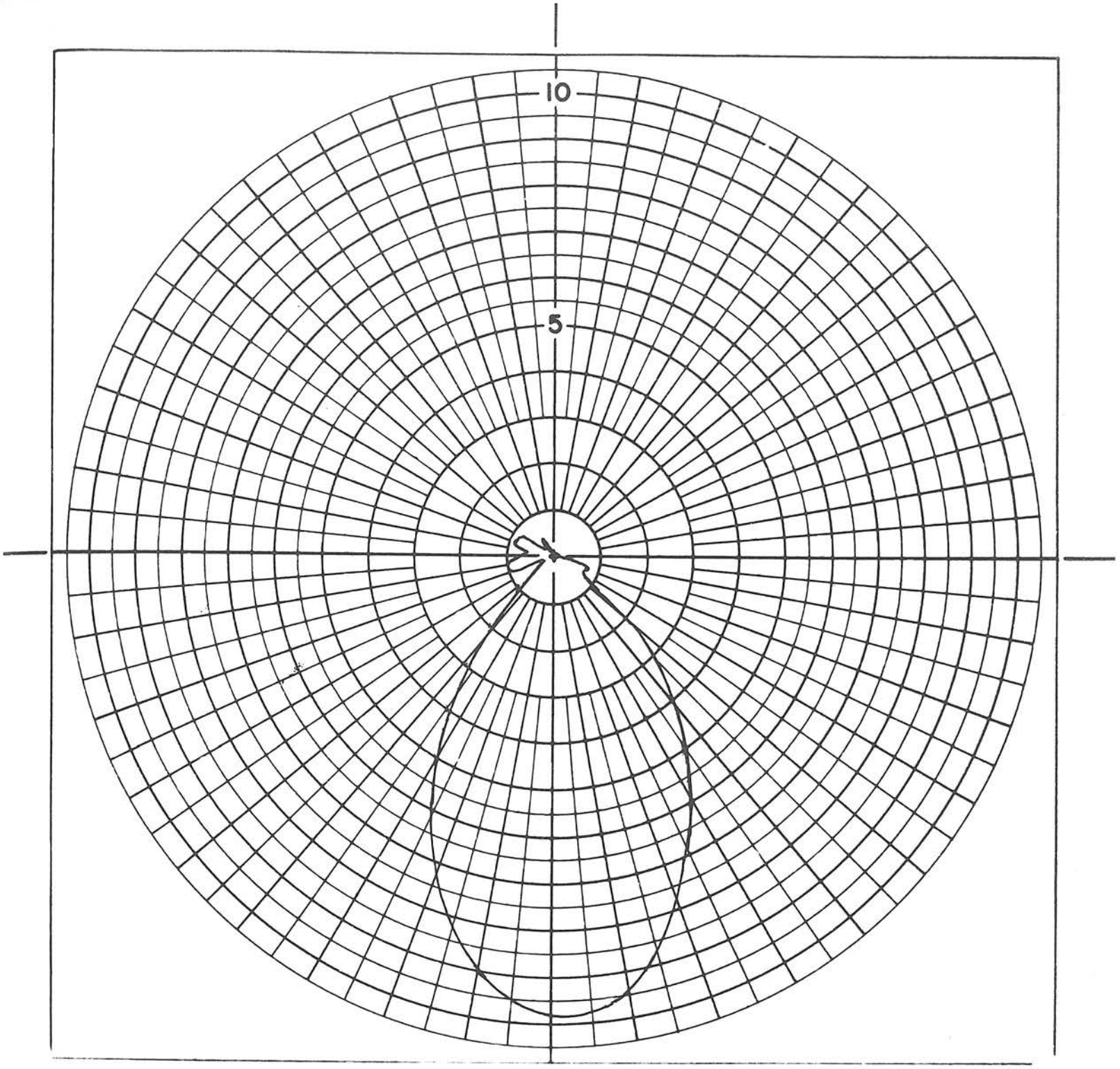

FIG 4.4.2 E_ϕ PATTERN FOR MODULATED HELIX 0·9 λ LONG

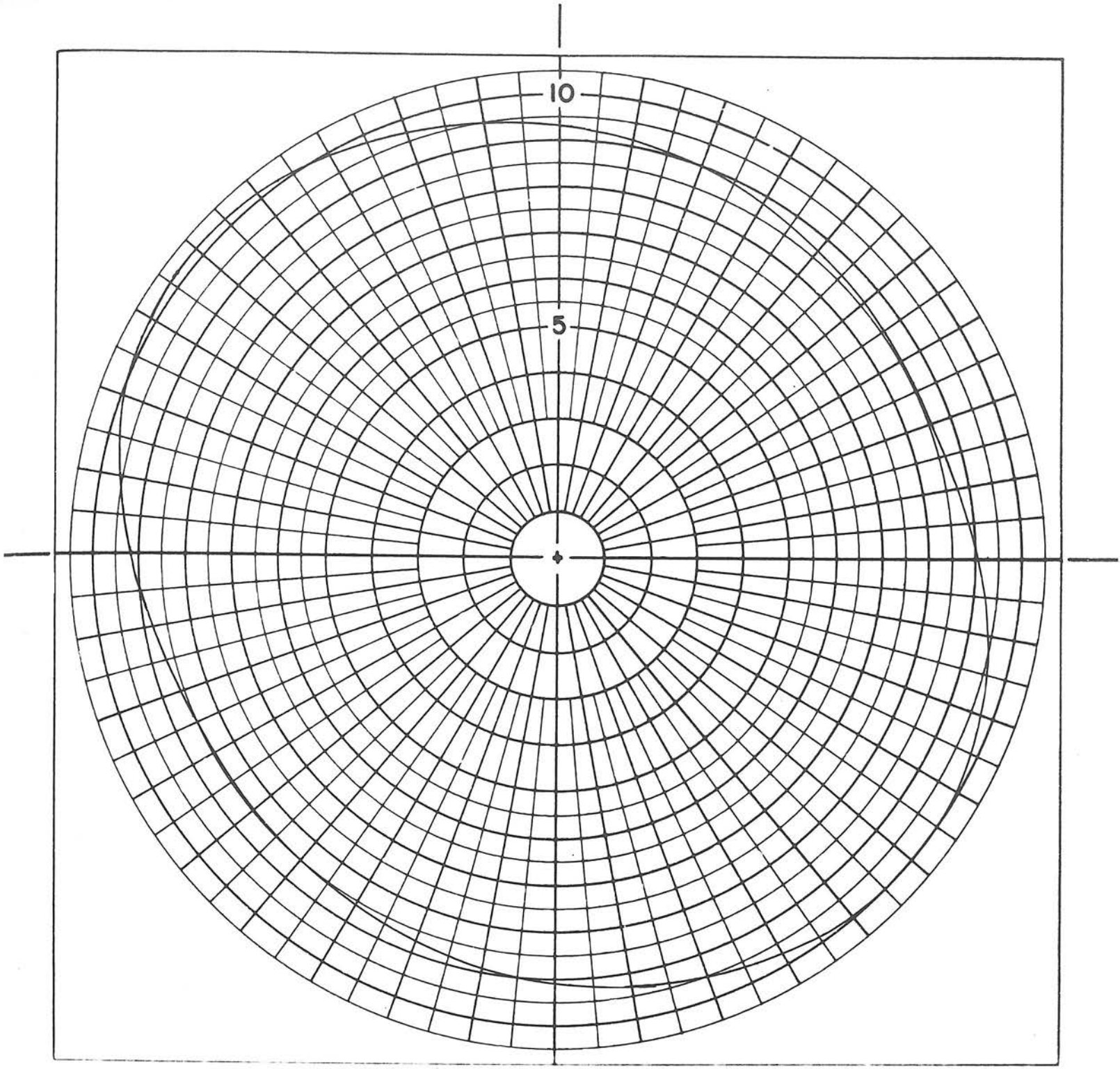

FIG 4.4.3 POLARISATION PATTERN FOR MODULATED HELIX

0·9λ LONG

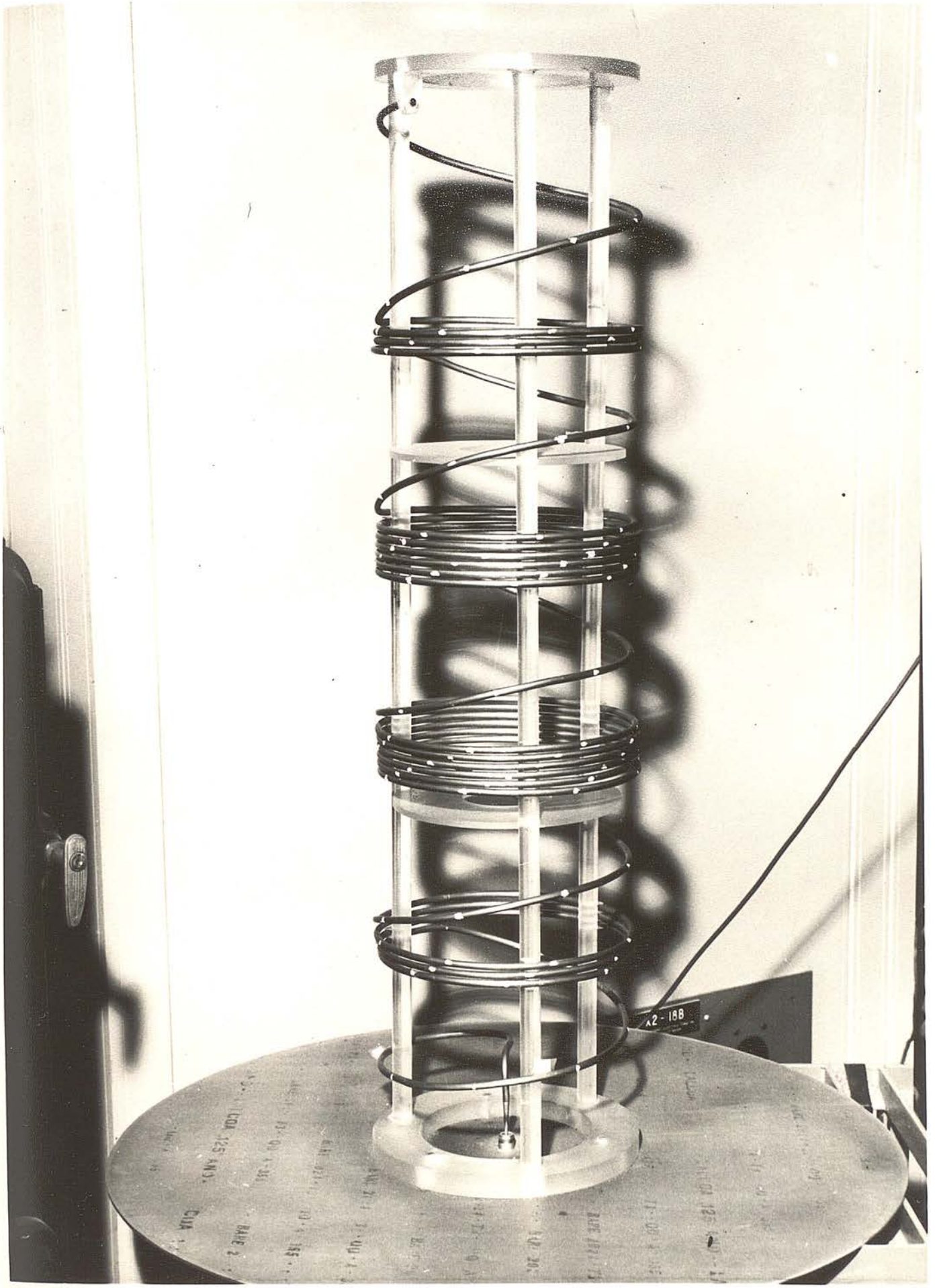

FIG 4.4.4

difficulties had their origin in the use of $\frac{1}{32}$" outside diameter coaxial cable. It was necessary to use this in order to ensure that the loop was not affected by the magnetic field of the closely spaced turns adjacent to the turn in which it was desired to measure the current. The conductor diameter used for the turns was $\frac{1}{4}$".

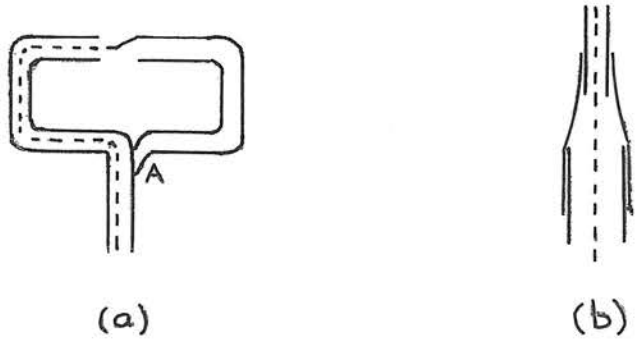

FIG 4.4.5

The first difficulty arose in the use of a normal 65 - Watt soldering iron in the making of soldered connection A. Even though the heat was only instantaneously applied at this junction, it invariably produced a short-circuit between the inner and outer of the narrow diameter coaxial cable. Since the outer conductor was a copper tube there was no visible evidence of the damage. Use of a 20-Watt soldering iron overcame this difficulty.

The second difficulty lay in the connection between the $\frac{1}{32}$" diameter coaxial cable and the normal $\frac{1}{4}$" diameter cable-type RG58U. Unless a truly coaxial correction is made, in which there is no possibility of currents flowing on the outside/

outside of the coaxial cable gaining access to the crystal load, it will be found that current readings can be obtained anywhere in the aerial vicinity, and not only in close proximity to the aerial conductor. In Figure 4.4.5.(b) the difficult outer connection is effected by the wrapping of aluminium foil tightly round both cables.

The results of some of the current measurements are shown in Figures 4.4.6. to 4.4.8. In Figure 4.4.6. a typical standing wave of current is shown for a frequency below that of the desired radiating mode. Figure 4.4.7. represents the current distribution in the narrow frequency band corresponding to a good pattern. It will be noted here that the standing wave is still substantial by comparison with the diagrams given by Marsh[9] for the uniform helix. In Figure 4.4.8. at a frequency above the useful band, the fluctuations are smaller in amplitude, but the phase velocity is no longer suitable for the desired mode of radiation. The current measurements in all cases were taken at a constant output by means of a calibrated attenuator on the signal generator.

FIG 4.4.6

CURRENT DISTRIBUTION ALONG MODULATED HELIX

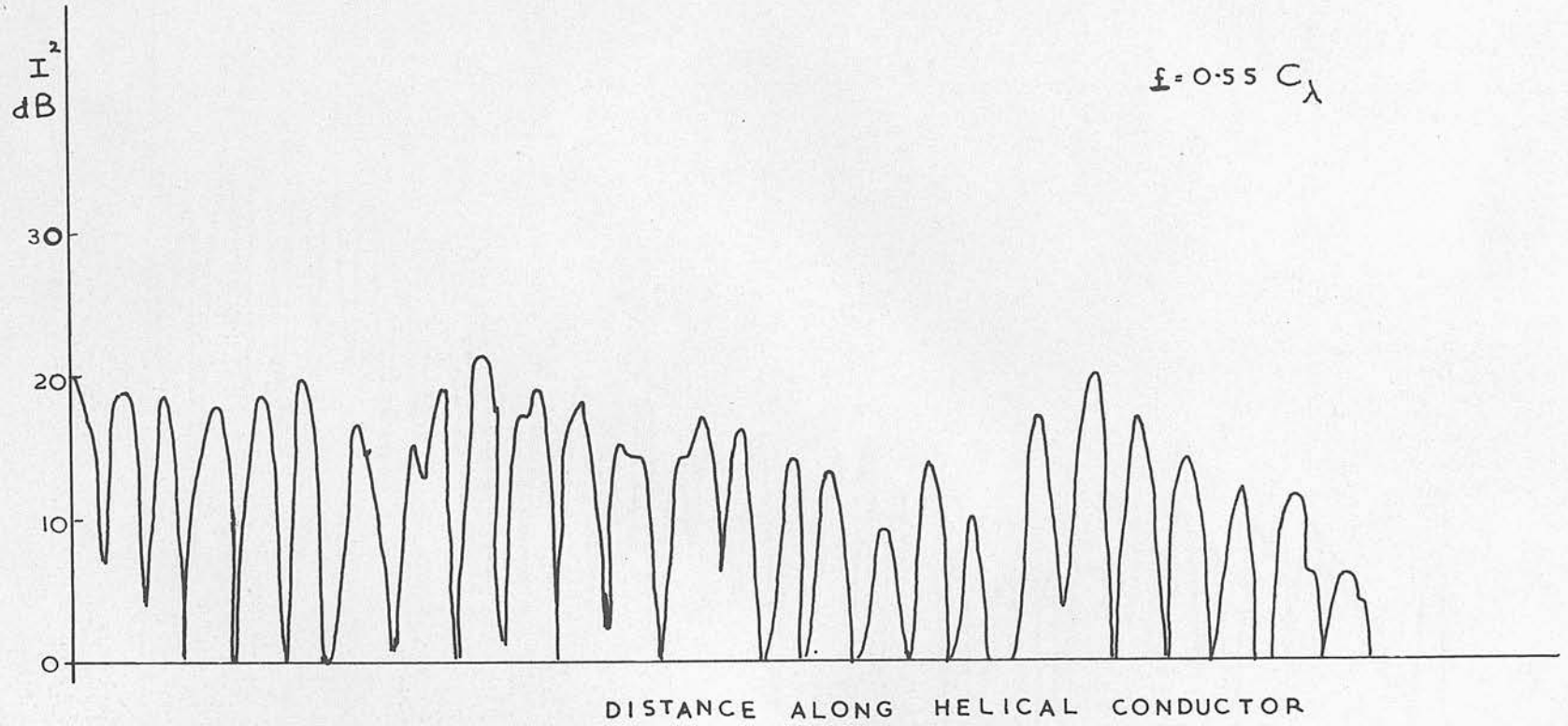

FIG. 4.4.7

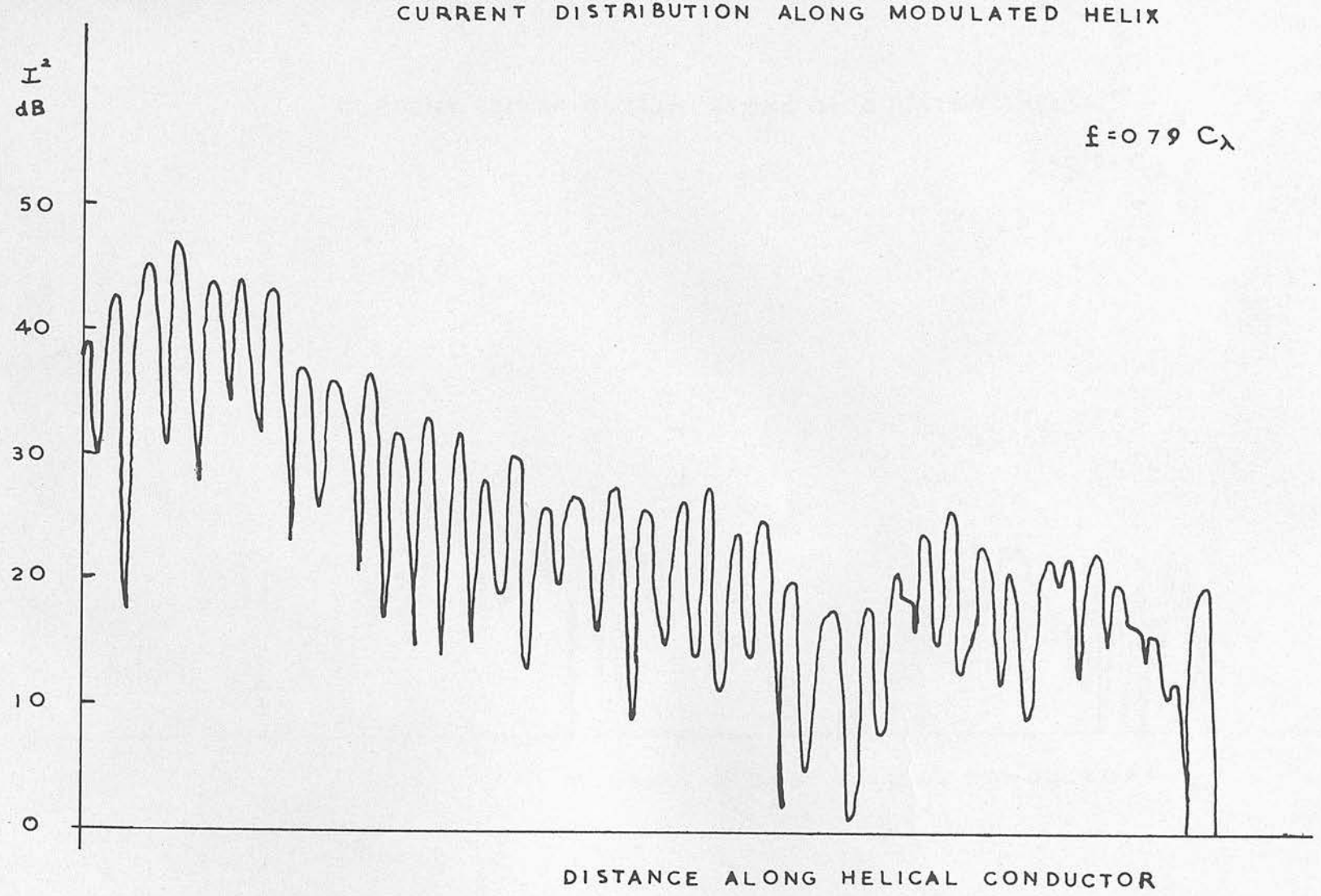
CURRENT DISTRIBUTION ALONG MODULATED HELIX
I^2
dB
$\ell = 0.79\ C_\lambda$
50
40
30
20
10
0
DISTANCE ALONG HELICAL CONDUCTOR

FIG 4.4.8

CUPPENT DISTRIBUTION ALONG MODULATED HELIX

$f = 0.94 C_\lambda$

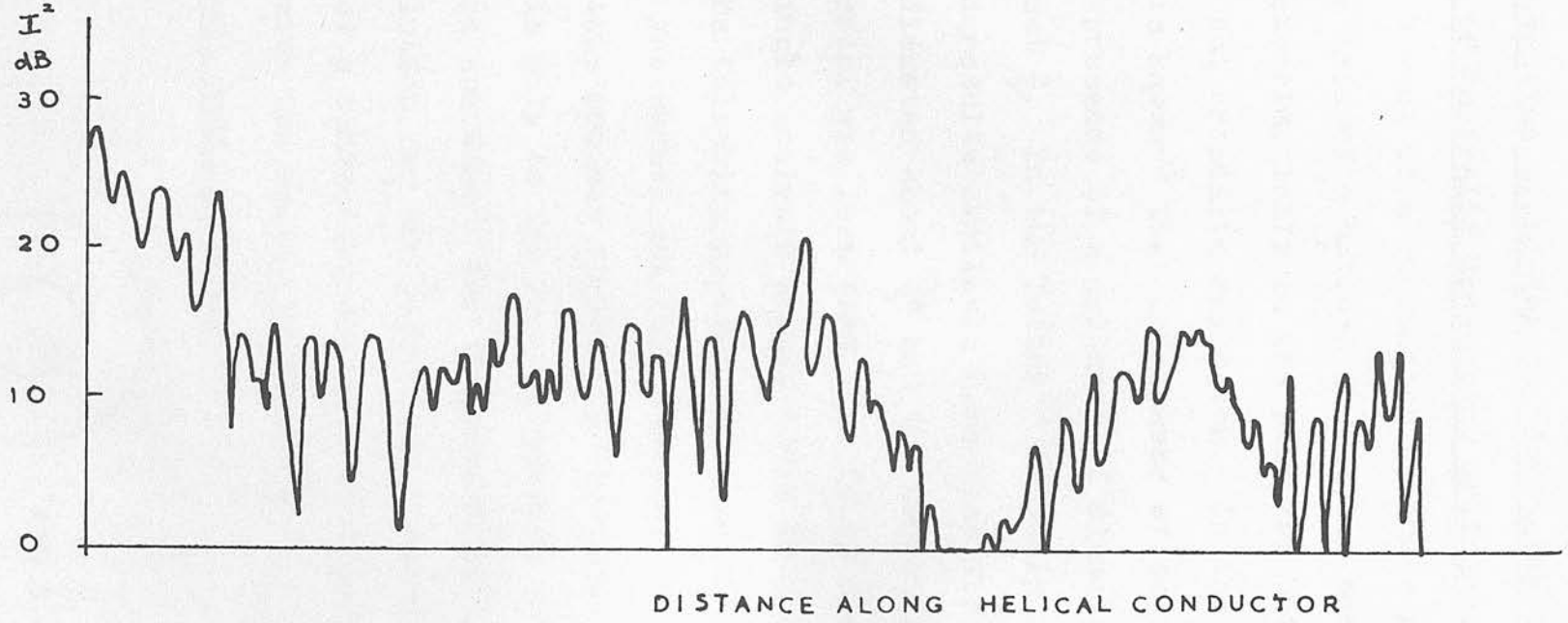

CHAPTER V

Wave Propagation Along Helical Conductor in Presence of Centrally Conducting Cylinder.

The effect of a conducting cylinder placed along the axis of a helical aerial has been studied experimentally in the past for both End-Fire and Broadside radiation. In the former case it is known[33] that no adverse effects result from the presence of a cylinder of diameter up to at least $\frac{\lambda}{5}$. In the latter[34] the only published results available have been for a mast of diameter about $\frac{3\lambda}{5}$ and the bandwidth of the aerial was less than 1%. It is clear that a single analysis should cover both cases, and in the following pages a solution is given for both the Sheath and Tape Helices. Previous work on this subject includes a treatment applicable only to the travelling-wave tube by Mathers and Kino[35] for the Sheath Helix, and a solution for the Tape Helix inverse problem of a conducting cylinder outside and coaxial with the helix, by Stark[36].

5.1. Sheath Helix Solution

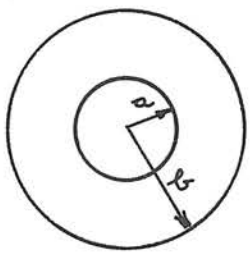

FIG 5.1

The wave equation solutions in this case are/

are necessarily of the same form as Equations 2.1.7 and 2.1.8. i.e.

$$E_z = [A_m I_m(\gamma r) + C_m K_m(\gamma r)] e^{j m\theta} e^{-j\beta z} \quad -- 5.1.1$$

$$H_z = [B_m I_m(\gamma r) + D_m K_m(\gamma r)] e^{j m\theta} e^{-j\beta z} \quad -- 5.1.2$$

It is convenient, however, to write these in such a way that they necessarily satisfy the boundary conditions for E_z^i and H_z^i at the surface of the conducting cylinder, viz.,

$$E_z^i = 0 \quad \text{at } r = a \quad -- 5.1.3$$

$$\frac{\partial H_z^i}{\partial r} = 0 \quad \text{at } r = a \quad -- 5.1.4$$

where the superscript i indicates the region internal to the helical surface ($a < r < b$). Superscript e will denote the external region ($r > b$).

A form which does satisfy these conditions is,

$$E_z^i = A_m' \left[I_m(\gamma r) - K_m(\gamma r) \frac{I_m(\gamma a)}{K_m(\gamma a)} \right] e^{j m\theta} e^{-j\beta z} \quad -- 5.1.5$$

$$= A_m \left[I_m(\gamma r) K_m(\gamma a) - K_m(\gamma r) I_m(\gamma a) \right] e^{j m\theta} e^{-j\beta z} \quad -- 5.1.6(a)$$

$$= A_m G_{mm}(\gamma r, \gamma a) e^{j m\theta} e^{-j\beta z} \quad -- 5.1.6(b)$$

where $G_{mm}(\gamma r, \gamma a) = I_m(\gamma r) K_m(\gamma a) - K_m(\gamma r) I_m(\gamma a)$ -- 5.1.7

Similarly

$$H_z^i = B_m' \left[I_m(\gamma r) - K_m(\gamma r) \frac{I_m'(\gamma a)}{K_m'(\gamma a)} \right] e^{j m\theta} e^{-j\beta z} \quad -- 5.1.8$$

$$= B_m \left[I_m(\gamma r) K_m'(\gamma a) - K_m(\gamma r) I_m'(\gamma a) \right] e^{j m\theta} e^{-j\beta z} \quad -- 5.1.9(a)$$

where $= B_m G_{mm'}(\gamma r, \gamma a) e^{j m\theta} e^{-j\beta z}$ -- 5.1.9(b)

$$G_{mm'}(\gamma r, \gamma a) = I_m(\gamma r) K_m'(\gamma a) - K_m(\gamma r) I_m'(\gamma a) \quad -- 5.1.10$$

$$E_z^e = C_m K_m(\gamma r) \quad -- 5.1.11$$

$$H_z^e = D_m K_m(\gamma r) \quad -- 5.1.12$$

The other field quantities can then be immediately written down,

$$E_r^i = \frac{j\beta A_m}{\gamma}\left[I_m'(\gamma r) K_m(\gamma a) - K_m'(\gamma r) I_m(\gamma a)\right] e^{jm\theta} e^{-j\beta z}$$

$$- \frac{\omega\mu m B_m}{\gamma^2 r}\left[I_m(\gamma r) K_m'(\gamma a) - K_m(\gamma r) I_m'(\gamma a)\right] e^{jm\theta} e^{-j\beta z}$$

$$= \left[\frac{j\beta A_m}{\gamma} G_{m'm}(\gamma r, \gamma a) - \frac{\omega\mu m B_m}{\gamma^2 r} G_{mm'}(\gamma r, \gamma a)\right] e^{jm\theta} e^{-j\beta z}$$

$$-- 5.1.13$$

where $G_{m'm}(\gamma r, \gamma a) = I_m'(\gamma r) K_m(\gamma a) - K_m'(\gamma r) I_m(\gamma a)$ -- 5.1.14

$$E_\theta^i = \left[-\frac{j\omega\mu}{\gamma} B_m^i G_{m'm'}(\gamma r, \gamma a) - \frac{m\beta}{\gamma^2 r} A_m^i G_{mm}(\gamma r, \gamma a)\right] e^{jm\theta} e^{-j\beta z}$$

-- 5.1.15(a)

where $G_{m'm'}(\gamma r, \gamma a) = I_m'(\gamma r) K_m'(\gamma a) - K_m'(\gamma r) I_m'(\gamma a)$ -- 5.1.15(b)

$$H_r^i = \left[\frac{j\beta}{\gamma} B_m^i G_{m'm'}(\gamma r, \gamma a) + \frac{m\omega\varepsilon}{\gamma^2 r} A_m^i G_{mm}(\gamma r, \gamma a)\right] e^{jm\theta} e^{-j\beta z} \quad -- 5.1.16$$

$$H_\theta^i = \left[\frac{j\omega\varepsilon}{\gamma} A_m^i G_{m'm}(\gamma r, \gamma a) - \frac{m\beta}{\gamma^2 r} B_m^i G_{mm'}(\gamma r, \gamma a)\right] e^{jm\theta} e^{-j\beta z} \quad -- 5.1.17$$

$$E_r^e = \left[\frac{j\beta}{\gamma} C_m K_m'(\gamma r) - \frac{m\omega\mu}{\gamma^2 r} D_m K_m(\gamma r)\right] e^{jm\theta} e^{-j\beta z} \quad --- 5.1.18$$

$$E_\theta^e = \left[-\frac{j\omega\mu}{\gamma} D_m K_m'(\gamma r) - \frac{m\beta}{\gamma^2 r} C_m K_m(\gamma r)\right] e^{jm\theta} e^{-j\beta z} \quad --- 5.1.19$$

$$H_r^e = \left[\frac{j\beta}{\gamma} D_m K_m'(\gamma r) + \frac{m\omega\varepsilon}{\gamma^2 r} C_m K_m(\gamma r)\right] e^{jm\theta} e^{-j\beta z} \quad --- 5.1.20$$

$$H_\theta^e = \left[\frac{j\omega\varepsilon}{\gamma} C_m K_m'(\gamma r) - \frac{m\beta}{\gamma^2 r} D_m K_m(\gamma r)\right] e^{jm\theta} e^{-j\beta z} \quad --- 5.1.21$$

Boundary Conditions at r = b

$$E_z^i = E_z^e \quad -- 5.1.22$$

$$E_\theta^i = E_\theta^e \quad -- 5.1.23$$

$$E_z^i = -E_\theta^i \cot\psi \quad -- 5.1.24$$

$$H_z^i + H_\theta^i \cot\psi = H_z^e + H_\theta^e \cot\psi \quad -- 5.1.25$$

From 5.1.22.

$$\frac{A_m}{C_m} = \frac{K_m(\gamma b)}{I_m(\gamma b)K_m(\gamma a) - K_m(\gamma b)I_m(\gamma a)} \quad -- \quad 5.1.26$$

From 5.1.23

$$\left[-\frac{j\omega\mu}{\gamma} B_m^i G_{m'm'}(\gamma b, \gamma a) - \frac{m\beta}{\gamma^2 b} A_m^i G_{mm}(\gamma b, \gamma a)\right] e^{jm\theta} e^{-j\beta z}$$

$$= \left[-\frac{j\omega\mu}{\gamma} D_m K_m'(\gamma b) - \frac{m\beta}{\gamma^2 b} C_m K_m(\gamma b)\right] e^{jm\theta} e^{-j\beta z} \quad -- \quad 5.1.27$$

From 5.1.24

$$A_m G_{mm}(\gamma b, \gamma a) = \frac{j\omega\mu}{\gamma} \cot\psi\, B_m^i G_{m'm'}(\gamma b, \gamma a) + \frac{m\beta\cot\psi}{\gamma^2 b} A_m^i G_{mm}(\gamma b, \gamma a)$$
$$-- \quad 5.1.28$$

Hence

$$\frac{A_m}{B_m} = \frac{j\omega\mu\gamma b \cot\psi G_{m'm'}(\gamma b, \gamma a)}{G_{mm}(\gamma b, \gamma a)[\gamma^2 b - m\beta\cot\psi]} \quad -- \quad 5.1.29$$

From Equations 5.1.26, 27, 29,

$$\frac{A_m}{D_m} = \frac{j\omega\mu\gamma b \cot\psi\, K_m'(\gamma b)}{G_{mm}(\gamma b, \gamma a)[\gamma^2 b - m\beta\cot\psi]} \quad -- \quad 5.1.30$$

Fields of Sheath Helix With Central Conducting Cylinder

$$E_z^i = A_m G_{mm}(\gamma r, \gamma a)\, e^{j m\theta}\, e^{-j\beta z} \qquad \text{5.1.31}$$

$$E_r^i = A_m\left[\frac{j\beta}{\gamma} G_{m'm}(\gamma r, \gamma a) - \frac{\omega\mu m}{\gamma^2 r}\,\frac{G_{mm}(\gamma b, \gamma a)\left[\gamma^2 b - m\beta\cot\psi\right]}{j\omega\mu\gamma b\cot\psi\, G_{m'm'}(\gamma b, \gamma a)}\, G_{mm'}(\gamma r, \gamma a)\right] e^{jm\theta} e^{-j\beta z} \qquad \text{5.1.32}$$

$$E_\theta^i = A_m\left[-\frac{m\beta}{\gamma^2 r} G_{mm}(\gamma r, \gamma a) - \frac{j\omega\mu}{\gamma}\,\frac{G_{mm}(\gamma b, \gamma a)\left[\gamma^2 b - m\beta\cot\psi\right]}{j\omega\mu\gamma b\cot\psi\, G_{m'm'}(\gamma b, \gamma a)}\, G_{m'm'}(\gamma r, \gamma a)\right] e^{jm\theta} e^{-j\beta z} \qquad \text{5.1.33}$$

$$H_z^i = A_m\left[\frac{G_{mm}(\gamma b, \gamma a)\left[\gamma^2 b - m\beta\cot\psi\right]}{j\omega\mu\gamma b\cot\psi\, G_{m'm'}(\gamma b, \gamma a)}\, G_{mm'}(\gamma r, \gamma a)\right] e^{jm\theta} e^{-j\beta z} \qquad \text{5.1.34}$$

$$H_r^i = A_m\left[\frac{j\beta}{\gamma}\,\frac{G_{mm}(\gamma b, \gamma a)\left[\gamma^2 b - m\beta\cot\psi\right]}{j\omega\mu\gamma b\cot\psi\, G_{m'm'}(\gamma b, \gamma a)}\, G_{m'm'}(\gamma r, \gamma a) + \frac{m\omega\varepsilon}{\gamma^2 r} G_{mm}(\gamma r, \gamma a)\right] e^{jm\theta} e^{-j\beta z} \qquad \text{5.1.35}$$

$$H_\theta^i = A_m\left[\frac{j\omega\varepsilon}{\gamma} G_{m'm}(\gamma r, \gamma a) - \frac{m\beta}{\gamma^2 r}\,\frac{G_{mm}(\gamma b, \gamma a)\left[\gamma^2 b - m\beta\cot\psi\right]}{j\omega\mu\gamma b\cot\psi\, G_{m'm'}(\gamma b, \gamma a)}\, G_{mm'}(\gamma r, \gamma a)\right] e^{jm\theta} e^{-j\beta z} \qquad \text{5.1.36}$$

$$E_z^a = A_m\,\frac{G_{mm}(\gamma b, \gamma a)}{K_m(\gamma b)} K_m(\gamma r)\, e^{jm\theta} e^{-j\beta z} \qquad \text{5.1.37}$$

$$E_r^a = A_m\left[\frac{j\beta}{\gamma}\,\frac{G_{mm}(\gamma b, \gamma a)}{K_m(\gamma b)} K_m'(\gamma r) - \frac{m\omega\mu}{\gamma^2 r}\,\frac{G_{mm}(\gamma b, \gamma a)\left[\gamma^2 b - m\beta\cot\psi\right]}{j\omega\mu\gamma b\cot\psi\, K_m'(\gamma b)} K_m(\gamma r)\right] e^{jm\theta} e^{-j\beta z} \qquad \text{5.1.38}$$

$$E_\theta^a = A_m\left[-\frac{j\omega\mu}{\gamma}\,\frac{G_{mm}(\gamma b, \gamma a)\left[\gamma^2 b - m\beta\cot\psi\right]}{j\omega\mu\gamma b\cot\psi\, K_m'(\gamma b)} K_m'(\gamma r) - \frac{m\beta}{\gamma^2 r}\,\frac{G_{mm}(\gamma b, \gamma a)}{K_m(\gamma b)} K_m(\gamma r)\right] e^{jm\theta} e^{-j\beta z} \qquad \text{5.1.39}$$

$$H_z^a = A_m\,\frac{G_{mm}(\gamma b, \gamma a)\left[\gamma^2 b - m\beta\cot\psi\right]}{j\omega\mu\gamma b\cot\psi\, K_m'(\gamma b)} K_m(\gamma r)\, e^{jm\theta} e^{-j\beta z} \qquad \text{5.1.40}$$

$$H_r^a = A_m\left[\frac{j\beta}{\gamma}\,\frac{G_{mm}(\gamma b, \gamma a)\left[\gamma^2 b - m\beta\cot\psi\right]}{j\omega\mu\gamma b\cot\psi\, K_m'(\gamma b)} K_m'(\gamma r) + \frac{m\omega\varepsilon}{\gamma^2 r}\,\frac{G_{mm}(\gamma b, \gamma a)}{K_m(\gamma b)} K_m(\gamma r)\right] e^{jm\theta} e^{-j\beta z} \qquad \text{5.1.41}$$

$$H_\theta^a = A_m\left[\frac{j\omega\varepsilon}{\gamma}\,\frac{G_{mm}(\gamma b, \gamma a)}{K_m(\gamma b)} K_m'(\gamma r) - \frac{m\beta}{\gamma^2 r}\,\frac{G_{mm}(\gamma b, \gamma a)\left[\gamma^2 b - m\beta\cot\psi\right]}{j\omega\mu\gamma b\cot\psi\, K_m'(\gamma b)} K_m(\gamma r)\right] e^{jm\theta} e^{-j\beta z} \qquad \text{5.1.42}$$

Characteristic Equation for Sheath Helix With Central Conducting Cylinder

From Equation 5.1.25

$$H_z^i + H_\theta^i \cot\psi = H_z^e + H_\theta^e \cot\psi$$

$$\frac{G_{mm}(\gamma b,\gamma a)[\gamma^2 b - m\beta\cot\psi]}{j\omega\mu\gamma b\cot\psi\, G_{m'm'}(\gamma b,\gamma a)} \cdot G_{mm'}(\gamma b,\gamma a) + \frac{j\omega\varepsilon\cot\psi}{\gamma} G_{m'm}(\gamma b,\gamma a)$$

$$- \frac{m\beta\cot\psi}{\gamma^2 b} \frac{G_{mm}(\gamma b,\gamma a)[\gamma^2 b - m\beta\cot\psi]}{j\omega\mu\gamma b\cot\psi\, G_{m'm}(\gamma b,\gamma a)} G_{mm'}(\gamma b,\gamma a)$$

$$= \frac{G_{mm}(\gamma b,\gamma a)[\gamma^2 b - m\beta\cot\psi]}{j\omega\mu\gamma b\cot\psi\, K_{m'}(\gamma b)} K_m(\gamma b) + \frac{j\omega\varepsilon\cot\psi}{\gamma} \frac{G_{mm}(\gamma b,\gamma a)}{K_m(\gamma b)} K_{m'}(\gamma b)$$

$$- \frac{m\beta\cot\psi}{\gamma^2 b} \frac{G_{mm}(\gamma b,\gamma a)[\gamma^2 b - m\beta\cot\psi]}{j\omega\mu\gamma b\cot\psi\, K_{m'}(\gamma b)} K_m(\gamma b) \qquad --- 5.1.43$$

Simplifying

$$\frac{G_{mm}(\gamma b,\gamma a)}{G_{m'm'}(\gamma b,\gamma a)} (\gamma^2 b - m\beta\cot\psi)\left[\left(1 - \frac{m\beta\cot\psi}{\gamma^2 b}\right)\left(G_{mm'}(\gamma b,\gamma a) - G_{m'm'}(\gamma b,\gamma a)\frac{K_m(\gamma b)}{K_{m'}(\gamma b)}\right)\right]$$

$$= k^2 b\cot^2\psi\left[G_{m'm}(\gamma b,\gamma a) - G_{mm}(\gamma b,\gamma a)\frac{K_{m'}(\gamma b)}{K_m(\gamma b)}\right] \qquad --- 5.1.44$$

Hence

$$\frac{k^2 b^2\gamma^2 b^2\cot^2\psi}{(\gamma^2 b^2 - m\beta b\cot\psi)^2} = -\frac{G_{mm}(\gamma b,\gamma a)}{G_{m'm'}(\gamma b,\gamma a)} \frac{K_m(\gamma b)}{K_{m'}(\gamma b)} \frac{K_{m'}(\gamma a)}{K_m(\gamma a)} \qquad --- 5.1.45$$

Note when a tends to zero this equation becomes

$$\frac{k^2 b^2\gamma^2 b^2\cot^2\psi}{(\gamma^2 b^2 - m\beta b\cot\psi)^2} = -\frac{K_m(\gamma b)}{K_{m'}(\gamma b)} \frac{\left[I_m(\gamma b) - K_m(\gamma b)\frac{I_m(\gamma a)}{K_m(\gamma a)}\right]}{\left[I'_m(\gamma b) - K_{m'}(\gamma b)\frac{I_{m'}(\gamma a)}{K_{m'}(\gamma a)}\right]}$$

$$= -\frac{K_m(\gamma b) I_m(\gamma b)}{K_{m'}(\gamma b) I_{m'}(\gamma b)} \qquad --- 5.1.46$$

This checks with Equation 2.1.27

5.1.1. Numerical Results for End-Fire Aerial

Some numerical results from Equation 5.1.45 are plotted for the -1 mode in Figure 5.1.2. with different ratios of central conductor to helix radius. The ratio $\frac{a}{b} = 0.05$ has been chosen as being representative of a mast used for support purposes. It is seen that the axial phase velocity variation with frequency is only slightly different from the case with no central mast, as far as upper frequency limit is concerned. The sheath helix approach, it will be remembered, gives no information about the lower frequency limit of the end-fire aerial, since the forbidden regions do not enter into its solution.

The slight increase in axial phase velocity which does exist will cause an increase of upper frequency limit which calculation shows to be of the order of 2-4% For the detection of this small increase a very carefully controlled experiment would have to be performed, and it is not surprising that this increase has not been observed. It is the author's opinion that with suitable equipment it should however be observable.

Increase of the conducting mast diameter raises the axial phase velocity still further as shown for the case $\frac{a}{b} = 0.9$ in the same diagram. This ratio has been chosen because it is close to the experimental value of 0.871 used for the Broadside Helical Aerial by Smith,[34] and avoids

FIG 5.1.2

SHEATH HELIX WITH COAXIAL CONDUCTING MAST :

PHASE VELOCITY VS CIRCUMFERENCE IN WAVELENGTHS

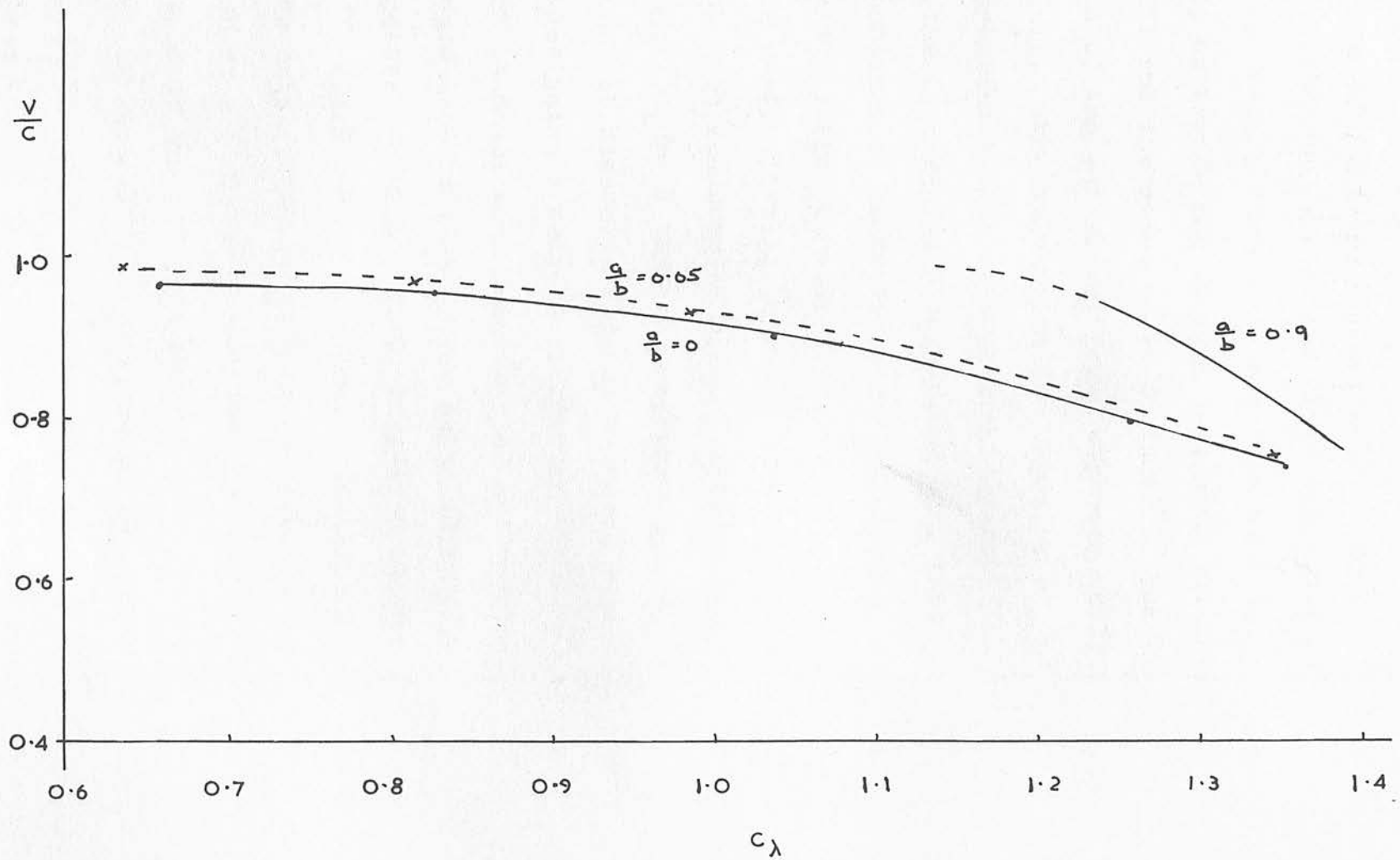

the interpolation in tables necessary with that value. When $\frac{a}{b}$ tends to unity the phase velocity will apprach the free space value as for the single wire transmission line.[22, 42].

5.1.2. Numerical Results for Broadside Aerial

The Broadside Helical Aerial as described by Smith[34] of Cornell University operates at a frequency corresponding to $c_\lambda \simeq 1.94$ when the ratio $\frac{a}{b}$ is 0.871 and the pitch angle ψ is 15°. The C_λ bandwidth of the aerial was found experimentally to be $< 1\%$. The explanation for choosing a circumferential length of approximately two wavelengths is given as a mechanical one, that the supporting mast necessary could not have a sufficiently large diameter if one wavelength per turn were used. It will be shown here that there is a much more fundamental reason, namely that it is not until $C_\lambda \simeq 2$ that the necessary phase conditions for broadside radiation become possible.

In designing a helical aerial for broadside radiation it might seem desirable to avoid a mode which would also radiate in the axial direction. This suggests avoiding a field variation of the form $e^{-j\theta}$, since such a wave travelling axially along the helix could be responsible for the radiation of a circularly polarised plane wave as in the case of the end-fire aerial. Any field variation of form $e^{-jm\theta}$, $m = 1$, could be expected to be superior in this respect.

Consequently, for the aerial described above

it would appear at first sight that m = 2 had been chosen. The calculated values of phase velocity for this case with $\psi = 13^{o}$ are shown in Fig. 5.1.3. for the two ratios $\frac{a}{b} = 0$ and $\frac{a}{b} = 0.9$. In order to locate the frequency of operation of such an aerial it is necessary to superimpose the phase variation with frequency for the broadside condition. This may be done as follows:-

The axial phase velocity v may be written as

$$v = \frac{w}{\beta} \qquad 5.1.47.$$

where w is the angular frequency and β is the axial phase shift per unit length.

For broadside radiation the array element currents must all be in phase, so that

$$\beta = \frac{2n\pi}{p} \qquad 5.1.48.$$

where n is an integer $\geqslant 0$, and p is the helical pitch. The value n = 0 however, implies infinite phase velocity in this case, and so may be excluded. For n = 1, which represents the highest finite axial phase velocity, Equation 5.1.47 may be written

$$v = fp \qquad 5.1.49$$

which in turn gives

$$\frac{v}{c} = C_{\lambda} \tan\psi \qquad 5.1.50$$

For $\psi = 13^{o}$ this does not intersect the curve for $\frac{a}{b} = 0.9$ within the range $C_{\lambda} < 2.65$ which has been plotted. While this range could readily be extended it is suggested that this is not the desired solution. If the -1 mode solution from

FIG 5.1.3

PHASE VELOCITY OF BROADSIDE HELICAL AERIAL

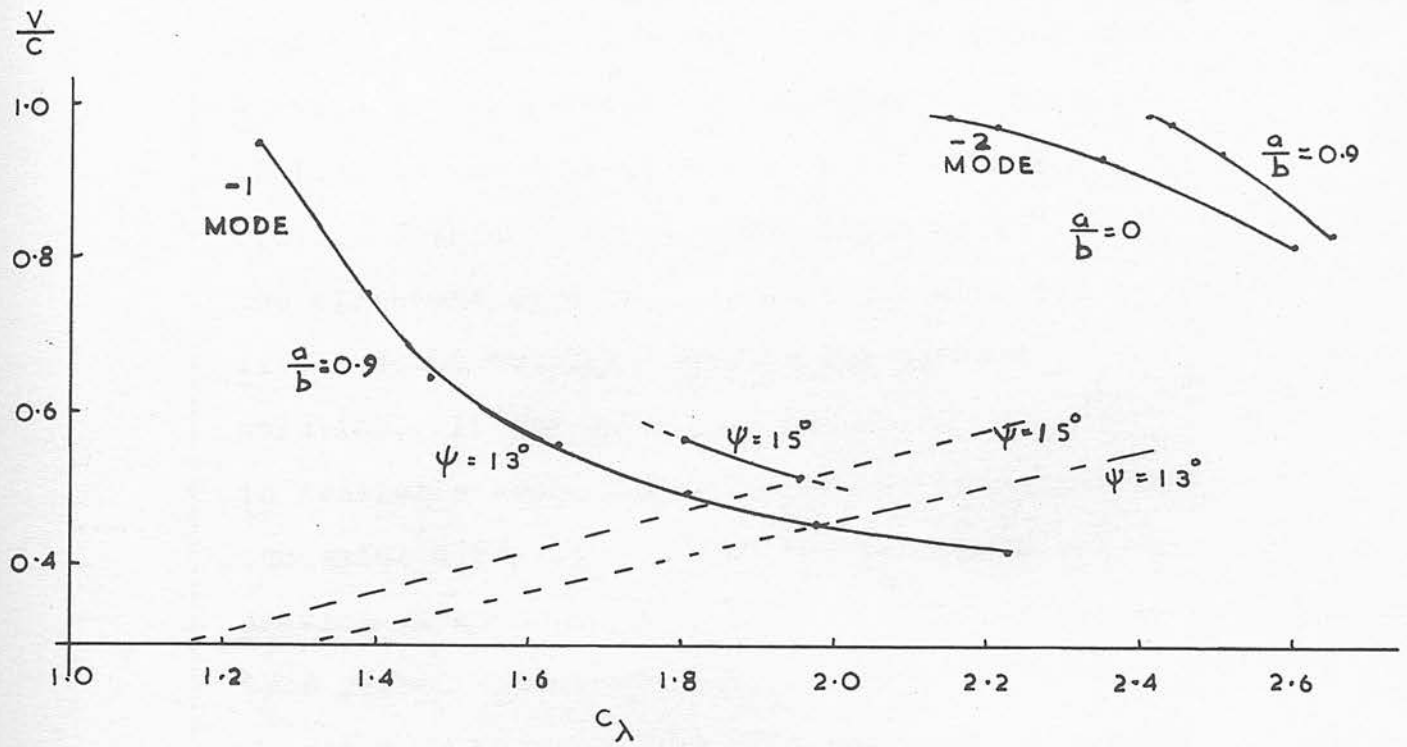

Figure 5.1.2. is extended however as shown in Figure 5.1.3. it is seen that a solution is obtained for $C_\lambda \simeq 1.96$. It must be remembered that this theoretical solution is applicable to the pitch angle of 15^o which has been used throughout with a ratio $\frac{a}{b} = 0.9$, while the experimental result of 1.94 is for a pitch angle of 15^o with $\frac{a}{b} = 0.871$. However, changing the angle to 15^o makes the agreement even better, so that there can be little doubt but that this is the correct solution. It may be noted that no information is available about radiation from this aerial in the axial direction, though the arguments previously advanced would suggest that this does take place. It is interesting that Reference 1 as cited by Kraus[19] shows this pronounced axial radiation for a helical aerial of similar type withouththe coaxial conducting cylinder.

It has been mentioned previously that the bandwidth of the Broadside Helical Aerial described by Smith has been found to be less than 1% The graphical construction used in Figure 5.1.3. shows clearly why this bandwidth is so much less than that of the End-Fire Aerial. There the necessary phase condition is a horizontal straight line for the axial phase velocity, while the theoretical solution begins by being horizontal and then diverges from this line. Here however the slope of the phase condition is positive, while that of the theoretical solution

is negative. Consequently there is a rapid divergence from the required phase condition for a small change of frequency.

Quantitatively, for a frequency change of 1% the phase velocity divergence can be estimated from the figure to be approximately 2%, corresponding to a phase shift of 7.2° between adjacent terms. The main beam of the aerial will therefore be swung away from the broadside position by an angle $\theta_o = \sin^{-1} \frac{\lambda\alpha}{2\pi p}$, where p is the helical pitch and α is the phase shift between sources. This gives a value of 2.5° for 1% frequency change, and the beam shift is proportional to frequency for angles such that the sine of the angle can be replaced by its radian measure. Hence the agreement with experiment can be regarded as satisfactory though an exact comparison is not possible, since the criterion for determining bandwidth used by Smith is not given in his paper.

5.2. Tape Helix Solution

Equations 5.1.1. to 5.1.21 for the Sheath Helix solution are also applicable to the solution for the tape helix when the subscript m is added to the field quantities on the left side of these equations, and to γ and β on the right side.

Boundary Conditions at r = b

$$E_z^i = E_z^e \quad -- \quad 5.2.1$$

$$E_\theta^i = E_\theta^e \quad -- \quad 5.2.2$$

$$H_z^i - H_z^e = J_\theta \quad -- \quad 5.2.3$$

$$H_\theta^e - H_\theta^i = J_z \quad -- \quad 5.2.4$$

From Equation 5.2.1.

$$\frac{A_m}{C_m} = \frac{K_m(\gamma_m b)}{G_{mm}(\gamma_m b, \gamma_m a)} \quad -- \quad 5.2.5$$

From Equation 5.2.2.

$$\left[-\frac{j\omega\mu}{\gamma_m} B_m G_{m'm'}(\gamma_m b, \gamma_m a) - \frac{m\beta_m}{\gamma_m^2 b} A_m G_{mm}(\gamma_m b, \gamma_m a)\right]$$

$$= \left[-\frac{j\omega\mu}{\gamma_m} D_m K_m'(\gamma_m b) - \frac{m\beta_m}{\gamma_m^2 b} C_m K_m(\gamma_m b)\right] \quad -- \quad 5.2.6$$

From Equation 5.2.3.

$$B_m G_{mm'}(\gamma_m b, \gamma_m a) - D_m K_m(\gamma_m b) = j_{\theta m} \quad -- \quad 5.2.7$$

From Equation 5.2.4.

$$\frac{j\omega\varepsilon}{\gamma_m} C_m K_m'(\gamma_m b) - \frac{m\beta_m}{\gamma_m^2 b} D_m K_m(\gamma_m b) - \frac{j\omega\varepsilon}{\gamma_m} A_m G_{m'm}(\gamma_m b, \gamma_m a)$$

$$+ \frac{m\beta_m}{\gamma_m^2 b} B_m G_{mm'}(\gamma_m b, \gamma_m a) = j_{zm} \quad -- \quad 5.2.8$$

Substituting for B_m in Equation 5.2.8. from Equation 5.2.7. gives

$$A_m = \frac{\gamma_m^2 b\, j_{zm} - m\beta_m j_{\theta m}}{\gamma_m^2 b} \cdot \frac{\gamma_m K_m(\gamma_m b)}{j\omega\varepsilon\left[G_{mm}(\gamma_m b, \gamma_m a) K_m'(\gamma_m b) - G_{m'm}(\gamma_m b, \gamma_m a) K_m(\gamma_m b)\right]}$$

$$-- \quad 5.2.9$$

From Equations 5.2.5. to 5.2.7.

$$D_m = j\theta_m \frac{G_{m'm'}(\gamma_m b, \gamma_m a)}{K_{m'}(\gamma_m b) G_{m'm'}(\gamma_m b, \gamma_m a) - K_m(\gamma_m b) G_{m'm'}(\gamma_m b, \gamma_m a)} \quad \text{--- 5.2.10}$$

Then

$$B_m = j\theta_m \frac{K_{m'}(\gamma_m b)}{K_{m'}(\gamma_m b) G_{mm'}(\gamma_m b, \gamma_m a) - K_m(\gamma_m b) G_{m'm'}(\gamma_m b, \gamma_m a)} \quad \text{--- 5.2.11}$$

From Equation 5.2.9

$$E^i_{zm} = \frac{\gamma_m K_m(\gamma_m b) G_{mm}(\gamma_m r, \gamma_m a) [\gamma_m^2 b\, j z_m - m\beta_m j\theta_m]}{j\omega\varepsilon [G_{mm}(\gamma_m b, \gamma_m a) K_{m'}(\gamma_m b) - G_{m'm}(\gamma_m b, \gamma_m a) K_m(\gamma_m b)] \gamma_m^2 b} \quad \text{--- 5.2.12}$$

i.e.

$$E^i_{zm} = \frac{-(\gamma_m b)^2}{j\omega\varepsilon b} \frac{K_m(\gamma_m b) G_{mm}(\gamma_m r, \gamma_m a)}{K_m(\gamma_m a)} \left(j z_m - \frac{m\beta_m}{\gamma_m^2 b} j\theta_m\right) \quad \text{--- 5.2.13}$$

since $$G_{mm'}(\gamma_m b, \gamma_m b) = -\frac{1}{\gamma_m b} \quad \text{--- 5.2.14}$$

From Equations 5.2.9. and 5.2.11.

$$E^i_{\theta m} = -\frac{j\omega\mu}{\gamma_m} B_m G_{m'm'}(\gamma_m r, \gamma_m a) - \frac{m\beta_m}{\gamma_m^2 b} A_m G_{mm}(\gamma_m r, \gamma_m a) \quad \text{--- 5.2.15}$$

simplifies to

$$E^i_{\theta m} = -\frac{j\omega\mu}{\gamma_m} j\theta_m \frac{K_{m'}(\gamma_m b) G_{m'm'}(\gamma_m r, \gamma_m a)}{K_{m'}(\gamma_m a) G_{mm'}(\gamma_m b, \gamma_m b)} - \frac{m\beta_m}{\gamma_m} \frac{\left(j z_m - \frac{m\beta_m}{\gamma_m^2 b} j\theta_m\right) \gamma_m K_m(\gamma_m b) G_{mm}(\gamma_m r, \gamma_m a)}{j\omega\varepsilon \quad K_m(\gamma_m a)} \quad \text{--- 5.2.16}$$

which further simplifies to

$$E^i_{\theta m} = j\theta_m \frac{-\omega^2\mu\varepsilon \gamma_m^2 b^2 K_{m'}(\gamma_m b) K_m(\gamma_m a) G_{m'm'}(\gamma_m r, \gamma_m a) - m^2\beta_m^2 K_m(\gamma_m b) K_{m'}(\gamma_m a) G_{mm}(\gamma_m r, \gamma_m a)}{j\gamma_m^2 a\omega\varepsilon K_m(\gamma_m a) K_{m'}(\gamma_m a)}$$

$$+ j z_m \frac{m\beta_m K_m(\gamma_m b) G_{mm}(\gamma_m r, \gamma_m a)}{j\omega\varepsilon K_m(\gamma_m a)} \quad \text{--- 5.2.17}$$

Making use of

$$E_{11m} = E_{zm} \sin\psi + E_{\theta m} \cos\psi \quad \text{--- 5.2.18}$$

$$j z_m = j_{11m} \sin\psi \quad \text{--- 5.2.19}$$

and

$$j\theta_m = j_{11m} \cos\psi \quad \text{--- 5.2.20}$$

as in the case of the simple tape helix, there results/

results

$$E_{\parallel m} = \left\{ \frac{-(\gamma_m b)^2}{j\omega\varepsilon b} \frac{K_m(\gamma_m b)\, G_{mm}(\gamma_m r, \gamma_m a)}{K_m(\gamma_m a)} \left[j_{\parallel m} \sin^2\psi - \frac{m\beta_m}{\gamma_m^2 b} j_{\parallel m} \sin\psi\cos\psi \right] \right.$$

$$+ j_{\parallel m} \cos^2\psi \; \frac{-\omega^2\mu\varepsilon\gamma_m^2 b^2 K_m'(\gamma_m b) K_m(\gamma_m a) G_{mm}'(\gamma_m r, \gamma_m a) - m^2\beta_m^2 K_m(\gamma_m b) K_m'(\gamma_m a) G_{mm}^{(\gamma_m r, \gamma_m a)}}{j\gamma_m^2 b\, \omega\varepsilon K_m(\gamma_m a) K_m'(\gamma_m a)}$$

$$\left. + \frac{m\beta_m K_m(\gamma_m b)\, G_{mm}(\gamma_m r, \gamma_m a)}{j\omega\varepsilon\, K_m(\gamma_m a)} j_{\parallel m} \cos\psi \sin\psi \right\} e^{-j\beta_0 z} e^{jm\theta} e^{-j\frac{2\pi m z}{h}}$$

— — — 5.2.21

which simplfies for r = b to

$$E_{\parallel m}\Big|_{r=b} = j \frac{e^{-j\beta_0 z} \sin^2\psi}{\omega\varepsilon b} \left\{ \frac{K_m(\gamma_m b)}{K_m(\gamma_m a)} \left[(\gamma_m b)^2 - 2m\beta_m b \cot\psi + \frac{m^2\beta_m^2 b^2}{\gamma_m^2 b^2} \cot^2\psi \right] \right.$$

$$G_{mm}(\gamma_m b, \gamma_m a)$$

$$\left. + k^2 b^2 \frac{K_m'(\gamma_m b)}{K_m'(\gamma_m a)} \cot^2\psi \; G_{m'm'}(\gamma_m b, \gamma_m a) \right\} e^{jm\theta} e^{-j\frac{2\pi m z}{h}} j_{\parallel m}$$

— — — 5.2.22

Since

$$E_{\parallel}\Big|_{r=b} = \sum_m E_{\parallel m}\Big|_{r=b}$$

— — — 5.2.23

$$E_{\parallel}\Big|_{r=b} = \frac{j e^{-j\beta_0 z} \sin^2\psi}{\omega\varepsilon b} \sum_m \left\{ \frac{K_m(\gamma_m b)}{K_m(\gamma_m a)} \left[\gamma_m^2 b^2 - 2m\beta_m b \cot\psi + \frac{m^2\beta_m^2 b^2 \cot^2\psi}{\gamma_m^2 b^2} \right] \right.$$

$$G_{mm}(\gamma_m b, \gamma_m a)$$

$$\left. + k^2 b^2 \cot^2\psi \frac{K_m'(\gamma_m b)}{K_m'(\gamma_m a)} G_{m'm'}(\gamma_m b, \gamma_m a) \right\} e^{jm\theta} e^{-j\frac{2\pi m z}{h}} j_{\parallel m}$$

— — — 5.2.24

Setting this expression equal to zero along the centre line of the tape at $z = \frac{h\theta}{2\pi} + \frac{\delta}{2}$ and using Equation 2.2.17 gives finally

$$0 = \sum_m \left\{ \left[\gamma_m^2 b^2 - 2m\beta_m b \cot\psi + \frac{m^2\beta_m^2 b^2 \cot^2\psi}{\gamma_m^2 b^2} \right] \frac{K_m(\gamma_m b)}{K_m(\gamma_m a)} G_{mm}(\gamma_m b, \gamma_m a) \right.$$

$$\left. + k^2 b^2 \cot^2\psi \frac{K_m'(\gamma_m b)}{K_m'(\gamma_m a)} G_{m'm'}(\gamma_m b, \gamma_m a) \right\} \frac{\sin\frac{\beta_m\delta}{2}}{\frac{\beta_m\delta}{2}}$$

— — — 5.2.25

5.2.2. Solution of Characteristic Equation for Tape Helix with Coaxial Conducting Cylinder

Although Equation 5.2.25 is of similar form to the characteristic equation of the Simple Helix it is unfortunately much less amenable to computation. A procedure is available as shown by Sensiper[14] and Watkins[21] for makin Equation 2.2.33 more rapidly convergent, by means of suitable approximations for the products $I_m(\gamma_m b) K_m(\gamma_m b)$ and $I_m'(\gamma_m b) K_m'(\gamma_m b)$. No similar approximations are known to the author for the more complicated functions that appear in Equation 5.2.25. Arrangements have accordingly been made to have the computations carried out by the digital computer at Ohio State University. Although these exact results are not yet available it is possible to estimate the solution when $\frac{a}{b}$ is small, as follows.

Consider the case when $\frac{a}{b}$ is 0.05 and the pitch angle ψ is 13°. It is known from the Sheath Helix solution that the phase velocity v will be increased by the presence of the coaxial conducting cylinder. However, at the low frequency end when $C_\lambda \simeq 0.8$ the existing solution for no conducting cylinder is so close to the edge of the forbidden region (see Figure 3.3.1) that the new solution cannot be significantly different from it though it is always above the first one. To the scale on

which the graph is drawn however the two solutions cannot be separated.

At the upper frequency limit it is not possible to estimate the solution so easily or accurately. However, a comparison of the most significant term in each of the two series for $\frac{a}{b}$ equal to 0 and 0.05 shows that they differ by only 1.25%. Since a change in the value of v of only 0.5% produces a change of the order of 50% in this same term for $\frac{a}{b}$ equal to zero, it is reasonable to assume that the change of v is again negligible. Consequently as mentioned in the discussion on the Sheath Helix, it is not surprising that no change in the bandwidth of the aerial has been observed. It is not at this stage possible to discuss whether such a change should be observeable, as was done with the Sheath Helix.

No numerical results for the case of $\frac{a}{b}$ equal to 0.9 are available, but it should be noted that the solutions for the Sheath and Tape Helices can be expected to converge when $\frac{a}{b}$ tends to unity. This may be responsible for the good agreement which was obtained with the Sheath Helix for $\frac{a}{b}$ equal to 0.9. The calculations to be performed on the digital computer will include this ratio, so as to complete this aspect of the investigation.

CHAPTER VI

Wave Propagation Along Tape Helix Wound on Dielectric Tube.

It is frequently necessary in model tests on helical aerials to wind the helical conductor on a dielectric former in order to provide it with mechanical support. The following analysis has been undertaken to obtain a formal solution to this problem so that the effect of the former on the bandwidth may be calculated. It will be seen, however, that the solution presents severe computational difficulties.

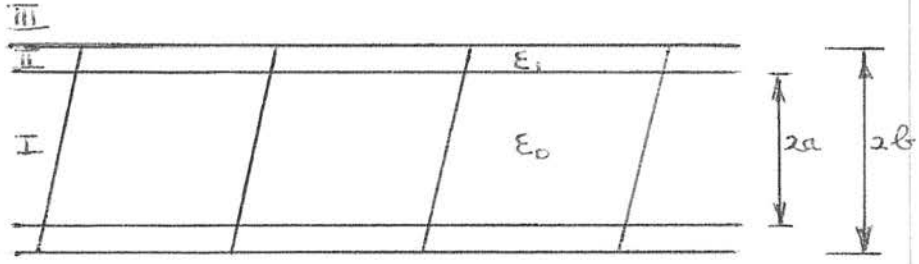

FIG 6.1

Region I $0 < r < a$

Let $E'_{zm} = A'_m I_m(\gamma_m r) e^{j m\theta} e^{-j\beta_m z}$ — — 6.1.1

$H'_{zm} = B'_m I_m(\gamma_m r) e^{j m\theta} e^{-j\beta_m z}$ — — 6.1.2

Hence

$$E'_{\theta m} = \left[-\frac{j\omega\mu}{\gamma_m} B'_m I'_m(\gamma_m r) - \frac{m\beta_m}{\gamma_m^2 r} A'_m I_m(\gamma_m r)\right] e^{j m\theta} e^{-j\beta_m z} \quad — \quad 6.1.3$$

$$E'_{rm} = \left[\frac{j\beta_m}{\gamma_m} A'_m I'_m(\gamma_m r) - \frac{\omega\mu m}{\gamma_m^2 r} B'_m I_m(\gamma_m r)\right] e^{j m\theta} e^{-j\beta_m z} \quad — \quad 6.1.4$$

$$H'_{\theta m} = \left[\frac{j\omega\varepsilon_0}{\gamma_m} A'_m I'_m(\gamma_m r) - \frac{m\beta_m}{\gamma_m^2 r} B'_m I_m(\gamma_m r)\right] e^{j m\theta} e^{-j\beta_m z} \quad — \quad 6.1.5$$

$$H'_{rm} = \left[\frac{j\beta_m}{\gamma_m} B'_m I'_m(\gamma_m r) + \frac{m\omega\varepsilon_0}{\gamma_m^2 r} A'_m I_m(\gamma_m r)\right] e^{j m\theta} e^{-j\beta_m z} \quad — \quad 6.1.6$$

Region II $a < r < b$

Note in this section the superscript 2 denotes/

denotes the second region and is not the symbol for the square of a field. Also the symbols which are primed denote propagation in the dielectric medium.

Let $E^2_{zm} = \left[A^2_m I_m(\gamma'_m r) + B^2_m K_m(\gamma'_m r) \right] e^{j m\theta} e^{-j\beta_m z}$ — 6.1.7

$H^2_{zm} = \left[C^2_m I_m(\gamma'_m r) + D^2_m K_m(\gamma'_m r) \right] e^{j m\theta} e^{-j\beta_m z}$ — 6.1.8

Hence

$$E^2_{rm} = \left\{ \frac{j\beta_m}{\gamma'_m} \left[A^2_m I'_m(\gamma'_m r) + B^2_m K'_m(\gamma'_m r) \right] - \frac{m\omega\mu}{\gamma'^2_m r} \left[C^2_m I_m(\gamma'_m r) + D^2_m K_m(\gamma'_m r) \right] \right\} e^{j m\theta} e^{-j\beta_m z} \quad \text{— 6.1.9}$$

$$E^2_{\theta m} = \left\{ -\frac{j\omega\mu}{\gamma'_m} \left[C^2_m I'_m(\gamma'_m r) + D^2_m K'_m(\gamma'_m r) \right] - \frac{m\beta_m}{\gamma'^2_m r} \left[A^2_m I_m(\gamma'_m r) + B^2_m K_m(\gamma'_m r) \right] \right\} e^{j m\theta} e^{-j\beta_m z} \quad \text{— 6.1.10}$$

$$H^2_{rm} = \left\{ \frac{j\beta_m}{\gamma'_m} \left[C^2_m I'_m(\gamma'_m r) + D^2_m K'_m(\gamma'_m r) \right] - \frac{m\beta_m}{\gamma'^2_m r} \left[A^2_m I_m(\gamma'_m r) + B^2_m K_m(\gamma'_m r) \right] \right\} e^{j m\theta} e^{-j\beta_m z} \quad \text{— 6.1.11}$$

$$H^2_{\theta m} = \left\{ \frac{j\omega\varepsilon_1}{\gamma'_m} \left[A^2_m I'_m(\gamma'_m r) + B^2_m K'_m(\gamma'_m r) \right] - \frac{m\beta_m}{\gamma'^2_m r} \left[C^2_m I_m(\gamma'_m r) + D^2_m K_m(\gamma'_m r) \right] \right\} e^{j m\theta} e^{-j\beta_m z} \quad \text{— 6.1.12}$$

Region III $b < r < \infty$

The superscript 3 used here denotes the third region, and is not the symbol for a cube.

Let $E^3_{zm} = A^3_m K_m(\gamma_m r) e^{j m\theta} e^{-j\beta_m z}$ — 6.1.13

$H^3_{zm} = B^3_m K_m(\gamma_m r) e^{j m\theta} e^{-j\beta_m z}$ — 6.1.14

Then

$E^3_{\theta m} = \left[-\frac{j\omega\mu}{\gamma_m} B^3_m K'_m(\gamma_m r) - \frac{m\beta_m}{\gamma^2_m r} A^3_m K_m(\gamma_m r) \right] e^{j m\theta} e^{-j\beta_m z}$ — 6.1.15

$E^3_{rm} = \left[\frac{j\beta_m}{\gamma_m} A^3_m K'_m(\gamma_m r) - \frac{\omega\mu m}{\gamma^2_m r} B^3_m K_m(\gamma_m r) \right] e^{j m\theta} e^{-j\beta_m z}$ — 6.1.16

$H^3_{\theta m} = \left[\frac{j\omega\varepsilon}{\gamma_m} A^3_m K'_m(\gamma_m r) - \frac{m\beta_m}{\gamma^2_m r} B^3_m K_m(\gamma_m r) \right] e^{j m\theta} e^{-j\beta_m z}$ — 6.1.17

$H^3_{rm} = \left[\frac{j\beta_m}{\gamma_m} B^3_m K'_m(\gamma_m r) + \frac{m\omega\varepsilon}{\gamma^2_m r} A^3_m K_m(\gamma_m r) \right] e^{j m\theta} e^{-j\beta_m z}$ — 6.1.18

Boundary Conditions

At r = a	At r = b
$E_z^1 = E_z^2$ — 6.1.19	$E_z^2 = E_z^3$ — 6.1.23
$E_\theta^1 = E_\theta^2$ — 6.1.20	$E_\theta^2 = E_\theta^3$ — 6.1.24
$H_z^1 = H_z^2$ — 6.1.21	$H_z^2 - H_z^3 = J_\theta$ — 6.1.25
$H_\theta^1 = H_\theta^2$ — 6.1.22	$H_\theta^3 - H_\theta^2 = J_z$ — 6.1.26

From 6.1.19

$$A_m^1 I_m(\gamma_m a) - A_m^2 I_m(\gamma_m^1 a) - B_m^2 K_m(\gamma_m^1 a) = 0 \quad — \quad 6.1.27$$

From 6.1.20

$$-\frac{j\omega\mu}{\gamma_m} B_m^1 I_m'(\gamma_m a) - \frac{m\beta_m}{\gamma_m^2 a} A_m^1 I_m(\gamma_m a) + \frac{j\omega\mu}{\gamma_m^1}\left[C_m^2 I_m'(\gamma_m^1 a) + D_m^2 K_m'(\gamma_m^1 a)\right]$$
$$+ \frac{m\beta_m}{\gamma_m^{12} a}\left[A_m^2 I_m(\gamma_m^1 a) + B_m^2 K_m(\gamma_m^1 a)\right] = 0 \quad — \quad 6.1.28$$

From 6.1.21

$$B_m^1 I_m(\gamma_m a) - C_m^2 I_m(\gamma_m^1 a) - D_m^2 K_m(\gamma_m^1 a) = 0 \quad — \quad 6.1.29$$

From 6.1.22

$$\frac{j\omega\varepsilon_0}{\gamma_m} A_m^1 I_m'(\gamma_m a) - \frac{m\beta_m}{\gamma_m^2 a} B_m^1 I_m(\gamma_m a) - \frac{j\omega\varepsilon_1}{\gamma_m^1}\left[A_m^2 I_m'(\gamma_m^1 a) + B_m^2 K_m'(\gamma_m^1 a)\right]$$
$$+ \frac{m\beta_m}{\gamma_m^{12} a}\left[C_m^2 I_m(\gamma_m^1 a) + D_m^2 K_m(\gamma_m^1 a)\right] = 0 \quad — \quad 6.1.30$$

From 6.1.23

$$A_m^2 I_m(\gamma_m^1 b) + B_m^2 K_m(\gamma_m^1 b) - A_m^3 K_m(\gamma_m b) = 0 \quad — \quad 6.1.31$$

From 6.1.24

$$-\frac{j\omega\mu}{\gamma_m^1}\left[C_m^2 I_m'(\gamma_m^1 b) + D_m^2 K_m'(\gamma_m^1 b)\right] - \frac{m\beta_m}{\gamma_m^{12} b}\left[A_m^2 I_m(\gamma_m^1 b) + B_m^2 K_m(\gamma_m^1 b)\right]$$
$$+ \frac{j\omega\mu}{\gamma_m} B_m^3 K_m'(\gamma_m b) + \frac{m\beta_m}{\gamma_m^2 b} A_m^3 K_m(\gamma_m b) = 0 \quad — \quad 6.1.32$$

From 6.1.25

$$C_m^2 I_m(\gamma_m^1 b) + D_m^2 K_m(\gamma_m^1 b) - B_m^3 K_m(\gamma_m b) = j_{\beta m} \quad — \quad 6.1.33$$

From 6.1.26

$$\frac{j\omega\varepsilon_0}{\gamma_m} A_m^3 K_m'(\gamma_m b) - \frac{m\beta_m}{\gamma_m^2 b} B_m^3 K_m(\gamma_m b) - \frac{j\omega\varepsilon_1}{\gamma_m^1}\left[A_m^2 I_m'(\gamma_m^1 b) + B_m^2 K_m'(\gamma_m^1 b)\right]$$
$$+ \frac{m\beta_m}{\gamma_m^{12} b}\left[C_m^2 I_m(\gamma_m^1 b) + D_m^2 K_m(\gamma_m^1 b)\right] = j z_m \quad — \quad 6.1.34$$

Coefficients

A_m^3	B_m^3	C_m^2	D_m^2	A_m^2	B_m^2	A_m^1	B_m^1	
0	0	0	0	$-I_m(\gamma_m' a)$	$-K_m(\gamma_m' a)$	$I_m(\gamma_m a)$	0	$=0$
0	0	$\frac{j\omega\mu}{\gamma_m'} I_m'(\gamma_m' a)$	$\frac{j\omega\mu}{\gamma_m'} K_m'(\gamma_m' a)$	$\frac{m\beta_m}{\gamma_m'^2 a} I_m(\gamma_m' a)$	$\frac{m\beta_m}{\gamma_m'^2 a} K_m(\gamma_m' a)$	$-\frac{m\beta_m}{\gamma_m^2 a} I_m(\gamma_m a)$	$-\frac{j\omega\mu}{\gamma_m} I_m'(\gamma_m a)$	$=0$
0	0	$-I_m(\gamma_m' a)$	$-K_m(\gamma_m' a)$	0	0	0	$I_m(\gamma_m a)$	$=0$
0	0	$\frac{m\beta_m}{\gamma_m'^2 a} I_m(\gamma_m' a)$	$\frac{m\beta_m}{\gamma_m'^2 a} K_m(\gamma_m' a)$	$-\frac{j\omega\varepsilon_1}{\gamma_m'} I_m'(\gamma_m' a)$	$-\frac{j\omega\varepsilon_1}{\gamma_m'} K_m'(\gamma_m' a)$	$\frac{j\omega\varepsilon_0}{\gamma_m} I_m'(\gamma_m a)$	$-\frac{m\beta_m}{\gamma_m^2 a} I_m(\gamma_m a)$	$=0$
$-K_m(\gamma_m b)$	0	0	0	$I_m(\gamma_m' b)$	$K_m(\gamma_m' b)$	0	0	$=0$
$\frac{m\beta_m}{\gamma_m^2 b} K_m(\gamma_m b)$	$\frac{j\omega\mu}{\gamma_m} K_m'(\gamma_m b)$	$-\frac{j\omega\mu}{\gamma_m'} I_m'(\gamma_m' b)$	$-\frac{j\omega\mu}{\gamma_m'} K_m'(\gamma_m' b)$	$\frac{-m\beta_m}{\gamma_m'^2 b} I_m(\gamma_m' b)$	$-\frac{m\beta_m}{\gamma_m'^2 b} K_m(\gamma_m' b)$	0	0	$=0$
0	$-K_m(\gamma_m b)$	$I_m(\gamma_m' b)$	$K_m(\gamma_m' b)$	0	0	0	0	$=j\alpha_m$
$\frac{j\omega\varepsilon_0}{\gamma_m} K_m'(\gamma_m b)$	$-\frac{m\beta_m}{\gamma_m^2 b} K_m(\gamma_m b)$	$\frac{m\beta_m}{\gamma_m'^2 b} I_m(\gamma_m' b)$	$\frac{m\beta_m}{\gamma_m'^2 b} K_m(\gamma_m' b)$	$-\frac{j\omega\varepsilon_1}{\gamma_m'} I_m'(\gamma_m' b)$	$-\frac{j\omega\varepsilon_1}{\gamma_m'} K_m'(\gamma_m' b)$	0	0	$=j\alpha_m$

In order to simplify the evaluation of the forthcoming determinants, the following abbreviations will be used,

$-I_m(\gamma_m' a) = a$

$-K_m(\gamma_m' a) = b$

$I_m(\gamma_m a) = c$

$\frac{j\omega\mu}{\gamma_m'} I_m'(\gamma_m' a) = d$

$\frac{j\omega\mu}{\gamma_m'} K_m'(\gamma_m' a) = e$

$\frac{m\beta_m}{\gamma_m'^2 a} I_m(\gamma_m' a) = f$

$\frac{m\beta_m}{\gamma_m'^2 a} K_m(\gamma_m' a) = g$

$\frac{-m\beta_m}{\gamma_m^2 a} I_m(\gamma_m a) = h$

$-\frac{j\omega\mu}{\gamma_m} I_m'(\gamma_m a) = k$

$-\frac{j\omega\varepsilon_1}{\gamma_m'} I_m'(\gamma_m' a) = m$

$-\frac{j\omega\varepsilon_1}{\gamma_m'} K_m'(\gamma_m' a) = n$

$\frac{j\omega\varepsilon_0}{\gamma_m} I_m'(\gamma_m a) = p$

$-K_m(\gamma_m b) = q$

$I_m(\gamma_m' b) = r$

$K_m(\gamma_m' b) = s$

$\frac{m\beta_m}{\gamma_m^2 b} K_m(\gamma_m b) = t$

$\frac{j\omega\mu}{\gamma_m} K_m'(\gamma_m b) = u$

$-\frac{j\omega\mu}{\gamma_m'} I_m'(\gamma_m' b) = v$

$-\frac{j\omega\mu}{\gamma_m'} K_m'(\gamma_m' b) = w$

$\frac{-m\beta_m}{\gamma_m'^2 b} I_m(\gamma_m' b) = x$

$-\frac{m\beta_m}{\gamma_m'^2 b} K_m(\gamma_m' b) = y$

$\frac{j\omega\varepsilon_0}{\gamma_m} K_m'(\gamma_m b) = z$

$-\frac{j\omega\varepsilon_1}{\gamma_m'} I_m'(\gamma_m' b) = \alpha$

$-\frac{j\omega\varepsilon_1}{\gamma_m'} K_m'(\gamma_m' b) = \lambda$

$j\theta_m = \delta$

$j z_m = \gamma$

— — 6.1.43

Then $A_m^3 = \frac{D_2}{D_1}$

where $D_1 =$

$$\begin{vmatrix} 0 & 0 & 0 & 0 & a & b & c & 0 \\ 0 & 0 & d & e & f & g & h & k \\ 0 & 0 & a & b & 0 & 0 & 0 & c \\ 0 & 0 & f & g & m & n & t & h \\ q & 0 & 0 & 0 & r & s & 0 & 0 \\ t & u & v & w & x & y & 0 & 0 \\ 0 & q & r & s & 0 & 0 & 0 & 0 \\ z & -t & -x & -y & \alpha & \lambda & 0 & 0 \end{vmatrix}$$

and $D_2 =$

$$\begin{vmatrix} 0 & 0 & 0 & 0 & a & b & c & 0 \\ 0 & 0 & d & e & f & g & h & k \\ 0 & 0 & a & b & 0 & 0 & 0 & 0 \\ 0 & 0 & f & g & m & n & t & h \\ 0 & 0 & 0 & 0 & r & s & 0 & 0 \\ 0 & u & v & w & x & y & 0 & 0 \\ s & q & r & s & 0 & 0 & 0 & 0 \\ r & -t & -x & -y & \alpha & \lambda & 0 & 0 \end{vmatrix}$$

Similarly $B_m{}^3 = \frac{D_3}{D_1}$

where $D_3 =$

$$\begin{vmatrix}
0 & 0 & 0 & 0 & a & b & c & 0 \\
0 & 0 & d & e & f & g & h & k \\
0 & 0 & a & b & 0 & 0 & 0 & c \\
0 & 0 & f & g & m & n & p & h \\
q & 0 & 0 & 0 & r & s & 0 & 0 \\
t & 0 & v & w & x & y & 0 & 0 \\
0 & \delta & \gamma & \varepsilon & 0 & 0 & 0 & 0 \\
\zeta & \eta & -x & -y & \alpha & \lambda & 0 & 0
\end{vmatrix}$$

Reduction of these determinants follows in the usual way[25]. Details of the manipulations will be omitted however as the work involved is straightforward, though laborious. After much algebra they simplify to,

$$D_1 = -\frac{cd}{a^3}(ae - bd) \times$$

$$\begin{vmatrix}
c(an - bm) & (ap - cm) & (ah - cf) \\
q(ay - bx) & (pt - xq) - & (av - qv) - \frac{(ah - cd)}{c(ae - bd)} \times \\
-t(as - br) & \frac{(ah - cf)}{c(ae - bd)}[q(av - bv) - u(as - br)] & [-q(av - bv) - u(as - br)] \\
-q(a\lambda - bd) & (\zeta p - dq) - & (qx - tv) - \frac{(ah - cd)}{c(ae - bd)} \times \\
-\zeta(as - br) & \frac{(ah - cf)}{c(ae - bd)}[q(bx - ay) + t(as - br)] & [q(bx - ay) + t(as - br)]
\end{vmatrix}$$

$$D_2 = \frac{1}{a^2 b} \times$$

$$\begin{vmatrix} (ae-bd) & (as-br)(ah-cf) & (ak-cd) \\ 0 & (as-br)(ap-cm) + cr(an-bm) & (ah-cf) \\ (aw-br)(q\tau+ts) + u\delta(bx-ay) - u\tau(as-br) & u\delta ca(r\lambda-\alpha s) & -cw(q\tau+ts) + uc(\alpha\delta+\tau r) \end{vmatrix}$$

$$D_3 = -\frac{(ae-bd)}{a^2 br(as-br)} \times$$

$$\begin{vmatrix} -q(an-bm) & (as-br)(ap-cm) + cr(an-bm) & (ah-cf) \\ t(as-br) - q(ay-bx) & cr(ay-bx) - c\alpha(as-br) - \frac{(aw-br)}{(ae-bd)}(as-br)(ah-cf) & -cw - \frac{(aw-br)(ak-cd)}{(ae-bd)} \\ \delta z(as-br) - \delta q(a\lambda-b\alpha) & cr\delta(a\lambda-b\alpha) - c\alpha\delta(as-br) - \frac{(as-br)(ah-cf)}{(ae-bd)}[\delta(bx-ay) - \tau(as-br)] & c(\alpha\delta+\tau r) - \frac{(ak-cd)}{(ae-bd)} \times [\delta(bx-ay) - \tau(as-br)] \end{vmatrix}$$

The evaluation of these determinants in terms of the modified Bessel Functions does not lead to a solution which can be described as simple. This is to be expected since even for the simpler case of wave propagation along a dielectric tube without any helix, the results obtained by Astrahan[26] are of considerable complexity.

In order to obtain a solution which can conveniently/

conveniently be written on one page, it is desirable to introduce further notation as follows:

Let

$$(ae-bd) = \Delta_1 = \frac{j\omega\mu}{\gamma_m'^2 a}$$

$$(fn-bm) = \Delta_2 = -\frac{j\omega\varepsilon}{\gamma_m'^2 a}$$

$$(af-cm) = \Delta_3 = -\frac{j\omega\varepsilon_0}{\gamma_m} I_m'(\gamma_m a) I_m(\gamma_m' a) + \frac{j\omega\varepsilon_1}{\gamma_m'} I_m'(\gamma_m' a) I_m(\gamma_m a)$$

$$(ah-cf) = \Delta_4 = \frac{m\beta_m}{a} I_m(\gamma_m a) I_m(\gamma_m' a)\left(\frac{1}{\gamma_m^2} - \frac{1}{\gamma_m'^2}\right)$$

$$(ag-bc) = \Delta_5 = \frac{m\beta_m}{\gamma_m'^2 b} G_{mm}(\gamma_m' a, \gamma_m' b)$$

$$(as-br) = \Delta_6 = -G_{mm}(\gamma_m' a, \gamma_m' b)$$

$$(rt-xq) = \Delta_7 = \frac{m\beta_m}{b} I_m(\gamma_m' b) K_m(\gamma_m b)\left(\frac{1}{\gamma_m^2} - \frac{1}{\gamma_m'^2}\right)$$

$$(au-bv) = \Delta_8 = \frac{j\omega\mu}{\gamma_m'} G_{mm'}(\gamma_m' a, \gamma_m' b) \qquad -- 6.1.44$$

$$(uv-qv) = \Delta_9 = \frac{j\omega\mu}{\gamma_m} I_m(\gamma_m' b) K_m'(\gamma_m b) - \frac{j\omega\mu}{\gamma_m'} I_m'(\gamma_m' b) K_m(\gamma_m b)$$

$$(ak-cd) = \Delta_{10} = \frac{j\omega\mu}{\gamma_m} I_m(\gamma_m' a) I_m'(\gamma_m a) - \frac{j\omega\mu}{\gamma_m'} I_m(\gamma_m a) I_m'(\gamma_m' a)$$

$$(a\lambda - b\alpha) = \Delta_{11} = \frac{j\omega\varepsilon_1}{\gamma_m'} G_{mm'}(\gamma_m' a, \gamma_m' b)$$

$$(gv-dq) = \Delta_{12} = \frac{j\omega\varepsilon_0}{\gamma_m} I_m(\gamma_m' b) K_m'(\gamma_m b) - \frac{j\omega\varepsilon_1}{\gamma_m'} I_m'(\gamma_m' b) K_m(\gamma_m b)$$

$$(q\tau + ts) = \Delta_{13} = K_m(\gamma_m b)\left[-jz_m + \frac{m\beta_m}{\gamma_m^2 b} j\theta_m\right] = j_{11m}\Delta_{13}^{i}$$

$$(\alpha s + \tau r) = \Delta_{14} = -I_m(\gamma_m' b)\left[-jz_m + \frac{m\beta_m}{\gamma_m'^2 b} j\theta_m\right] = j_{11m}\Delta_{14}^{i}$$

$$(r\lambda - ds) = \Delta_{15} = -\frac{j\omega\varepsilon_1}{\gamma_m'} G_{mm'}(\gamma_m' b, \gamma_m' b) = \frac{j\omega\varepsilon_1}{\gamma_m'^2 b}$$

where

$$G_{mm}(\gamma_m' a, \gamma_m' b) = I_m(\gamma_m' a) K_m(\gamma_m' b) - K_m(\gamma_m' a) I_m(\gamma_m' b) \qquad -- 6.1.45$$

$$G_{mm'}(\gamma_m' a, \gamma_m' b) = I_m(\gamma_m' a) K_m'(\gamma_m' b) - K_m(\gamma_m' a) I_m'(\gamma_m' b) \qquad -- 6.1.46$$

Then D_1

$$= -\frac{cd}{a^3}\Delta_1\Big\{c\Delta_2\Big[\Big[\Delta_7 - \frac{\Delta_4}{c\Delta_1}(q\Delta_8 - u\Delta_6)\Big]\Big[-\Delta_7 - \frac{\Delta_{10}}{c\Delta_1}(-q\Delta_5 + t\Delta_6)\Big]$$
$$-\Big[\Delta_9 - \frac{\Delta_{10}}{c\Delta_1}(q\Delta_8 - u\Delta_6)\Big]\Big[\Delta_{12} - \frac{\Delta_4}{c\Delta_1}(-q\Delta_5 + t\Delta_6)\Big]\Big]$$
$$+\Delta_3\Big[\Big[\Delta_9 - \frac{\Delta_{10}}{c\Delta_1}(q\Delta_8 - u\Delta_6)\Big]\Big[q\Delta_{11} - z\Delta_6\Big]$$
$$-\Big[-\Delta_7 - \frac{\Delta_{10}}{c\Delta_1}(-q\Delta_5 + t\Delta_6)\Big]\Big[q\Delta_5 - t\Delta_6\Big]\Big]$$
$$+\Delta_4\Big[\Big[q\Delta_5 - t\Delta_6\Big]\Big[\Delta_{12} - \frac{\Delta_4}{c\Delta_1}(-q\Delta_5 + t\Delta_6)\Big]$$
$$-\Big[q\Delta_{11} - z\Delta_6\Big]\Big[\Delta_7 - \frac{\Delta_4}{c\Delta_1}(q\Delta_8 - u\Delta_6)\Big]\Big]\Big\} \quad -- \ 6.1.47$$

Similarly D_2

$$= \frac{1}{a^2 b}\Big\{\Delta_1\Big[\Big[\Delta_6\Delta_3 + cr\Delta_2\Big]\Big[-cr\Delta_{13} + uc\Delta_{14}\Big] - \Delta_4\Big[u\delta ca\Delta_{15}\Big]\Big]$$
$$+\Delta_6\Delta_4\Big[\Big[\Delta_4\Big]\Big[\Delta_8\Delta_{13} - u\delta\Delta_5 - u\tilde{\iota}\Delta_6\Big]\Big]$$
$$+\Delta_{10}\Big[-\Big[\Delta_6\Delta_3 + cr\Delta_2\Big]\Big[\Delta_8\Delta_{13} - u\delta\Delta_5 - u\tilde{\iota}\Delta_6\Big]\Big]\Big\} \quad -- \ 6.1.48$$

$$= \frac{jlm}{a^2 b}\Big\{\Delta_1\Big[(\Delta_6\Delta_3 + cr\Delta_2)(-cr\Delta_{13}^1 + uc\Delta_{14}^1) - u\cos\psi ca\Delta_{15}\Delta_4\Big]$$
$$+\Big[\Delta_8\Delta_{13}^1 - u\cos\psi\Delta_5 - u\sin\psi\Delta_6\Big]\Big[\Delta_6\Delta_4^2 - \Delta_{10}(\Delta_6\Delta_3 + cr\Delta_2)\Big]\Big\}$$

so that

$$A_m^3 = \frac{D_2}{D_1}$$
$$= jlm\,\frac{\frac{1}{a^2 b}\Big\{\Delta_1\Big[\Delta_6\Delta_3 + cr\Delta_2)(-cr\Delta_{13}^1 + uc\Delta_{14}^1) - u\cos\psi ca\Delta_{15}\Delta_4\Big] + \Big[\Delta_8\Delta_{13}^1 - u\cos\psi\Delta_5 - u\sin\psi\Delta_6\Big]\Big[\Delta_6\Delta_4^2 - \Delta_{10}(\Delta_6\Delta_3 + cr\Delta_2)\Big]\Big\}}{D_1 \text{ as above}}$$

$$-- \ 6.1.49$$

Also D_3

$$= -\frac{\Delta_1}{a^2 b \Delta_6}\Bigg\{ -q\Delta_2\Bigg[\Big[c\gamma\Delta_5 - c\alpha\Delta_6 - \frac{\Delta_8\Delta_6\Delta_4}{\Delta_1}\Big]\Big[c\Delta_{14} - \frac{\Delta_{10}}{\Delta_1}\big(-\delta\Delta_5 - \gamma\Delta_6\big)\Big]$$

$$- \Big[c\gamma\delta\Delta_{11} - c\alpha\delta\Delta_6 - \frac{\Delta_6\Delta_4}{\Delta_1}\big(-\delta\Delta_5 - \gamma\Delta_6\big)\Big]\Big[-c\gamma - \frac{\Delta_8\Delta_{10}}{\Delta_1}\Big]$$

$$+ \big(\Delta_6\Delta_3 + c\gamma\Delta_2\big)\Bigg[\Big[-c\gamma - \frac{\Delta_8\Delta_{10}}{\Delta_1}\Big]\big[\delta\gamma\Delta_6 - \delta q\Delta_{11}\big]$$

$$- \big[t\Delta_6 - q\Delta_5\big]\Big[c\Delta_{14} - \frac{\Delta_{10}}{\Delta_1}\big(-\delta\Delta_5 - \gamma\Delta_6\big)\Big]\Bigg]$$

$$+ \Delta_4\Bigg[\big[t\Delta_6 - q\Delta_5\big]\Big[c\gamma\delta\Delta_{11} - c\alpha\delta\Delta_6 - \frac{\Delta_6\Delta_4}{\Delta_1}\big(-\delta\Delta_5 - \gamma\Delta_6\big)\Big]$$

$$- \big[\delta\gamma\Delta_6 - \delta q\Delta_{11}\big]\Big[c\gamma\Delta_5 - c\alpha\Delta_6 - \frac{\Delta_8\Delta_6\Delta_4}{\Delta_1}\Big]\Bigg]\Bigg\} \qquad -- 6.1.50$$

so that

$$B_m^{\,3} = \frac{D_3}{D_1}$$

$$-\frac{\Delta_1}{a^2 b \Delta_6}\Bigg\{ -q\Delta_2\Bigg[\Big[c\gamma\Delta_5 - c\alpha\Delta_6 - \frac{\Delta_4\Delta_6\Delta_8}{\Delta_1}\Big]\Big[c\Delta_{14}' - \frac{\Delta_{10}}{\Delta_1}\big(-\cos\psi\Delta_5 - \sin\psi\Delta_6\big)\Big]$$

$$- \Big[c\gamma\cos\psi\Delta_{11} - c\alpha\cos\psi\Delta_6 - \frac{\Delta_4\Delta_6}{\Delta_1}\big(-\cos\psi\Delta_5 - \sin\psi\Delta_6\big)\Big]\Big[-c\gamma - \frac{\Delta_8\Delta_{10}}{\Delta_1}\Big]\Bigg]$$

$$+ \big(\Delta_3\Delta_6 + c\gamma\Delta_2\big)\Bigg[\Big[-c\gamma - \frac{\Delta_8\Delta_{10}}{\Delta_1}\Big]\big[\cos\psi\gamma\Delta_6 - \cos\psi q\Delta_{11}\big]$$

$$- \big[t\Delta_6 - q\Delta_5\big]\Big[c\Delta_{14}' - \frac{\Delta_{10}}{\Delta_1}\big(-\cos\psi\Delta_5 - \sin\psi\Delta_6\big)\Big]\Bigg]$$

$$+ \Delta_4\Bigg[\big[t\Delta_6 - q\Delta_5\big]\Big[c\gamma\cos\psi\Delta_{11} - c\alpha\cos\psi\Delta_6 - \frac{\Delta_4\Delta_6}{\Delta_1}\big(-\cos\psi\Delta_5 - \sin\psi\Delta_6\big)\Big]$$

$$- \big[\cos\psi\gamma\Delta_6 - \sin\psi q\Delta_{11}\big]\Big[c\gamma\Delta_5 - c\alpha\Delta_6 - \frac{\Delta_4\Delta_6\Delta_8}{\Delta_1}\Big]\Bigg]\Bigg\}$$

$$= j_{11m} \qquad\qquad D_1 \qquad\qquad -- 6.1.51$$

At $r = b$,

$$E^3_{zm} = A^3_m K_m(\gamma_m b)\, e^{j m\theta}\, e^{-j\beta_m z} \qquad -- 6.1.13$$

$$E^3_{\theta m} = \left[-\frac{j\omega\mu}{\gamma_m} B^3_m K'_m(\gamma_m b) - \frac{m\beta_m}{\gamma_m^2 b} A^3_m K_m(\gamma_m b) \right] e^{j m\theta}\, e^{-j\beta z} \qquad -- 6.1.15.$$

Then since

$$E_{\parallel m}\Big|_{r=b} = E^3_{zm} \sin\psi + E^3_{\theta m} \cos\psi$$

$$= \left\{ A^3_m \left[K_m(\gamma_m b) \sin\psi - \frac{m\beta_m}{\gamma_m^2 b} K_m(\gamma_m b) \cos\psi \right] - B^3_m \frac{j\omega\mu}{\gamma_m} K'_m(\gamma_m b) \cos\psi \right\} e^{j m\theta}\, e^{-j\beta_m z} \qquad -- 6.1.52$$

and since $E_{\parallel}\big|_{r=b}$ has to be equated to zero along the centre line of the tape, these results for the characteristic equation:-

$$\Big[K_m(\gamma_m b)\Big(\sin\psi - \frac{m\beta_m}{\gamma_m^2 b}\cos\psi\Big)\times$$

$$\frac{1}{\alpha^2 b}\Big\{\Delta_1\Big[(\Delta_3\Delta_6 + cr\,\Delta_2)\Big(-cr\,\Delta_{13}' + \mu c\,\Delta_{14}'\Big) - \mu\cos\psi\,\alpha\,\Delta_4\Delta_{15}\Big]$$

$$+\Big[\Delta_8\Delta_{13}' - \mu\cos\psi\,\Delta_5 - \mu\sin\psi\,\Delta_6\Big]\Big[\Delta_6\Delta_4^2 - \Delta_{16}(\Delta_3\Delta_6 + cr\,\Delta_2)\Big]\Big\}$$

$$+\frac{j\omega\mu}{\gamma_m}K_m'(\gamma_m b)\cos\psi\,\frac{\Delta_1}{\alpha^2 b\,\Delta_6}\Big\{-q\,\Delta_2\Big[\Big[cr\,\Delta_5 - c\alpha\,\Delta_6 - \frac{\Delta_4\Delta_6\Delta_8}{\Delta_1}\Big]$$

$$\Big[c\Delta_{14}' - \frac{\Delta_{10}}{\Delta_1}(-\cos\psi\,\Delta_5 - \sin\psi\,\Delta_6)\Big]$$

$$-\Big[cr\cos\psi\,\Delta_{11} - c\alpha\cos\psi\,\Delta_6 - \frac{\Delta_4\Delta_6}{\Delta_1}(-\cos\psi\,\Delta_5 - \sin\psi\,\Delta_6)\Big]\Big[-cr - \frac{\Delta_8\Delta_{10}}{\Delta_1}\Big]\Big]$$

$$+(\Delta_3\Delta_6 + cr\,\Delta_2)\Big[\Big[-cr - \frac{\Delta_8\Delta_{10}}{\Delta_1}\Big]\Big[\cos\psi\,\gamma\,\Delta_6 - \cos\psi\,q\,\Delta_{11}\Big]$$

$$-\Big[t\Delta_6 - q\,\Delta_5\Big]\Big[c\Delta_{14}' - \frac{\Delta_{10}}{\Delta_1}(-\cos\psi\,\Delta_5 - \sin\psi\,\Delta_6)\Big]\Big]$$

$$+\Delta_4\Big[\Big[t\Delta_6 - q\Delta_5\Big]\Big[cr\,\Delta_{11}\cos\psi - c\alpha\,\Delta_6\cos\psi - \frac{\Delta_4\Delta_6}{\Delta_1}\Big(-\Delta_5\cos\psi - \Delta_6\sin\psi\Big)\Big]$$

$$-\Big[\gamma\,\Delta_6\cos\psi - q\,\Delta_{11}\sin\psi\Big]\Big[cr\,\Delta_5 - c\alpha\,\Delta_6 - \frac{\Delta_4\Delta_6\Delta_8}{\Delta_1}\Big]\Big]\Big]\Big]\frac{\sin\frac{\beta_m\delta}{2}}{\frac{\beta_m\delta}{2}}$$

$$0 \doteq \sum_m \frac{}{}$$

$$-\frac{cd}{a^3}\Delta_1\Big\{c\Delta_2\Big[\Big[\Delta_7 - \frac{\Delta_4}{c\Delta_1}(q\Delta_8 - \mu\Delta_6)\Big]\Big[-\Delta_7 - \frac{\Delta_{10}}{c\Delta_1}(-q\Delta_5 + t\Delta_6)\Big]$$

$$-\Big[\Delta_9 - \frac{\Delta_{10}}{c\Delta_1}(q\Delta_8 - \mu\Delta_6)\Big]\Big[\Delta_{12} - \frac{\Delta_4}{c\Delta_1}(-q\Delta_5 + t\Delta_6)\Big]\Big]$$

$$+\Delta_3\Big[\Big[\Delta_9 - \frac{\Delta_{10}}{c\Delta_1}(q\Delta_8 - \mu\Delta_6)\Big]\Big[q\Delta_{11} - \gamma\Delta_6\Big]$$

$$-\Big[-\Delta_7 - \frac{\Delta_{10}}{c\Delta_1}(-q\Delta_5 + t\Delta_6)\Big]\Big[q\Delta_5 - t\Delta_6\Big]\Big]$$

$$+\Delta_4\Big[\Big[q\Delta_5 - t\Delta_6\Big]\Big[\Delta_{12} - \frac{\Delta_4}{c\Delta_1}(-q\Delta_5 + t\Delta_6)\Big]$$

$$-\Big[q\Delta_{11} - \gamma\Delta_6\Big]\Big[\Delta_7 - \frac{\Delta_4}{c\Delta_1}(q\Delta_8 - \mu\Delta_6)\Big]\Big]\Big\}$$

— — — 6.1.53

It is desirable to check the solution for the case $\varepsilon_1 = \varepsilon_0$ i.e. when the dielectric disappears to leave the simple helix alone. In this case from Equation 6.1.44, $\Delta_3 = \Delta_4 = \Delta_7 = \Delta_{10} = 0$

Hence the characterstic equation becomes

$$0 = \sum_m \frac{\left\{ K_m(\gamma_m b)\left(\sin\psi - \frac{m\beta_m}{\gamma_m^2 b}\cos\psi\right)\frac{1}{a^2 b}\left[c^2 \gamma \Delta_1 \Delta_2 \left(-v\Delta_{13}^{i} + u\Delta_{14}^{i}\right)\right] + \frac{j\omega\mu}{\gamma_m} K_m'(\gamma_m b)\cos\psi \frac{\Delta_1}{a^2 b \Delta_6}\left[c^2 v \cos\psi \Delta_2 \Delta_6 (q\alpha - \gamma z)\right]\right\}\left(\frac{\sin\frac{\beta_m \delta}{2}}{\frac{\beta_m \delta}{2}}\right)}{\frac{c^2 d}{a^3}\Delta_1 \Delta_2 \Delta_9 \Delta_{12}} \quad \text{-- 6.1.54}$$

This readily simplifies to

$$0 = \sum_m \frac{\left\{ \frac{j\omega\mu}{\gamma_m}\frac{1}{\gamma_m b}\frac{k^2}{(\gamma_m^2 a)^2}\frac{I_m(\gamma_m b) K_m(\gamma_m b)}{K_m(\gamma_m a)}\sin^2\psi\left(1 - \frac{m\beta_m}{\gamma_m^2 b}\cot\psi\right)^2 - \frac{j\omega\mu}{\gamma_m}\frac{k^4 K_m'(\gamma_m b) I_m'(\gamma_m b)\cos^2\psi}{(\gamma_m^2 a^2)^2 \gamma_m^2 \gamma_m b K_m(\gamma_m a)}\right\}\left(\frac{\sin\frac{\beta_m \delta}{2}}{\frac{\beta_m \delta}{2}}\right)}{\frac{j\omega\mu}{\gamma_m}\frac{I_m'(\gamma_m a)}{I_m(\gamma_m a)}\frac{k^4}{(\gamma_m^2 a)^2}\frac{1}{(\gamma_m^2 b)^2}} \quad \text{-- 6.1.55}$$

from which by equating the numerator to zero there follows

$$0 = \sum_m \left\{\left[\gamma_m^2 b^2 - 2m\beta_m b\cot\psi + \frac{m^2\beta_m^2 b^2 \cot^2\psi}{\gamma_m^2 b^2}\right] I_m(\gamma_m b) K_m(\gamma_m b) + k^2 b^2 \cot^2\psi\, I_m'(\gamma_m b) K_m'(\gamma_m b)\right\}\frac{\sin\frac{\beta_m \delta}{2}}{\frac{\beta_m \delta}{2}} \quad \text{-- 6.1.56}$$

This checks with Equation 2.2.33

CHAPTER VII

Wave Propagation Along Two Coaxial Sheath Helices

This problem has been studied for the case of travelling-wave tubes by Wade[27] and the treatment here merely extends his analysis so that it may be of use to the problem of two coaxial helical aerials. Some experimental work on the aerial aspect has been carried out by Ko[28] at Ohio State University, but his results up to the present have been restricted to one particular length of aerial. It is clear from these results which showed effective use of only the inner aerial that some mathematical analysis is necessary for their interpretation. More experimental work is also necessary, particularly for varying lengths of aerial, to find out whether energy transfer of the kind one would expect from coupled-mode theory takes place. Only the formal solution of the problem is given here.

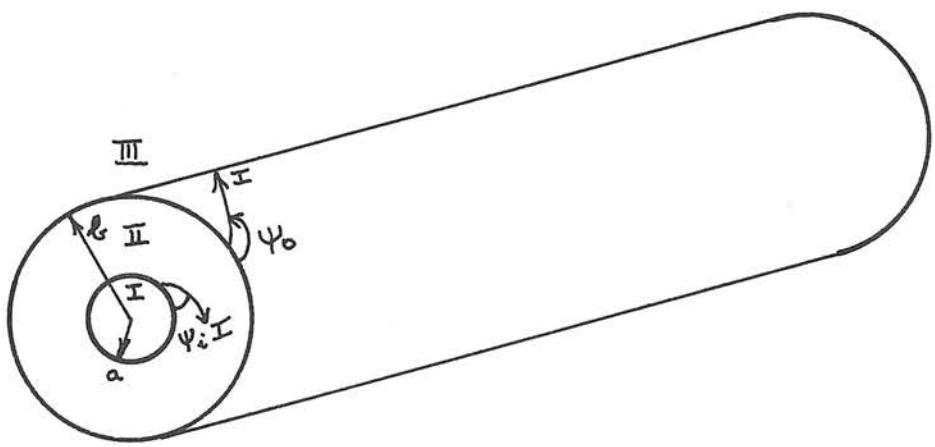

FIG 7.1

Region I $\quad o < r < a$

Let

$$E_{z_i} = A_m^i I_m(\gamma r)\, e^{j m\theta}\, e^{-j\beta z} \qquad -\ -\ 7.1.1$$

$$H_{z_i} = B_m^i I_m(\gamma r)\, e^{j m\theta}\, e^{-j\beta z} \qquad -\ -\ 7.1.2$$

Hence

$$E_{\theta_i} = \left[-\frac{m\beta}{\gamma^2 r} A_m^i I_m(\gamma r) - \frac{j\omega\mu}{\gamma} B_m^i I_m'(\gamma r)\right] e^{j m\theta}\, e^{-j\beta z} \qquad -\ -\ 7.1.3$$

$$E_{r_i} = \left[\frac{j\beta}{\gamma} A_m^i I_m'(\gamma r) - \frac{\omega\mu m}{\gamma^2 r} B_m^i I_m(\gamma r)\right] e^{j m\theta}\, e^{-j\beta z} \qquad -\ -\ 7.1.4$$

$$H_{\theta_i} = \left[\frac{j\omega\varepsilon}{\gamma} A_m^i I_m'(\gamma r) - \frac{m\beta}{\gamma^2 r} B_m^i I_m(\gamma r)\right] e^{j m\theta}\, e^{-j\beta z} \qquad -\ -\ 7.1.5$$

$$H_{r_i} = \left[\frac{m\omega\varepsilon}{\gamma^2 r} A_m^i I_m(\gamma r) + \frac{j\beta}{\gamma} B_m^i I_m'(\gamma r)\right] e^{j m\theta}\, e^{-j\beta z} \qquad -\ -\ 7.1.6$$

Region II $\quad a < r < b$

Let

$$E_{z_2} = \left[C_{m1} I_m(\gamma r) + C_{m2} K_m(\gamma r)\right] e^{j m\theta}\, e^{-j\beta z} \qquad -\ -\ 7.1.7$$

$$H_{z_2} = \left[C_{m3} I_m(\gamma r) + C_{m4} K_m(\gamma r)\right] e^{j m\theta}\, e^{-j\beta z} \qquad -\ -\ 7.1.8$$

Then

$$E_{\theta_2} = \left\{-\frac{j\omega\mu}{\gamma}\left[C_{m3} I_m'(\gamma r) + C_{m4} K_m'(\gamma r)\right] - \frac{m\beta}{\gamma^2 r}\left[C_{m1} I_m(\gamma r) + C_{m2} K_m(\gamma r)\right]\right\} \times e^{j m\theta}\, e^{-j\beta z} \qquad -\ -\ 7.1.9$$

$$E_{r_2} = \left\{\frac{j\beta}{\gamma}\left[C_{m1} I_m'(\gamma r) + C_{m2} K_m'(\gamma r)\right] - \frac{\omega\mu m}{\gamma^2 r}\left[C_{m3} I_m(\gamma r) + C_{m4} K_m(\gamma r)\right]\right\} \times e^{j m\theta}\, e^{-j\beta z} \qquad -\ -\ 7.1.10$$

$$H_{\theta_2} = \left\{\frac{j\omega\varepsilon}{\gamma}\left[C_{m1} I_m'(\gamma r) + C_{m2} K_m'(\gamma r)\right] - \frac{m\beta}{\gamma^2 r}\left[C_{m3} I_m(\gamma r) + C_{m4} K_m(\gamma r)\right]\right\} \times e^{j m\theta}\, e^{-j\beta z} \qquad -\ -\ 7.1.11$$

$$H_{r_2} = \left\{\frac{j\beta}{\gamma}\left[C_{m3} I_m'(\gamma r) + C_{m4} K_m'(\gamma r)\right] + \frac{m\omega\varepsilon}{\gamma^2 r}\left[C_{m1} I_m(\gamma r) + C_{m2} K_m(\gamma r)\right]\right\} \times e^{j m\theta}\, e^{-j\beta z} \qquad -\ -\ 7.1.12$$

Region III $b < r < \infty$

Let

$$E_{z3} = A_m^e K_m(\gamma r) e^{j m\theta} e^{-j\beta z} \quad -- 7.1.13$$

$$H_{z3} = B_m^e K_m(\gamma r) e^{j m\theta} e^{-j\beta z} \quad -- 7.1.14$$

Hence

$$E_{\theta 3} = \left[-\frac{m\beta}{\gamma^2 r} A_m^e K_m(\gamma r) - \frac{j\omega\mu}{\gamma} B_m^e K_m'(\gamma r) \right] e^{j m\theta} e^{-j\beta z} \quad -- 7.1.15$$

$$E_{r3} = \left[\frac{j\beta}{\gamma} A_m^e K_m'(\gamma r) - \frac{m\omega\mu}{\gamma^2 r} B_m^e K_m(\gamma r) \right] e^{j m\theta} e^{-j\beta z} \quad -- 7.1.16$$

$$H_{\theta 3} = \left[\frac{j\omega\varepsilon}{\gamma} A_m^e K_m'(\gamma r) - \frac{m\beta}{\gamma^2 r} B_m^e K_m(\gamma r) \right] e^{j m\theta} e^{-j\beta z} \quad -- 7.1.17$$

$$H_{r3} = \left[\frac{m\omega\varepsilon}{\gamma^2 r} A_m^e K_m(\gamma r) + \frac{j\beta}{\gamma} B_m^e K_m'(\gamma r) \right] e^{j m\theta} e^{-j\beta z} \quad -- 7.1.18$$

Boundary Conditions

At $r = a$	At $r = b$
$E_{z1} = -E_{\theta 1} \cot\psi_i$ — 7.1.19	$E_{z3} = -E_{\theta 3} \cot\psi_o$ — 7.1.23
$E_{z1} = E_{z2}$ — — 7.1.20	$E_{z2} = E_{z3}$ — — 7.1.24
$E_{\theta 1} = E_{\theta 2}$ — — 7.1.21	$E_{\theta 2} = E_{\theta 3}$ — — 7.1.25
$H_{z1} = H_{z2} + H_{\theta 2}\cot\psi_i - H_{\theta 1}\cot\psi_i$ — — 7.1.22	$H_{z2} = H_{z3} + H_{\theta 3}\cot\psi_o - H_{\theta 2}\cot\psi_o$ — — 7.1.26

From 7.1.19

$$A_m^i I_m(\gamma a)\left[1 - \frac{m\beta\cot\psi_i}{\gamma^2 a}\right] - \frac{j\omega\mu}{\gamma} B_m^i I_m'(\gamma a)\cot\psi_i = 0 \quad -- 7.1.27$$

From 7.1.20

$$A_m^i I_m(\gamma a) - C_{m1} I_m(\gamma a) - C_{m2} K_m(\gamma a) = 0 \quad -- 7.1.28$$

From 7.1.21

$$-\frac{m\beta}{\gamma^2 a} A_m^i I_m(\gamma a) - \frac{j\omega\mu}{\gamma} B_m^i I_m'(\gamma a) + \frac{m\beta}{\gamma^2 a} C_{m1} I_m(\gamma a)$$

$$+\frac{m\beta}{\gamma^2 a} C_{m2} K_m(\gamma a) + \frac{j\omega\mu}{\gamma} C_{m3} I_m'(\gamma a) + \frac{j\omega\mu}{\gamma} C_{m4} K_m'(\gamma a) = 0 \quad -- 7.1.29$$

From 7.1.22

$$\frac{j\omega\varepsilon}{\gamma}\cot\psi_i A_m^i I_m'(\gamma a) + B_m^i I_m(\gamma a)\left[1 - \frac{m\beta\cot\psi_i}{\gamma^2 a}\right] - \frac{j\omega\varepsilon\cot\psi_i}{\gamma} C_{m1} I_m'(\gamma a)$$

$$-\frac{j\omega\varepsilon}{\gamma}\cot\psi_i C_{m2} K_m'(\gamma a) - C_{m3} I_m(\gamma a)\left[1 - \frac{m\beta\cot\psi_i}{\gamma^2 a}\right] - C_{m4} K_m(\gamma a)\left[1 - \frac{m\beta\cot\psi_i}{\gamma^2 a}\right] = 0$$

From 7.1.26 — — 7.1.30

$$-\frac{j\omega\varepsilon}{\gamma}\cot\psi_o I_m'(\gamma b) - \frac{j\omega\varepsilon}{\gamma}\cot\psi_o K_m'(\gamma b) - C_{m3} I_m(\gamma b)\left[1 - \frac{m\beta\cot\psi_o}{\gamma^2 b}\right]$$

$$-C_{m4} K_m(\gamma b)\left[1 - \frac{m\beta\cot\psi_o}{\gamma^2 b}\right] + A_m^e \frac{j\omega\varepsilon}{\gamma}\cot\psi_o K_m'(\gamma b) + B_m^e K_m(\gamma b)\left[1 - \frac{m\beta\cot\psi_o}{\gamma^2 b}\right] = 0 \quad 7.1.31$$

From 7.1.25

$$-\frac{m\beta}{\gamma^2 a} C_{m1} I_m(\gamma a) - \frac{m\beta}{\gamma^2 a} C_{m2} K_m(\gamma a) - \frac{j\omega\mu}{\gamma} C_{m3} I_m'(\gamma a)$$

$$-\frac{j\omega\mu}{\gamma} C_{m4} K_m'(\gamma a) + \frac{m\beta}{\gamma^2 a} A_m^e K_m(\gamma a) + \frac{j\omega\mu}{\gamma} B_m^e K_m'(\gamma a) = 0 \quad -- \quad 7.1.32$$

From 7.1.24

$$-C_{m1} I_m(\gamma a) \quad -C_{m2} K_m(\gamma a) + A_m^e K_m(\gamma a) \quad = 0 \quad -- \quad 7.1.33$$

From 7.1.23

$$A_m^e K_m(\gamma a)\left[1 - \frac{m\beta \cot\psi_0}{\gamma^2 a}\right] - B_m^e \frac{j\omega\mu}{\gamma} \cot\psi_0 K_m'(\gamma a) = 0 \quad -- \quad 7.1.34$$

A_m^i	B_m^i	C_{m1}	C_{m2}	C_{m3}	C_{m4}	A_m^e	B_m^e	
$I_m(\gamma a)\left[1-\frac{m\beta\cot\psi_i}{\gamma^2 a}\right]$	$-\frac{j\omega\mu}{\gamma}\cot\psi_i I_m'(\gamma a)$	0	0	0	0	0	0	$=0$
$-I_m(\gamma a)$	0	$I_m(\gamma a)$	$K_m(\gamma a)$	0	0	0	0	$=0$
$\frac{-m\beta}{\gamma^2 a} I_m(\gamma a)$	$-\frac{j\omega\mu}{\gamma} I_m'(\gamma a)$	$\frac{m\beta}{\gamma^2 a} I_m(\gamma a)$	$\frac{m\beta}{\gamma^2 a} K_m(\gamma a)$	$\frac{j\omega\mu}{\gamma} I_m'(\gamma a)$	$\frac{j\omega\mu}{\gamma} K_m'(\gamma a)$	0	0	$=0$
$\frac{j\omega\varepsilon}{\gamma}\cot\psi_i I_m'(\gamma a)$	$\frac{I_m(\gamma a)}{\left[1-\frac{m\beta\cot\psi_i}{\gamma^2 a}\right]}$	$-\frac{j\omega\varepsilon}{\gamma}\cot\psi_i I_m'(\gamma a)$	$-\frac{j\omega\varepsilon\cot\psi_i}{\gamma} K_m'(\gamma a)$	$\frac{-I_m(\gamma a)}{\left[1-\frac{m\beta}{\gamma^2 a}\cot\psi_i\right]}$	$\frac{-K_m(\gamma a)}{\left[1-\frac{m\beta\cot\psi_i}{\gamma^2 a}\right]}$	0	0	$=0$
0	0	$-\frac{j\omega\varepsilon}{\gamma}\cot\psi_o I_m'(\gamma b)$	$-\frac{j\omega\varepsilon\cot\psi_o}{\gamma} K_m'(\gamma b)$	$\frac{-I_m(\gamma b)}{\left[1-\frac{m\beta\cot\psi_o}{\gamma^2 b}\right]}$	$\frac{-K_m(\gamma b)}{\left[1-\frac{m\beta\cot\psi_o}{\gamma^2 b}\right]}$	$\frac{j\omega\varepsilon\cot\psi_o}{\gamma} K_m'(\gamma b)$	$\frac{K_m(\gamma b)}{\left[1-\frac{m\beta\cot\psi_o}{\gamma^2 b}\right]}$	$=0$
0	0	$-\frac{m\beta}{\gamma^2 b} I_m(\gamma b)$	$-\frac{m\beta}{\gamma^2 b} K_m(\gamma b)$	$-\frac{j\omega\mu}{\gamma} I_m'(\gamma b)$	$-\frac{j\omega\mu}{\gamma} K_m'(\gamma b)$	$\frac{m\beta}{\gamma^2 b} K_m(\gamma b)$	$\frac{j\omega\mu}{\gamma} K_m'(\gamma b)$	$=0$
0	0	$-I_m(\gamma b)$	$-K_m(\gamma b)$	0	0	$K_m(\gamma b)$	0	$=0$
0	0	0	0	0	0	$\frac{K_m(\gamma b)}{\left[1-\frac{m\beta\cot\psi_o}{\gamma^2 b}\right]}$	$\frac{-j\omega\mu\cot\psi_o}{\gamma} K_m'(\gamma b)$	$=0$

- - - 7.1.35 -42

Since Equations 7.1.27 to 7.1.34 will be solved by the use of determinants it is desirable to use the following abbreviations,

$I_m(\gamma a)\left[1 - \frac{m\beta \cot\psi_i}{\gamma^2 a}\right] = a$

$\frac{j\omega\mu}{\gamma} \cot\psi_i \, I_m'(\gamma a) = b$

$\frac{j\omega\mu}{\gamma} I_m'(\gamma a) = c$

$\frac{j\omega\mu}{\gamma} K_m'(\gamma a) = d$

$K_m(\gamma a) = e$

$\frac{j\omega\varepsilon}{\gamma} \cot\psi_i \, I_m'(\gamma a) = f$

$\frac{j\omega\varepsilon}{\gamma} \cot\psi_i \, K_m'(\gamma a) = h$

$\frac{j\omega\mu}{\gamma} I_m'(\gamma b) = i$

$\frac{j\omega\mu}{\gamma} K_m'(\gamma b) = j$

$K_m(\gamma b)\left[1 - \frac{m\beta \cot\psi_o}{\gamma^2 b}\right] = k$

$\frac{j\omega\mu}{\gamma} \cot\psi_o \, K_m'(\gamma b) = l$

$I_m(\gamma b) = m$

$\frac{j\omega\varepsilon}{\gamma} \cot\psi_o \, I_m'(\gamma b) = n$

$\frac{j\omega\varepsilon}{\gamma} \cot\psi_o \, K_m'(\gamma b) = p$

$\frac{m\beta}{\gamma^2 a} I_m(\gamma a) = \alpha$

$\frac{m\beta}{\gamma^2 a} K_m(\gamma a) = \beta$

$I_m(\gamma a) = \gamma$

$K_m(\gamma a)\left[1 - \frac{m\beta \cot\psi_i}{\gamma^2 a}\right] = \delta$

$\frac{m\beta}{\gamma^2 b} I_m(\gamma b) = \varepsilon$

$\frac{m\beta}{\gamma^2 b} K_m(\gamma b) = \kappa$

$K_m(\gamma b) = \mu$

$I_m(\gamma b)\left[1 - \frac{m\beta \cot\psi_o}{\gamma^2 b}\right] = \rho$

— — — 7.1.43

The determinantal solution then becomes

$$\begin{vmatrix} a & -b & 0 & 0 & 0 & 0 & 0 & 0 \\ -\alpha & -c & \alpha & \beta & c & d & 0 & 0 \\ -\gamma & 0 & \gamma & e & 0 & 0 & 0 & 0 \\ f & a & -f & -h & -a & -\delta & 0 & 0 \\ 0 & 0 & -\varepsilon & -\kappa & -i & -j & \kappa & j \\ 0 & 0 & 0 & 0 & 0 & 0 & k & -l \\ 0 & 0 & -m & -\mu & 0 & 0 & \mu & 0 \\ 0 & 0 & -n & -p & -q & -k & p & k \end{vmatrix} = 0 \quad -- 7.1.44$$

This determinant may be reduced in the normal way[25]. Details of the reduction will not be given, however, as the working is straightforward. The following third order determinant results

$$\begin{vmatrix} \kappa m b - \mu(ia + \varepsilon b) & be(\kappa m - \varepsilon\mu)(ad - \delta c) - id\mu b(hy - fe) & j \\ kmb & bk(me - \gamma\mu)(ad - \delta c) + lc\mu b(hy - fe) & -l \\ pmb - \mu(pa + nb) & be(mp - n\mu)(ad - \delta c) - pd\mu b(hy - fe) & k \end{vmatrix} = 0 \quad -- 7.1.45$$

This simplifies to

$$\begin{aligned} (ad - \delta c)\big[&-\kappa m b^2 k^2 \gamma\mu - \mu b k^2 (ia + \varepsilon b)(me - \gamma\mu) - \kappa m b^2 l e n\mu - \mu l b e (ia + \varepsilon b)(mp - n\mu) \\ &+ l p m b^2 e \varepsilon\mu + l\mu b e (pa + nb)(\kappa m - \varepsilon\mu) + k^2 m b^2 e \varepsilon\mu \\ &- j k m b^2 e n\mu + j p m b^2 k \gamma\mu + j b k \mu (pa + nb)(me - \gamma\mu)\big] \\ + (hy - fe)\big[&k l c \mu b^2 \kappa m - k l c \mu^2 b (ia + \varepsilon b) + id\mu b^2 l p m - id\mu^2 b^2 l n \\ &+ id\mu b^2 k^2 m - j l c \mu b^2 p m + j l c \mu^2 b (pa + nb) - pd\mu b^2 l \kappa m \\ &+ pd\mu^2 b l \varepsilon b - j k m b^2 pd\mu\big] = 0 \end{aligned} \quad -- 7.1.46$$

After considerable further working this becomes

$$\begin{aligned} &(ad - \delta c)\{[ik - je][\mu y a k - m e a k] + [mp - n\mu][jkby - idle]\} \\ &+ (hy - fe)\{[ik - je][kmdb - \mu l c a] + [mp - n\mu][idbl - jlcb]\} = 0 \end{aligned} \quad -- 7.1.47$$

The substitution of the modified Bessel Functions from Equations 7.1.43 in Equation 7.1.47, gives finally for the characteristic equation after further simplification

$$\frac{k^4}{\gamma^4}\cot^2\psi_i\cot^2\psi_0 I_m'(\gamma a)K_m'(\gamma b)G_{m'm'}(\gamma a,\gamma b)$$
$$+\frac{k^2}{\gamma^2}\Big\{2\cot\psi_i\cot\psi_0 I_m(\gamma a)K_m(\gamma b)I_m'(\gamma a)K_m'(\gamma b)\Big[1-\frac{m\beta}{\gamma^2 a}\cot\psi_i\Big]\Big[1-\frac{m\beta}{\gamma^2 b}\cot\psi_0\Big]$$
$$-\cot^2\psi_i I_m(\gamma b)K_m(\gamma b)I_m'(\gamma a)K_m'(\gamma a)\Big[1-\frac{m\beta}{\gamma^2 b}\cot\psi_0\Big]^2$$
$$-\cot^2\psi_0 I_m(\gamma a)K_m(\gamma a)I_m'(\gamma b)K_m'(\gamma b)\Big[1-\frac{m\beta}{\gamma^2 a}\cot\psi_i\Big]^2\Big\}$$
$$+\Big[1-\frac{m\beta}{\gamma^2 a}\cot\psi_i\Big]^2\Big[1-\frac{m\beta}{\gamma^2 b}\cot\psi_0\Big]^2 I_m(\gamma a)K_m(\gamma b)G_{mm}(\gamma a,\gamma b)=0 \qquad --7.1.48$$

Particular Cases of Characteristic Equation

Case (i) No Angular Variation of Fields

As a check on Equation 7.1.48 consider the form the equation takes when the fields do not vary with angle Θ, i.e. the type of propagation associated with the helices used in travelling-wave tubes. For this case m = 0 and the characteristic equation becomes

$$\frac{k^4}{\gamma^4}\cot^2\psi_i\cot^2\psi_0 I_1(\gamma a)K_1(\gamma b)G_{11}(\gamma a,\gamma b)$$
$$+\frac{k^2}{\gamma^2}\Big\{-2\cot\psi_i\cot\psi_0 I_0(\gamma a)K_0(\gamma b)I_1(\gamma a)K_1(\gamma b)$$
$$+\cot^2\psi_i I_0(\gamma b)K_0(\gamma b)I_1(\gamma a)K_1(\gamma a)$$
$$+\cot^2\psi_0 I_0(\gamma a)K_0(\gamma a)I_1(\gamma b)K_1(\gamma b)\Big\}$$
$$+I_0(\gamma a)K_0(\gamma b)G_{00}(\gamma a,\gamma b)=0 \qquad --7.1.49$$

This is identical with the equation obtained by Wade.[27]

Case (ii) Reduction to Simple Helix When Outer Radius Tends to Infinity

The following asymptotic expressions for the modified Bessel Functions are required:-

For $x \longrightarrow \infty$

$$I_m(x) \longrightarrow \frac{e^x}{(2\pi x)^{\frac{1}{2}}}\left[1 - \frac{(4m^2-1^2)}{8x}\right] \quad -- \quad 7.1.50(a)$$

$$I_m'(x) \longrightarrow \frac{e^x}{(2\pi x)^{\frac{1}{2}}}\left[1 - \frac{(4m^2+3)}{8x}\right] \quad -- \quad 7.1.50(b)$$

$$K_m(x) \longrightarrow e^{-x}\left(\frac{\pi}{2x}\right)^{\frac{1}{2}}\left[1 + \frac{(4m^2-1^2)}{8x}\right] \quad -- \quad 7.1.50(c)$$

$$K_m'(x) \longrightarrow -e^{-x}\left(\frac{\pi}{2x}\right)^{\frac{1}{2}}\left[1 + \frac{4m^2+3}{8x}\right] \quad -- \quad 7.1.50(d)$$

For the outer radius b tending to infinity, Equation 7.1.48 becomes

$$\frac{k^4}{\gamma^4}\cot^2\psi_i \cot^2\psi_o\, I_m'(\gamma a)(-1)\, e^{-\gamma b}\left(\frac{\pi}{2\gamma b}\right)^{\frac{1}{2}}\left[1 + \frac{4m^2+3}{8\gamma b}\right] \times$$

$$\left\{I_m'(\gamma a)(-1)\, e^{-\gamma b}\left(\frac{\pi}{2\gamma b}\right)^{\frac{1}{2}}\left[1 + \frac{4m^2+3}{8\gamma b}\right] - K_m'(\gamma a)\frac{e^{\gamma b}}{(2\pi\gamma b)^{\frac{1}{2}}}\left[1 - \frac{4m^2+3}{8\gamma b}\right]\right\}$$

$$+ \frac{k^2}{\gamma^2}\left\{2\cot\psi_i \cot\psi_o I_m(\gamma a)\, e^{-\gamma b}\left(\frac{\pi}{2\gamma b}\right)^{\frac{1}{2}}\left[1 + \frac{(4m^2-1^2)}{8\gamma b}\right] I_m'(\gamma a)(-) \times \right.$$

$$e^{-\gamma b}\left(\frac{\pi}{2\gamma b}\right)^{\frac{1}{2}}\left[1 + \frac{4m^2+3}{8\gamma b}\right]\left[1 - \frac{m\beta}{\gamma^2 a}\cot\psi_i\right]\left[1 - \frac{m\beta}{\gamma^2 b}\cot\psi_o\right]$$

$$- \cot^2\psi_i \frac{e^{\gamma b}}{(2\pi\gamma b)^{\frac{1}{2}}}\left[1 - \frac{(4m^2-1^2)}{8\gamma b}\right] e^{-\gamma b}\left(\frac{\pi}{2\gamma b}\right)^{\frac{1}{2}}\left[1 + \frac{(4m^2-1^2)}{8\gamma b}\right] \times$$

$$I_m'(\gamma a) K_m'(\gamma a)\left[1 - \frac{m\beta}{\gamma^2 b}\cot\psi_o\right]^2$$

$$- \cot^2\psi_o\, I_m(\gamma a) K_m(\gamma a)\frac{e^{\gamma b}}{(2\pi\gamma b)^{\frac{1}{2}}}\left[1 - \frac{(4m^2+3)}{8\gamma b}\right](-1) \times$$

$$\left. e^{-\gamma b}\left(\frac{\pi}{2\gamma b}\right)^{\frac{1}{2}}\left[1 + \frac{(4m^2+3)}{8\gamma b}\right]\left[1 - \frac{m\beta}{\gamma^2 a}\cot\psi_i\right]^2\right\}$$

$$+ \left[1 - \frac{m\beta}{\gamma^2 a}\cot\psi_i\right]^2\left[1 - \frac{m\beta}{\gamma^2 b}\cot\psi_o\right]^2 I_m(\gamma a)\, e^{-\gamma b}\left(\frac{\pi}{2\gamma b}\right)^{\frac{1}{2}}\left[1 + \frac{(4m^2-1^2)}{8\gamma b}\right] \times$$

$$\left\{I_m(\gamma a)\, e^{-\gamma b}\left(\frac{\pi}{2\gamma b}\right)^{\frac{1}{2}}\left[1 + \frac{(4m^2-1^2)}{8\gamma b}\right] - \frac{e^{\gamma b}}{(2\pi\gamma b)^{\frac{1}{2}}}\left[1 - \frac{(4m^2-1^2)}{8\gamma b}\right] K_m(\gamma a)\right\}$$

$$= 0 \quad -- \quad 7.1.51$$

i.e.

$$-\frac{1}{2\gamma\ell}\left\{-\frac{k^4}{\gamma^4}\cot^2\psi_i\cot^2\psi_o I_m'(\gamma a)K_m'(\gamma a)\right.$$

$$+\frac{k^2}{\gamma^2}\left[\cot^2\psi_i I_m'(\gamma a)K_m'(\gamma a)-\cot^2\psi_o I_m(\gamma a)K_m(\gamma a)\left(1-\frac{m\beta}{\gamma^2 a}\cot\psi_i\right)^2\right]$$

$$\left.+\left(1-\frac{m\beta}{\gamma^2 a}\cot\psi_i\right)^2 I_m(\gamma a)K_m(\gamma a)\right\} \quad -- \ 7.1.52$$

$$= 0$$

This gives

$$-\frac{1}{2\gamma\ell}\left[-I_m'(\gamma a)K_m'(\gamma a)\frac{k^2}{\gamma^2}\cot^2\psi_i\left(\frac{k^2}{\gamma^2}\cot^2\psi_o-1\right)\right.$$

$$\left.-I_m(\gamma a)K_m(\gamma a)\left(1-\frac{m\beta}{\gamma^2 a}\cot\psi_i\right)^2\left(\frac{k^2}{\gamma^2}\cot^2\psi_o-1\right)\right]=0$$

$$-- \ 7.1.53$$

so that

$$\frac{I_m'(\gamma a)K_m'(\gamma a)}{I_m(\gamma a)K_m(\gamma a)} = -\frac{(\gamma^2 a^2-m\beta a\cot\psi_i)^2}{k^2a^2\gamma^2a^2\cot^2\psi_i}$$

$$-- \ 7.1.54$$

This is identical with Equation 2.1.27

CHAPTER VIII

Wave Propagation Along Sheath Helix Encapsulated in Dielectric

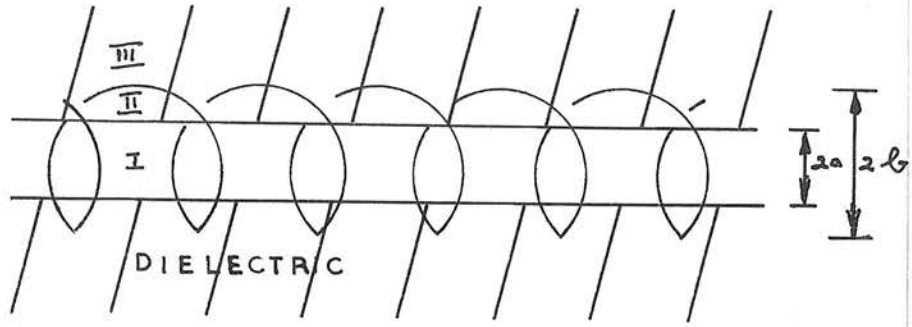

FIG 8.1

Experiments by Jones [11] have indicated that operation of the helical aerial is not in general adversely affected by encapsulation in low loss dielectrics. An exact analysis even of the sheath helix encapsulated in a dielectric would be extremely difficult. The approximation is accordingly made here that the dielectric outside the helix extends to infinity. This reduces the number of boundary conditions from twelve to eight, making the evaluation of the determinant more manageable. A similar approximation has been made by Olving[29] in his treatment of the helix for travelling-wave tubes It should perhaps be stated explicitly that the encapsulation referred to here allows the presence of a hollow coaxial tube as shown in Figure 8.1., in order to make the treatment fairly general.

Region I $0 < r < a$

Let $$E_{z1} = A_m' I_m(\gamma r) e^{j m\theta} e^{-j\beta z} \qquad \text{8.1.1}$$

$$H_{z1} = B_m' I_m(\gamma r) e^{j m\theta} e^{-j\beta z} \qquad \text{8.1.2}$$

Then

$$E_{\theta 1} = \left[\frac{-m\beta}{\gamma^2 r} A_m' I_m(\gamma r) - \frac{j\omega\mu}{\gamma} B_m' I_m'(\gamma r) \right] e^{j m\theta} e^{-j\beta z} \qquad \text{8.1.3}$$

$$E_{r1} = \left[\frac{j\beta}{\gamma} A_m' I_m'(\gamma r) - \frac{m\omega\mu}{\gamma^2 r} B_m' I_m(\gamma r) \right] e^{j m\theta} e^{-j\beta z} \qquad \text{8.1.4}$$

$$H_{\theta 1} = \left[\frac{j\omega\varepsilon_0}{\gamma} A_m' I_m'(\gamma r) - \frac{m\beta}{\gamma^2 r} B_m' I_m(\gamma r) \right] e^{j m\theta} e^{-j\beta z} \qquad \text{8.1.5}$$

$$H_{r1} = \left[\frac{m\omega\varepsilon_0}{\gamma^2 r} A_m' I_m(\gamma r) + \frac{j\beta}{\gamma} B_m' I_m'(\gamma r) \right] e^{j m\theta} e^{-j\beta z} \qquad \text{8.1.6}$$

Region II $a < r < b$

Let $$E_{z2} = \left[A_m^2 I_m(\gamma' r) + B_m^2 K_m(\gamma' r) \right] e^{j m\theta} e^{-j\beta z} \qquad \text{8.1.7}$$

$$H_{z2} = \left[C_m^2 I_m(\gamma' r) + D_m^2 K_m(\gamma' r) \right] e^{j m\theta} e^{-j\beta z} \qquad \text{8.1.8}$$

Then

$$E_{\theta 2} = \left[-\frac{j\omega\mu}{\gamma'} \left[C_m^2 I_m'(\gamma' r) + D_m^2 K_m'(\gamma' r) \right] - \frac{m\beta}{\gamma'^2 r} \left[A_m^2 I_m(\gamma' r) + B_m^2 K_m(\gamma' r) \right] \right] \times e^{j m\theta} e^{-j\beta z} \qquad \text{8.1.9}$$

$$E_{r2} = \left[\frac{j\beta}{\gamma'} \left[A_m^2 I_m'(\gamma' r) + B_m^2 K_m'(\gamma' r) \right] - \frac{m\omega\mu}{\gamma'^2 r} \left[C_m^2 I_m(\gamma' r) + D_m^2 K_m(\gamma' r) \right] \right] \times e^{j m\theta} e^{-j\beta z} \qquad \text{8.1.10}$$

$$H_{\theta 2} = \left[\frac{j\omega\varepsilon_1}{\gamma'} \left[A_m^2 I_m'(\gamma' r) + B_m^2 K_m'(\gamma' r) \right] - \frac{m\beta}{\gamma'^2 r} \left[C_m^2 I_m(\gamma' r) + D_m^2 K_m(\gamma' r) \right] \right] \times e^{j m\theta} e^{-j\beta z} \qquad \text{8.1.11}$$

$$H_{r2} = \left[\frac{j\beta}{\gamma'} \left[C_m^2 I_m'(\gamma' r) + D_m^2 K_m'(\gamma' r) \right] + \frac{m\omega\varepsilon_1}{\gamma'^2 r} \left[A_m^2 I_m(\gamma' r) + B_m^2 K_m(\gamma' r) \right] \right] \times e^{j m\theta} e^{-j\beta z} \qquad \text{8.1.12}$$

Region III $b < r < \infty$

Let $$E_{z3} = A_m^3 K_m(\gamma' r) e^{j m\theta} e^{-j\beta z} \qquad \text{8.1.13}$$

$$H_{z3} = B_m^3 K_m(\gamma' r) e^{j m\theta} e^{-j\beta z} \qquad \text{8.1.14}$$

Then

$$E_{\theta 3} = \left[-\frac{j\omega\mu}{\gamma'} B_m^3 K_m'(\gamma' r) - \frac{m\beta}{\gamma'^2 r} A_m^3 K_m(\gamma' r) \right] e^{j m\theta} e^{-j\beta z} \qquad \text{8.1.15}$$

$$E_{r3} = \left[\frac{j\beta}{\gamma'} A_m^3 K_m'(\gamma' r) - \frac{m\omega\mu}{\gamma'^2 r} B_m^3 K_m(\gamma' r) \right] e^{j m\theta} e^{-j\beta z} \qquad \text{8.1.16}$$

$$H_{\theta 3} = \left[\frac{j\omega\varepsilon}{\gamma'} A_m^3 K_m'(\gamma' r) - \frac{m\beta}{\gamma'^2 r} B_m^3 K_m(\gamma' r) \right] e^{j m\theta} e^{-j\beta z} \qquad \text{8.1.17}$$

$$H_{r3} = \left[\frac{j\beta}{\gamma'} B_m^3 K_m'(\gamma' r) + \frac{m\omega\varepsilon_1}{\gamma'^2 r} A_m^3 K_m(\gamma' r) \right] e^{j m\theta} e^{-j\beta z} \qquad \text{8.1.18}$$

In Equations 8.1.7. to 8.1.18 the prime on the propagation constant γ indicates that it is the dielectric medium which is being considered.

Boundary Conditions

At r = a	At r = b
$E_{z1} = E_{z2}$ — — 8.1.19	$E_{z2} = E_{z3}$ — — 8.1.23
$E_{\theta 1} = E_{\theta 2}$ — — 8.1.20	$E_{\theta 2} = E_{\theta 3}$ — — 8.1.24
$H_{z1} = H_{z2}$ — — 8.1.21	$E_{z2} = -E_{\theta 2} \cot\psi$ — — 8.1.25
$H_{\theta 1} = H_{\theta 2}$ — — 8.1.22	$H_{z2} + H_{\theta 2}\cot\psi = H_{z3} + H_{\theta 3}\cot\psi$ — — 8.1.26

From 8.1.19

$$A_m^1 I_m(\gamma a) - A_m^2 I_m(\gamma' a) - B_m^2 K_m(\gamma' a) = 0 \quad \text{— —} \quad 8.1.27$$

From 8.1.20

$$-\frac{m\beta}{\gamma^2 a} A_m^1 I_m(\gamma a) - \frac{j\omega\mu}{\gamma} B_m^1 I_m'(\gamma a) + \frac{j\omega\mu}{\gamma'} C_m^2 I_m'(\gamma' a)$$
$$+ \frac{j\omega\mu}{\gamma'} D_m^2 K_m'(\gamma' a) + \frac{m\beta}{\gamma'^2 a} A_m^2 I_m(\gamma' a) + \frac{m\beta}{\gamma'^2 a} B_m^2 K_m(\gamma' a) = 0 \quad \text{— —} \quad 8.1.28$$

From 8.1.21.

$$B_m^1 I_m(\gamma a) - C_m^2 I_m(\gamma' a) - D_m^2 K_m(\gamma' a) = 0 \quad \text{— —} \quad 8.1.29$$

From 8.1.22

$$\frac{j\omega\varepsilon_0}{\gamma} A_m^1 I_m'(\gamma a) - \frac{m\beta}{\gamma^2 a} B_m^1 I_m(\gamma a) - \frac{j\omega\varepsilon_1}{\gamma'} A_m^2 I_m'(\gamma' a)$$
$$- \frac{j\omega\varepsilon_1}{\gamma'} B_m^2 K_m'(\gamma' a) + \frac{m\beta}{\gamma'^2 a} C_m^2 I_m(\gamma' a) + \frac{m\beta}{\gamma'^2 a} D_m^2 K_m(\gamma' a) = 0 \quad \text{— —} \quad 8.1.30$$

From 8.1.23

$$A_m^2 I_m(\gamma' b) + B_m^2 K_m(\gamma' b) - A_m^3 K_m(\gamma' b) = 0 \quad \text{— —} \quad 8.1.31$$

From 8.1.24

$$-\frac{j\omega\mu}{\gamma'} C_m^2 I_m'(\gamma' b) - \frac{j\omega\mu}{\gamma'} D_m^2 K_m'(\gamma' b) - \frac{m\beta}{\gamma'^2 b} A_m^2 I_m(\gamma' b)$$
$$- \frac{m\beta}{\gamma'^2 b} B_m^2 K_m(\gamma' b) + \frac{j\omega\mu}{\gamma'} B_m^3 K_m'(\gamma' b) + \frac{m\beta}{\gamma'^2 b} A_m^3 K_m(\gamma' b) = 0 \quad \text{— —} \quad 8.1.32$$

From 8.1.25

$$A_m^2 I_m(\gamma' b) + B_m^2 K_m(\gamma' b) - \frac{j\omega\mu\cot\psi}{\gamma'} C_m^2 I_m'(\gamma' r)$$
$$- \frac{j\omega\mu\cot\psi}{\gamma'} D_m^2 K_m'(\gamma' b) - \frac{m\beta\cot\psi}{\gamma'^2 b} A_m^2 I_m(\gamma' b)$$
$$- \frac{m\beta\cot\psi}{\gamma'^2 b} B_m^2 K_m(\gamma' b) = 0 \quad \text{— —} \quad 8.1.33$$

From 8.1.26

$$C_m^2 I_m(\gamma' b)\left[1 - \frac{m\beta\cot\psi}{\gamma'^2 b}\right] + D_m^2 K_m(\gamma' b)\left[1 - \frac{m\beta\cot\psi}{\gamma'^2 b}\right]$$

$$+ \frac{j\omega\varepsilon_1\cot\psi}{\gamma'} A_m^2 I_m'(\gamma' b) + \frac{j\omega\varepsilon_1\cot\psi}{\gamma'} B_m^2 K_m'(\gamma' b)$$

$$- B_m^3 K_m(\gamma' b) - \frac{j\omega\varepsilon_1\cot\psi}{\gamma'} A_m^3 K_m'(\gamma' b)$$

$$+ \frac{m\beta\cot\psi}{\gamma'^2 b} B_m^3 K_m(\gamma' b) \qquad = 0 \quad -- \quad 8.1.34$$

A_m^1	B_m^1	A_m^2	B_m^2	C_m^2	D_m^2	A_m^3	B_m^3	
$I_m(\gamma a)$	0	$-I_m(\gamma' a)$	$-K_m(\gamma' a)$	0	0	0	0	$=0$
$-\frac{m\beta}{\gamma^2 a} I_m(\gamma a)$	$-\frac{j\omega\mu}{\gamma} I_m'(\gamma a)$	$\frac{m\beta}{\gamma'^2 a} I_m(\gamma' a)$	$\frac{m\beta}{\gamma'^2 a} K_m(\gamma' a)$	$\frac{j\omega\mu}{\gamma'} I_m'(\gamma' a)$	$\frac{j\omega\mu}{\gamma'} K_m'(\gamma' a)$	0	0	$=0$
0	$I_m(\gamma a)$	0	0	$-I_m(\gamma' a)$	$-K_m(\gamma' a)$	0	0	$=0$
$\frac{j\omega\varepsilon_0}{\gamma} I_m'(\gamma a)$	$-\frac{m\beta}{\gamma^2 a} I_m(\gamma a)$	$-\frac{j\omega\varepsilon_1}{\gamma'} I_m'(\gamma' a)$	$-\frac{j\omega\varepsilon_1}{\gamma'} K_m'(\gamma' a)$	$\frac{m\beta}{\gamma'^2 a} I_m(\gamma' a)$	$\frac{m\beta}{\gamma'^2 a} K_m(\gamma' a)$	0	0	$=0$
0	0	$I_m(\gamma' b)$	$K_m(\gamma' b)$	0	0	$-K_m(\gamma' b)$	0	$=0$
0	0	$-\frac{m\beta}{\gamma'^2 b} I_m(\gamma' b)$	$-\frac{m\beta}{\gamma'^2 b} K_m(\gamma' b)$	$-\frac{j\omega\mu}{\gamma'} I_m'(\gamma' b)$	$-\frac{j\omega\mu}{\gamma'} K_m'(\gamma' b)$	$\frac{m\beta}{\gamma'^2 b} K_m(\gamma' b)$	$\frac{j\omega\mu}{\gamma'} K_m'(\gamma' b)$	$=0$
0	0	$\frac{I_m(\gamma' b)}{\left[1-\frac{m\beta \cot\psi}{\gamma'^2 b}\right]}$	$\frac{K_m(\gamma' b)}{\left[1-\frac{m\beta \cot\psi}{\gamma'^2 b}\right]}$	$-\frac{j\omega\mu \cot\psi}{\gamma'} I_m'(\gamma' b)$	$-\frac{j\omega\mu \cot\psi}{\gamma'} K_m'(\gamma' b)$	0	0	$=0$
0	0	$\frac{j\omega\varepsilon_1 \cot\psi}{\gamma'} I_m'(\gamma' b)$	$\frac{j\omega\varepsilon_1 \cot\psi}{\gamma'} K_m'(\gamma' b)$	$\frac{I_m(\gamma' b)}{\left[1-\frac{m\beta \cot\psi}{\gamma'^2 b}\right]}$	$\frac{K_m(\gamma' b)}{\left[1-\frac{m\beta \cot\psi}{\gamma'^2 b}\right]}$	$-\frac{j\omega\varepsilon_1 \cot\psi}{\gamma'} K_m'(\gamma' b)$	$\frac{-K_m(\gamma' b)}{\left[1-\frac{m\beta \cot\psi}{\gamma'^2 b}\right]}$	$=0$

It is convenient to introduce the following abbreviations, in order to make the determinant more easily handled,

Let

$I_m(\gamma a) = a$ $\qquad$ $I_m(\gamma' b) = s$

$-I_m(\gamma' a) = b$ $\qquad$ $K_m(\gamma' b) = t$

$-K_m(\gamma' a) = c$ $\qquad$ $-\frac{m\beta}{\gamma'^2 b} I_m(\gamma' b) = u$

$-\frac{m\beta}{\gamma^2 a} I_m(\gamma a) = d$ $\qquad$ $-\frac{m\beta}{\gamma'^2 b} K_m(\gamma' b) = v$

$-\frac{j\omega\mu}{\gamma} I_m'(\gamma a) = e$ $\qquad$ $-\frac{j\omega\mu}{\gamma'} I_m'(\gamma' b) = w$

$\frac{m\beta}{\gamma'^2 a} I_m(\gamma' a) = f$ $\qquad$ $-\frac{j\omega\mu}{\gamma'} K_m'(\gamma' b) = x$

$\frac{m\beta}{\gamma'^2 a} K_m(\gamma' a) = g$ $\qquad$ $I_m(\gamma' b)\left[1 - \frac{m\beta \cot\psi}{\gamma'^2 b}\right] = y$

$\frac{j\omega\mu}{\gamma'} I_m'(\gamma' a) = h$ $\qquad$ $K_m(\gamma' b)\left[1 - \frac{m\beta \cot\psi}{\gamma'^2 b}\right] = z$

$\frac{j\omega\mu}{\gamma'} K_m'(\gamma' a) = m$ $\qquad$ $-\frac{j\omega\mu}{\gamma'} \cot\psi\, I_m'(\gamma' b) = \alpha$

$\frac{j\omega\varepsilon_0}{\gamma} I_m'(\gamma a) = n$ $\qquad$ $-\frac{j\omega\mu}{\gamma'} \cot\psi\, K_m'(\gamma' b) = \beta$

$-\frac{j\omega\varepsilon_1}{\gamma'} I_m'(\gamma' a) = q$ $\qquad$ $\frac{j\omega\varepsilon_1 \cot\psi}{\gamma'} I_m'(\gamma' b) = \gamma$

$-\frac{j\omega\varepsilon_1}{\gamma'} K_m'(\gamma' a) = r$ $\qquad$ $\frac{j\omega\varepsilon_1 \cot\psi}{\gamma'} K_m'(\gamma' b) = \delta$

— — — 8.1.43

The determinantal solution then becomes,

$$\begin{vmatrix} a & o & b & c & o & o & o & o \\ d & e & f & g & h & m & o & o \\ o & a & o & o & b & c & o & o \\ n & d & q & r & f & g & o & o \\ o & o & s & t & o & o & -t & o \\ o & o & u & v & w & x & -v & -x \\ o & o & y & z & \alpha & \beta & o & o \\ o & o & \gamma & \delta & y & z & -\delta & -z \end{vmatrix} = 0 \qquad \text{— — — 8.1.44}$$

This determinant may be reduced in the usual way[25] to the following third order one,

$$\begin{vmatrix} x(\gamma t - \delta s)(be - ah) - t(bd - af)(wz - xy) & (ag - cd) & (am - ca) \\ x(\gamma t - \delta s)(bd - af) - t(bn - aq)(wz - xy) & (ar - nc) & (ag - cd) \\ -\alpha x(\gamma t - \delta s) + ty(wz - xy) & \gamma & \beta \end{vmatrix} = 0 \qquad \text{— — — 8.1.45}$$

from which after substitution of the modified Bessel Functions, and considerable simplification, there results for the characteristic equation,

$$-\frac{(\gamma'^2 b - m\beta c \cot\psi)^2}{\gamma'^2 b^2 k_1^2 b^2 \cot^2\psi} = \frac{K_m'(\gamma' b)}{K_m(\gamma' b)} \times \frac{\left(\frac{m\beta}{b}\right)^2 I_m^2(\gamma a) K_m(\gamma' a) G_{mm}'(\gamma' b, \gamma' a)\left(\frac{1}{\gamma'^2} - \frac{1}{\gamma^2}\right)^2 + I_m'(\gamma a) G_{mm'}(\gamma' a, \gamma' b)\left[\frac{k_0^2}{\gamma^2} I_m'(\gamma a) K_m(\gamma' a) - \frac{k_1^2}{\gamma\gamma'} I_m(\gamma a) K_m'(\gamma' a)\right] + I_m(\gamma a) G_{m'm'}(\gamma' a, \gamma' b)\left[\frac{k_1^2}{\gamma'^2} I_m(\gamma a) K_m'(\gamma' a) - \frac{k_0^2}{\gamma\gamma'} K_m(\gamma' a) I_m'(\gamma a)\right]}{k_0^2 I_m'(\gamma a) G_{mm}(\gamma' b, \gamma' a)\left[\frac{1}{\gamma\gamma'} I_m(\gamma a) K_m'(\gamma' a) - \frac{1}{\gamma^2} I_m'(\gamma a) K_m(\gamma' a)\right] + k_1^2 I_m(\gamma a) G_{mm'}(\gamma' b, \gamma' a)\left[\frac{1}{\gamma\gamma'} I_m'(\gamma a) K_m(\gamma' a) - \frac{1}{\gamma'^2} I_m(\gamma a) K_m'(\gamma' a)\right] + \left(\frac{m\beta}{b}\right)^2 I_m^2(\gamma a) K_m(\gamma' a) G_{mm}(\gamma' b, \gamma' a)\left(\frac{1}{\gamma'^2} - \frac{1}{\gamma^2}\right)}$$

— — — 8.1.46

Reduction to Simple Helix When $\varepsilon_1 = \varepsilon_0$

For $\varepsilon_1 = \varepsilon_0$, $\gamma^1 = \gamma$ and Equation 8.1.46 becomes

$$-\frac{(\gamma^2 b^2 - m\beta b \cot\psi)^2}{\gamma^2 b^2 k^2 b^2 \cot^2\psi} = \frac{K_m'(\gamma b)}{K_m(\gamma b)} \times \frac{\left[I_m'(\gamma a) G_{mm'}(\gamma' a, \gamma' b) \frac{k^2}{\gamma^2}\frac{1}{\gamma a} - I_m(\gamma a) G_{mm'}(\gamma a, \gamma b)\frac{k^2}{\gamma^2}\frac{1}{\gamma a}\right]}{\left[-\frac{k^2}{\gamma^2} I_m'(\gamma a) G_{mm}(\gamma' b, \gamma' a)\frac{1}{\gamma a} + \frac{k^2}{\gamma^2} I_m(\gamma a) G_{mm'}(\gamma b, \gamma a)\frac{1}{\gamma a}\right]} \quad \text{--- 8.1.47}$$

This simplifies readily to

$$-\frac{(\gamma^2 b^2 - m\beta b \cot\psi)^2}{\gamma^2 b^2 k^2 b^2 \cot^2\psi} = \frac{I_m'(\gamma b) K_m'(\gamma b)}{I_m(\gamma b) K_m(\gamma b)} \quad \text{--- 8.1.48}$$

which is identical with Equation 2.1.27

CHAPTER IX

Some Related End-Fire Travelling-Wave Aerials

9.1.1. Multiwire Helices

Propagation of electromagnetic waves along multiwire helices has been considered by both Sensiper[14] and Watkins[21]. It is clear that the theoretical solutions obtained will be dependent on the relative phases of the currents flowing in the different wires at a cross-section of constant z. This is in turn dependent on the feeding arrangements to the different wires. Since the groundplane type of feed provides an excellent launching mechanism for the unidirectional end-fire aerial it seems desirable to retain this in any new type of aerial employing helical wires. In order also to eliminate frequency-sensitive phase shifting devices at the feed so as not to reduce the intrinsic bandwidth of the aerial it then becomes necessary to feed all the wires in phase.

Consideration of the simplest type of multiwire helix - the bifilar - shows that when both wires fed in phase are wound in the same direction there is zero radiation along the axis of the aerial. However, if the two wires, fed in phase, are wound in opposite directions there will be a maximum of radiation along the axis as for the single wire helix. Hence a new type of aerial, the Contra Wound Bifilar Helix is proposed/

proposed.

9.1.2. The Contra-Wound Bifilar Helix

This is a linearly polarised aerial, since the resultant wave is composed of two equal circularly or elliptically polarised waves rotating in opposite directions. It should be noted that if this type of aerial were to be used for the reception of a circularly polarised wave, the single helix which could support this type of polarisation would re-radiate part of the "available" received energy through the other helix. Hence it is not an aerial which can receive linearly or circularly polarised signals equally efficiently - it is simply a linearly polarised aerial.

Analytically this may be shown as follows. Referring to Figure 3.6.1 and denoting the helix shown there by the numeral 1, and the contra-wound helix by the numeral 2, the following equations hold,

Helix 1	Helix 2
$x = a\cos u$ -- 9.1.1	$x = a\cos u$ -- 9.1.4
$y = a\sin u$ -- 9.1.2	$y = -a\sin u$ -- 9.1.5
$z = \frac{s}{2\pi} u$ -- 9.1.3	$z = \frac{s}{2\pi} u$ -- 9.1.6

Then using the same notation as in Chapter III, Section 6 the rectangular components of vector potential can be written as follows for Helix 1,

$$A_{x_1} = -\frac{\mu_0 I_0 a}{4\pi}\frac{e^{-j\beta R}}{R}\left[\int_{u_1}^{u_2} e^{-j[H_1 u - z(\cos u - \phi)]} \sin u\, du\right] \quad \text{---} \quad 9.1.7$$

$$A_{y_1} = \frac{\mu_0 I_0 a}{4\pi}\frac{e^{-j\beta R}}{R}\left[\int_{u_1}^{u_2} e^{-j[H_1 u - z\cos(u-\phi)} \cos u\, du\right] \quad \text{---} \quad 9.1.8$$

$$A_{z_1} = \frac{\mu_0 I_0}{4\pi}\frac{S}{2\pi}\frac{e^{-j\beta R}}{R}\left[\int_{u_1}^{u_2} e^{-j[H_1 u - z\cos(u-\phi)]} du\right] \quad \text{---} \quad 9.1.9$$

For Helix 2 the corresponding equations are

$$A_{x_2} = -\frac{\mu_0 I_0 a}{4\pi}\frac{e^{-j\beta R}}{R}\left[\int_{u_1}^{u_2} e^{-j[H_1 u - z\cos(u+\phi)]} \sin u\, du\right] \quad \text{---} \quad 9.1.10$$

$$A_{y_2} = -\frac{\mu_0 I_0 a}{4\pi}\frac{e^{-j\beta R}}{R}\left[\int_{u_1}^{u_2} e^{-j[H_1 u - z\cos(u+\phi)]} \cos u\, du\right] \quad \text{---} \quad 9.1.11$$

$$A_{z_2} = \frac{\mu_0 I_0}{4\pi}\frac{S}{2\pi}\frac{e^{-j\beta R}}{R}\left[\int_{u_1}^{u_2} e^{-j[H_1 u - z\cos(u+\phi)]} du\right] \quad \text{---} \quad 9.1.12$$

The integrals in these equations can be evaluated in terms of Bessel Functions[39], and for the particular case of H_1 equal to unity and N integral turns the equations become,

$$A_{x_1} = jKN\pi e^{-j\phi}\left[J_2(z)e^{-j\phi} + J_0(z)e^{j\phi}\right]\frac{e^{-j\beta R}}{R} \quad \text{---} \quad 9.1.13$$

$$A_{y_1} = -KN\pi e^{-j\phi}\left[J_2(z)e^{-j\phi} - J_0(z)e^{j\phi}\right]\frac{e^{-j\beta R}}{R} \quad \text{---} \quad 9.1.14$$

$$A_{z_1} = jK\frac{NS}{a}e^{-j\phi}J_1(z)\frac{e^{-j\beta R}}{R} \quad \text{---} \quad 9.1.15$$

and

$$A_{x2} = j^{KN\pi} e^{j\varphi}\left[J_2(z)e^{j\varphi} + J_0(z)e^{-j\varphi}\right]\frac{e^{-jkR}}{R} \qquad \text{--- 9.1.16}$$

$$A_{y2} = KN\pi e^{j\varphi}\left[J_2(z)e^{j\varphi} - J_0(z)e^{-j\varphi}\right]\frac{e^{-jkR}}{R} \qquad \text{--- 9.1.17}$$

$$A_{z2} = j\frac{KNS}{a} e^{j\varphi} J_1(z)\frac{e^{-jkR}}{R} \qquad \text{--- 9.1.18}$$

The two components E_θ and E_φ of radiation field can then be derived from the equations relating unit vectors $\hat{\theta}$ and $\hat{\varphi}$ to unit vectors $\hat{x}$, $\hat{y}$ and $\hat{z}$ as follows,

$$\hat{\theta} = \hat{x}\cos\theta\cos\varphi + \hat{y}\cos\theta\sin\varphi - \hat{z}\sin\theta \qquad \text{--- 9.1.19}$$

$$\hat{\varphi} = -\hat{x}\sin\varphi + \hat{y}\cos\varphi \qquad \text{--- 9.1.20}$$

Carrying out the summations of the vector potentials there results,

$$E_\theta \propto j^{2NK\pi}\frac{J_1(z)}{z}\cos\theta\left[e^{i\varphi}+e^{-i\varphi}\right] - j\frac{KNS}{a}J_1(z)\sin\theta\left[e^{i\varphi}+e^{-i\varphi}\right] \qquad \text{--- 9.1.21}$$

$$E_\varphi \propto 2NK\pi J_1'(z)\left[e^{i\varphi}-e^{-i\varphi}\right] \qquad \text{--- 9.1.22}$$

Along the axis of the helices, i.e. for $\theta = 0^\circ$, these equations reduce to

$$E_\theta \propto j2NK\pi\cos\varphi \qquad \text{--- 9.1.23}$$

$$E_\varphi \propto -j2KN\pi\sin\varphi \qquad \text{--- 9.1.24}$$

showing that the aerial is linearly polarised in this direction.

It was mentioned in Chapter I that a theoretical solution to the problem of wave propagation along contra wound helices had been given by Chodorow and Chu[16]. Numerical calculations

have been carried out by these authors for a pitch angle of 10° and from their graphs it is a simple matter to compute the phase velocity along the helical conductor as a function of frequency. This has been done in Fig. 9.1.1.

In order to estimate how useful an aerial this contra-wound helix may be, it is necessary to compare it with the graph of the phase velocity which is required to satisfy the Hansen-Woodyard condition for an infinitely long aerial. When this is done it is found that the two graphs are coincident within the thickness of the curve over the range from an estimated C_{λ} equal to 0.88 up to slightly over C_{λ} equal to 1.20. This rather astonishing result would tend to suggest that if the condition of increased directivity were satisfied for this finite helix as for the single finite helix, the bandwidth would be independent of aerial length. It is not surprising to learn therefore that the above estimated bandwidth does not hold in practice. Up to the present the maximum useful value of C_{λ} has been found to be 1.03, even for a short helix of 3 turns. Figures 9.1.2. and 9.1.3. show an experimental plot of pattern and axial ratio.

It should be noted that it is not too surprising to find the agreement between theory and experiment for the contra-wound helix less good than for the single helix. It is much more difficult to approximate the boundary conditions over the rhombus formed by the intersecting

FIG 9.1.1

CONDUCTOR PHASE VELOCITY FOR CONTRA WOUND HELIX

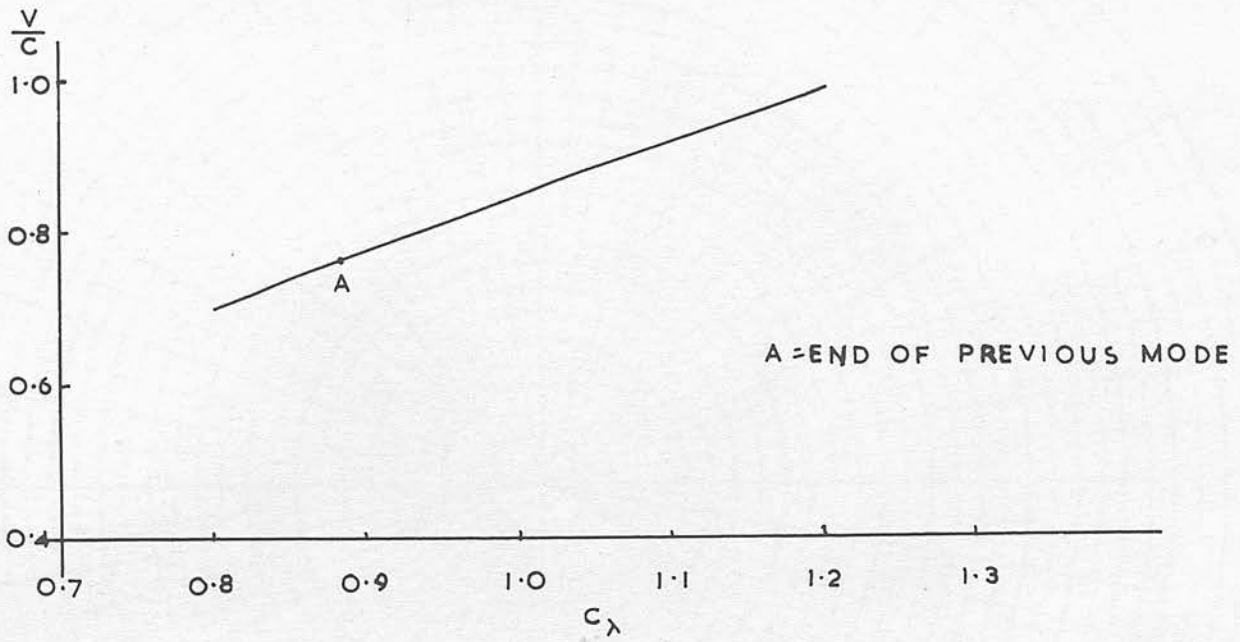

FIG 9.1.2

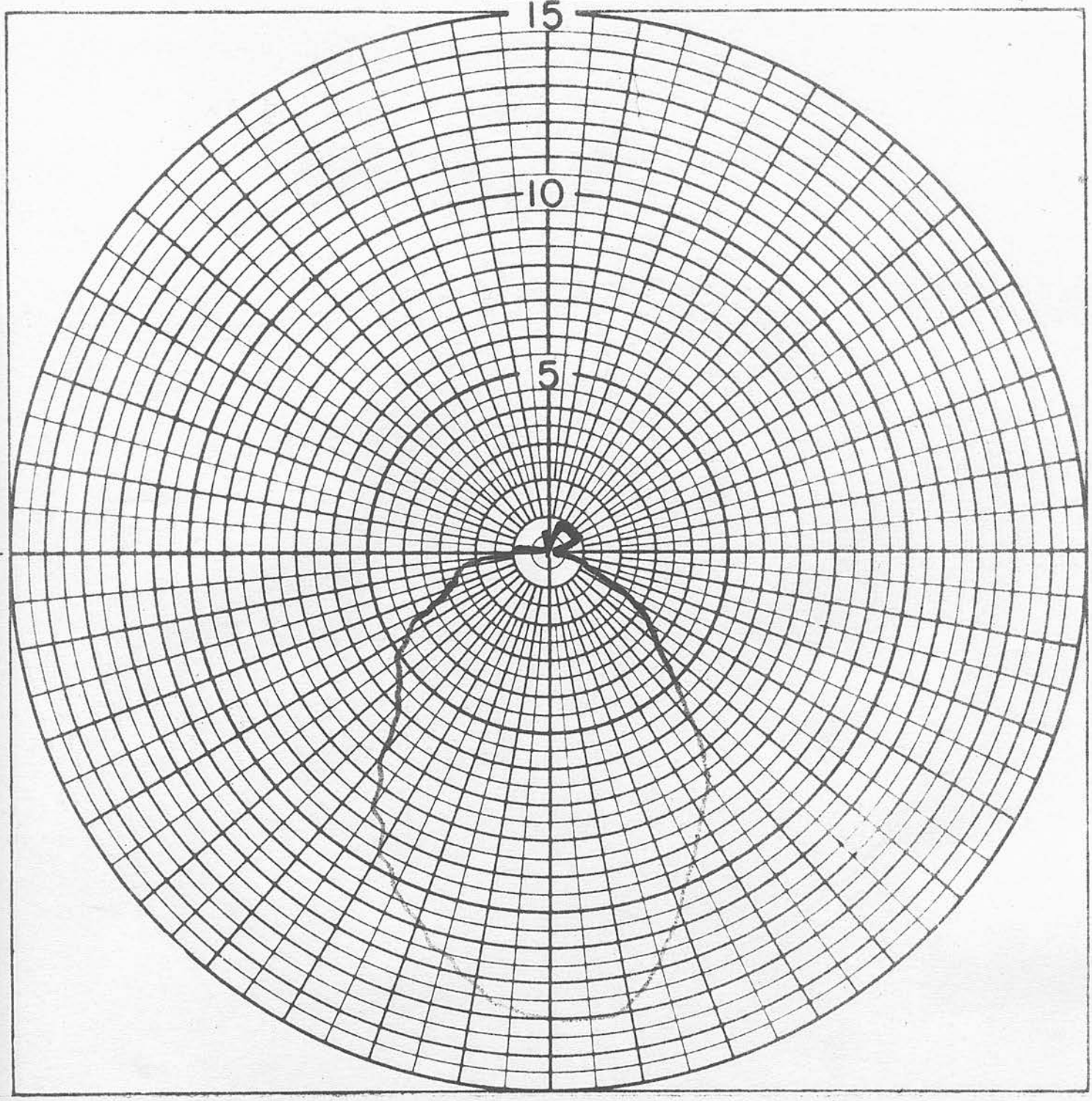

RADIATION PATTERN FOR 3-TURN CONTRA-WOUND HELIX

FIG 9, 1. 3

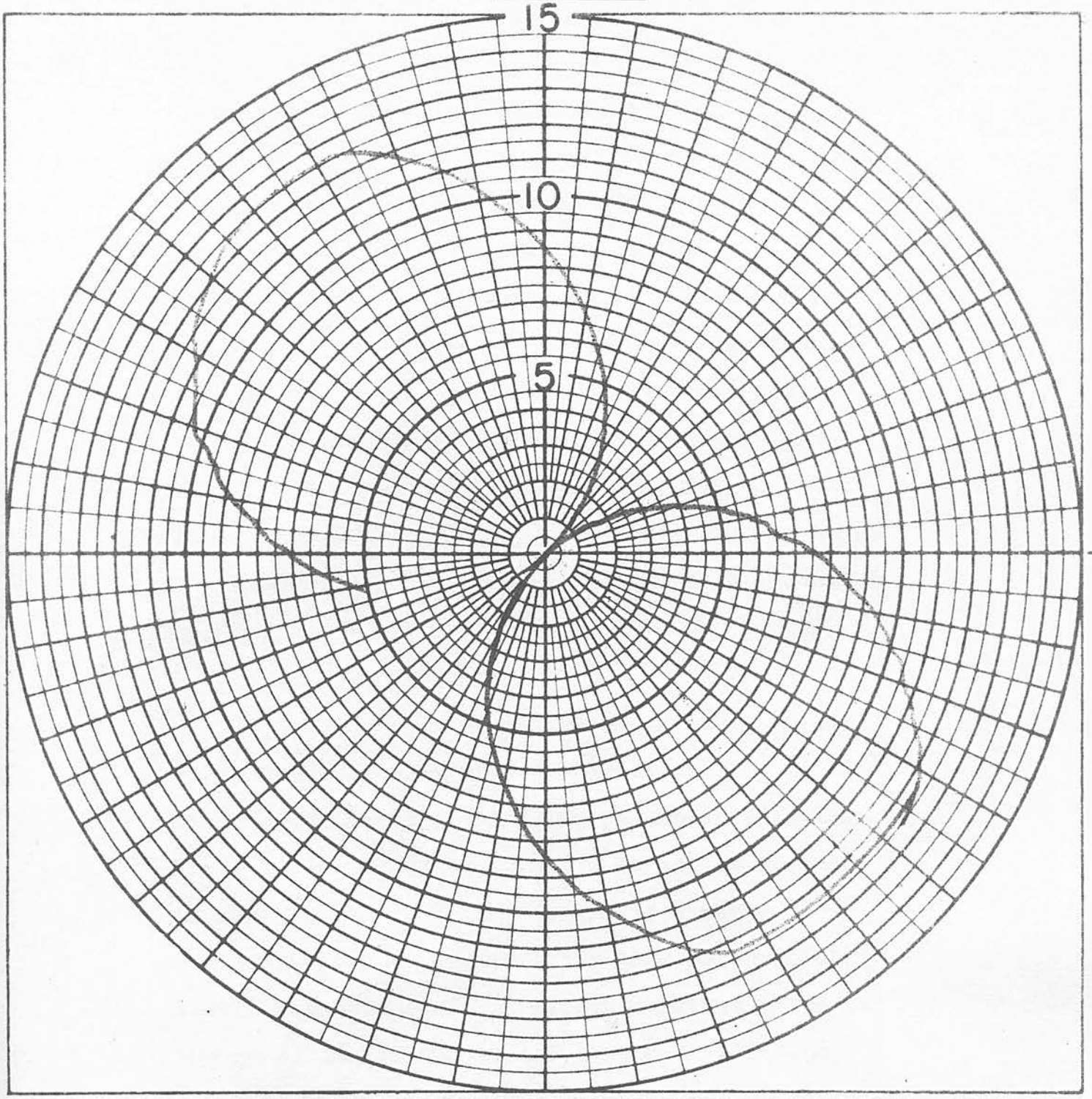

POLARISATION PATTERN FOR 3-TURN CONTRA-WOUND HELIX

wires than over the rectangle formed by the single helix.

Nevertheless this aerial offers an alternative to the zig-zag Aerial[37] as a linearly polarized development of the single helix. A complete investigation of it has not been made, but the preliminary results are sufficient to justify further measurements. From elementary considerations the input impedance with a ground plane type of launching device would seem to be of a suitable value for feeding direct from a coaxial cable.

9.2. Yagi-Uda Aerial

The current distribution along the Yagi-Uda aerial has been measured by Ehrensheck and Poehler[17]. Their results bear a striking resemblance to the distribution along the helical aerial as measured by Marsh[9]. In both cases there is a rapid diminution of current near the feed point which levels out quickly to an almost constant value for the remainder of the aerial length. Since the radiation patterns for both aerials can be derived from the Aerial Array Factor satisfying the Hansen-Woodyard condition, provided the number of elements n is greater than about 4, it is natural to try to find out why the bandwidth of the helical aerial is so much greater than that of the Yagi-Uda aerial.

It is claimed by Reynolds[32] that the pattern bandwidth of the Yagi-Uda aerial, and also of the

dielectric rod, parallel plate, and corrugated surface aerials is inherently large and equal to that of the helix, and that where a low bandwidth exists it is due to inadequate launching of the travelling wave. He has performed experiments to support his claim on a Yagi-Uda aerial 10λ long, where the launching has been carried out by a V aerial instead of the normal dipole. The results shown, covering a bandwidth of 2:1, are claimed to support his theory.

The following objections to this interesting theory are raised:-

(a) Although the radiation patterns of both the helical and Yagi-Uda aerials are derivable from the same formula, this has no relevance to the frequency range over which the formula is applicable. This frequency range is a function solely of the phase velocity along the aerial.

(b) The frequency variation of the phase velocity referred to in (a) has not been shown to be the same for the two aerials. It is now known from Chapter III how the pattern bandwidth of the helical aerial can be predicted from the theoretical phase velocity of the infinite helix. The corresponding phase velocity for the Yagi-Uda aerial consisting of conducting strips is not yet available. It is true that if the strips are replaced by cylindrical rods the phase velocity variation with frequency is known from work carried out by Serracchioli and

Levis[38], but these results show that the phase velocity depends markedly on rod diameter. In the case of the tape helix there is very little such dependence on tape width. Consequently it is not possible yet to make an accurate comparison between the two cases.

(c) The inherently large pattern bandwidth ratio of these end-fire aerials is assumed by Reynolds to be 2:1 for any length of aerial. This ratio has unfortunately been associated with the helix almost from the time of its invention. In the author's submission it has never been substantiated, and a much more realistic figure is 1.7 for short helices and a much lower value for long helices, tending to 1.0 as the length approaches infinity.

(d) The experimental results which Reynolds uses to support his claim can hardly be said to do so. Applying the same criterion of sidelobe level to his results, as has been used in Chapter III gives an acceptable bandwidth ratio of about 1.1 instead of the 2.0 which is claimed.

Nevertheless the theory which he has put forward, though wrong in detail, is sufficiently interesting to justify a more complete investigation and comparison between the different types of aerial in the end-fire travelling wave category. There is much to do both in anlysis and computation before a final comparison can be made.

CHAPTER X

Conclusions

1. The theory of electromagnetic wave propagation along an infinite helical conductor using

(a) the Sheath Helix model and

(b) the Tape Helix model

has been applied to the helical aerial. As a result the following predictions have been made for the first time, for any pitch angle

(i) the upper frequency limit of the Endfire Helical Aerial by means of the Sheath Helix Model

(ii) the upper and lower frequency limits of the Endfire Helical Aerial by means of the Tape Helix Model.

(iii) the upper and lower frequency limits of the Broadside Helical Aerial with Coaxial Conducting Cylinder using the Sheath Helix Model.

2. As a result of the above theoretical investigations it has been predicted and confirmed experimentally that the upper frequency limit of the helical aerial is not independent of length as had previously been reported. The form of this variation can be computed and the theoretical values agree with experiment to an accuracy of better than 10%

3. The prediction has been further made and confirmed that what was previously believed to be a lower limit of pitch angle of 5° for the Endfire Helical Aerial does not in fact exist. Satisfactory experiments have been carried out with pitch angles as low as 1.8°, which was the lowest physically possible at the frequency of operation used. It is believed now that there is no lower limit of pitch angle.

4. It has been predicted and confirmed that the free space circumferential length C_{λ} equal to unity is not the centre frequency of operation of the helical aerial in general. It is the centre frequency only for short aerials using a medium helical pitch angle. For low pitch angle helices C_{λ} equal to unity is well above the upper frequency limit of the aerial, and for long helices this may also be the case even for a medium pitch angle.

5. It has been found that it is not always possible to neglect the effect of the ground screen on the radiation pattern of the helix. Specifically when the ground screen is

(a) several wavelengths in diameter

or (b) constructed of n radial wires

the pattern is profoundly affected, adversely. Experiment has been limited to $n \leq 8$.

6. A Tchebycheff type of current distribution has been proposed for the helical aerial. It has been shown theoretically, using the assumption of a constant amplitude travelling wave, that the prospect of increased directivity from this distribution is severely restricted because of the linking up turns necessary. Reduced side-lobe level has been obtained however, in agreement with the above simplified theory, over the small frequency range determined by the narrow pitch turns. The measured current distribution shows large fluctuations by comparison with the simple uniform helix.

7. General theoretical solutions which in principle enable the phase velocity to be calculated, and hence the frequency limits of the aerial to be predicted, have been obtained for the first time for each of the following cases:-

(i) The Sheath and Tape Helix with a Coaxial Conducting Cylinder

(ii) The Tape Helix wound on a dielectric tube

(iii) The Sheath Helix embedded in a dielectric medium, with a hollow coaxial tube.

(iv) Two Coaxial Sheath Helices.

Calculations have been carried out only in Case (i) for the Sheath Helix and approximate calculations for the Tape Helix.

8. What is believed to be a new type of helical aerial - the linearly polarised Contra-Wound Helix is proposed. Some measurements have been made, and the travelling-wave analysis for the simple helix has been extended to include this case.

9. A critical review has been made of the theory that all End-Fire Travelling-Wave aerials intrinsically possess the same pattern bandwidth.

Acknowlegements: The author wishes to acknowledge the suggestion of the helical aerial as a subject of study by Mr. W. E. J. Farvis of Edinburgh University, the provision of certain experimental facilities by Professor R. N. Arnold of the same University and the use of the larger facilities at Ohio State University through the kindness of Professors T. E. Tice and R. G. Kouyoumjian there. Acknowledgements are also made to Professor R. N. Arnold for having granted leave of absence to visit Ohio State University and to Professor J. D. Kraus there for his interest and encouragement.

REFERENCES

1. H. Chireix U.S. Patent 1,843,445, Feb 2, 1932 cited by Kraus in "Antennas" McGraw-Hill 1950.
2. Private Communication from J.F. Ramsay, Marconi Co.
3. J. D. Kraus "Helical Beam Antenna" Electronics 20, pp 109-111, April 1947.
4. J. D. Kraus and J. C. Williamson "Characteristics of Helical Antennas Radiating in the Axial Mode" J.A.P. 19, pp.87-96, January 1948.
5. O. J. Glasser and J. D. Kraus "Measured Impedances of Helical Beam Antennas". J.A.P. 19, pp.193-197, February 1948.
6. J. D. Kraus "Helical Beam Antennas for Wide-Band Applications" Proc. I.R.E. 36, pp.1236-1242, October, 1948.
7. J. D. Kraus "The Helical Antenna" Proc. I.R.E. 37, pp.263-272, March 1949.
8. T. E. Rice and J. D. Kraus "The Influence of Conductor Size on the Properties of Helical Beam Antennas". Proc. I.R.E. 37 p.1296-Nov. 1949.
9. James A. Marsh "Measured Current Distributions on Helical Antennas" Proc. I.R.E. 39, pp.668-675, June 1951.
10. O. C. Haycock and J. S. Ajioka "Radiation Characteristics of Helical Antennas of Few Turns". Proc.I.R.E. 40, pp.989-991, 1952.
11. G. C. Jones "An Experimental Design Study of Some S and X-Band Helical Aerial Systems." Proc. I.E.E. - Vol.103, Pt.B. pp.764-771. 1956.

12. Y. J. Wong and S. C. Loh "Radiation Field of an Elliptical Helical Antenna" Trans I.R.E., Antennas and Propagation Group, January 1959.

13. H. A. Wheeler "A Helical Antenna for Circular Polarisation" Proc. I.R.E. 35, 1484-1488, Dec. 1947.

14. S. Sensiper Electromagnetic Wave Propagation on Helical Conductors Report No. 194. Research Laboratory of Electronics M.I.T. 1951 This is a shortened version of Sensiper's D.Sc. Thesis on the same subject. An abbreviated form appears in Proc.I.R.E. 43, 1955 pp.149-161

15. W. W. Hansen and J. R. Woodyard "A New Principle in Directional Antenna Design" Proc. I.R.E. 26, pp.333-345, 1938

16. M. Chodorow and E. L. Chu" Cross-Wound Helices for Travelling-Wave Tubes" Journ. App. Phys. 26, pp.33-43, January, 1955. This is an abbreviated version of Stanford Microwave Lab. Report No.249. Nov. 1954 with the same title.

17. H. W. Ehrenspeck and H. Poehler "A New Method of Obtaining Maximum Gain from Yagi Antennas" Proceedings of Wescon Symposium 1953.

18. D. G. Kiely "Dielectric Aerials" Methven and Co., Ltd. 1953.

19. J. D. Kraus "Antennas" McGraw-Hill Co. 1950

20. J. R. Pierce "Travelling-Wave Tubes" Van Nostrand 1950

21. D. A. Watkins "Topics in Electromagnetic Theory" Wiley and Sons Inc. 1958

22. Ramo and Whinnery "Fields and Waves in Modern Radio" Wiley and Sons Inc. 1953

23. Goward F. K. "An Improvement in End-Fire Arrays" J. I. E. E. Vol. 94, Part III 1947

24. R. H. Du Hamel "Optimum Patterns for Endfire Arrays" Proc. I.R.E. May 1953

25. E. T. Whittaker and G. Robinson "Calculus of Observations" Blackie and Sons. 1924

26. M. M. Astrakan Dissertation for Degree of Doctor of Philosophy, Northwestern University, Illinois 1949, cited by D. G. Kiely in Reference 18.

27. G. Wade "Study of Microwave Noise in Beam Type Devices" Stanford University Technical Report 75, 1954

28. Private Communication from H. C. Ko, Ohio State University.

29. S. Olving "Electromagnetic Wave Propagation on Helical Conductors Embedded in Dielectric Medium". Chalmers University of Technology, Research Laboratory of Electronics Report No. 33, 1951.

30. Cutler, King and Kock "Microwave Antenna Measurements" Proc. I.R.E. Dec. 1947

31. S. A. Schelkunoff "Electromagnetic Waves" Van Nostrand 1943.

32. D. K. Reynolds "Broadband Travelling-Wave Antennas". I.R.E. National Convention. Record 1957.

33. J. C. Williamson Unpublished M.Sc. Thesis Ohio State University 1947

34. H. G. Smith High Gain Side-Firing Helical Antennas for V.H.F. Television Broadcasting Trans. A.I.E.E. Pt.1, May 1954 pp.135-138

35. G.W.C.Mathers and G. S. Lino "Some Properties of a Sheath Helix with a Centre Conductor or External Shield". Report No. 65 Electronics Research Laboratory, Stanford University 1953.

36. L. Stark "Lower Modes of a Concentric Line Having a Helical Inner Conductor". Jour. App. Phys. September 1954, pp.1155-1162.

37. W. A. Cumming "A Nonresonant Endfire Array for V.H.F. and U.H.F." Trans I.R.E. Antennas and Propagation Group, April 1955, pp.52-58.

38. F. Serrachioli and C. A. Levis "The Calculated Phase Velocity of Long End-Fire Uniform Dipole Arrays" Presented at U.R.S.I. Symposium on E.M. Theory. June 1959 (To be published in Trans. I.R.E. 1959)

39. H. L. Knudsen "Radiation from Helical Antennas" Trans. Danish Academy of Technical Sciences, 1950.

40. E. T. Kornhauser "Radiation Field of Helical Antennas with Sinusoidal Current" Jour. App. Phys. July 1951.

41. H. L. Knudsen "Field Radiated by Ring Quasi-Array of Infinite Number of Tangential or Radial Dipoles" Proc. I.R.E. June 1953.

42. J. A. Stratton "Electromagnetic Theory" McGraw-Hill, 1941

43. H. Unz "Linear Arrays with Arbitrarily Distributed Elements" University of California Electronics Research Report No. 56, November 1956.